Universiteit Gent(U.G.)
Faculteit toegepaste wetenschappen
Elektrische Energie, Systemen en
Automatisering
Technologiepark-Zwijnaarde 913
B-9052 Zwijnaarde
EESA

Katholieke Universiteit Leuven(K.U.L.)
Faculteit toegepaste wetenschappen
Departement Elektrotechniek
Kasteelpark Arenberg 10
3001 Leuven (Heverlee)
ESAT/SCD-SISTA

GLOBAL STABILIZATION OF A NONLINEAR CHEMICAL PROCESS BY LINEAR FEEDBACK

Jury:
Prof.Dr.Ir. Mia Loccufier, promotor
Prof.Dr.Ir. Erik Noldus, promotor
Prof.Dr.Ir. Joos Vandewalle, promotor
Prof.Dr.Ir. Jan Van Impe, promotor
Prof.Dr.Ir. Joris De Schutter(Mechanica, KULeuven)
Prof.Dr.Ir. Georges Bastin (Cesame, UCL)
Prof.Dr.Ir. André Barbé (SISTA/COSIC, KULeuven)
Prof.Dr.Ir. Johan Suykens (SISTA/COSIC, KULeuven)

Proefschrift voorgedragen tot
het behalen van het doctoraat
in de toegepaste wetenschappen
door
José Aldemar Muñoz H.

U.D.C. 66.0

January 2005

©Katholieke Universiteit Leuven- Faculteit Toegepaste Wetenschappen
Arenbergkasteel,B-3001 Heverlee (Belgium)

Alle rechten voorbehouden. Niets uit deze uitgave mag vermenigvuldigd en/of openbaar gemaakt worden door mideelvan druk, fotocopie, **microfilm , elektronish** of op welke andere wijze ook zonder voorafgaande schrifteleijke toestemming van de uitgever.

All rights reserved. No part of the publication may be reproduced in any form **by print, photoprint, microfilm or any other means without** written permission from the publisher.

D/2004/7515/94
ISBN 90-5682-556-9

Acknowledgment

First of all, I should like to express my sincere gratitude to the initiators and promotors of the VLIR-UOS Colombia project (AEIN 1999 PR 221, E.I.99 : 13V43499) : Ir. Jean Louis Lams, Prof. Achiel Van Cauwenberghe, Prof. Joos Vandewalle, Prof. Erik Noldus, Prof. Robain De Keyser and Ir. Bernard Baeyens. Without their permanent support and dedication the successful progress of this project would not have been possible.

I want to thank my research supervisors : Prof. Mia Loccufier and Prof. Erik Noldus for proposing the research subject and the methods of investigation, for providing a well organized PhD programme and giving many valuable comments on the manuscript, as well as for being available for many discussions concerning various control problems and for coauthoring the publication of the obtained results. I would like to express my gratitude to my daily supervisor Prof. Erik Noldus for his encouragement, support and constructive criticism during all the work and for the great enthusiasm he has always shown for our cooperation.

I want to thank the heads of departments : Prof. Belmans from ESAT (KULeuven) and Prof. J. Melkebeek from EESA (UGent) for giving me the opportunity to follow the doctoral programme at their prestigious universities, to thank all members of the Electrical Energy, Systems and Automation Department (EESA) from Ghent University and the staff at the department of SCD-SISTA group from Leuven University who have contributed by creating pleasant and stimulating working conditions. I extend my gratitude to the Coruniversitaria's rector Dr. Leonidas López for being a person outstanding by his great interest in the Tolima people's education. Also I thank all members of my team at the Automatic Control Department at Coruniversitaria for providing the creative and friendly atmosphere which makes work a pleasure.

I also thank the promotors of this thesis : Prof. Mia Loccufier, Prof. Erik Noldus, Prof, Joos Vandewalle and Prof. J. Van Impe and the advisors : Prof. André Barbé and Prof. Johan Suykens.

Finally, I thank my parents Delia and Ernesto, my wife Lida and my children Mauricio and Katerine who in one or another way made this dream a reality. Their sacrifice and support helped me to continue till the end. Two special

persons who unfortunately died during my studies will always be remembered, Nestor my friend and Niray, my youngest brother: Thanks for being kind and for all the nice things you always shared with me.

Contents

Contents i

1 Introduction 1

1.1 Problem statement 2

1.1.1 Description of the CSTR 2

1.1.2 The control problem 5

1.1.3 Working conditions in an industrial environment 8

1.1.4 Choice of the set point 9

1.1.5 Stabilization technique 11

1.1.6 Physical dynamic equations vs dimensionless equations . 12

1.2 State of the art 16

1.3 Objective of the thesis 19

1.4 Basic concepts and results 19

1.4.1 Principles from Liapunov theory 19

1.4.2 The linearization principle 24

1.4.3 Principles from dissipativity and passivity 25

1.4.4 The Kalman-Yacubovich-Popov main lemma 28

1.5 Overview and personal contribution 30

2 Single input PD-control 33

2.1 Open loop process dynamics and control law 34

2.2 Closed loop stability analysis 35

2.2.1 Closed loop stability analysis using passivity theory . . 36

2.2.2 Closed loop stability analysis using Liapunov theory . . 37

2.3 Phase portrait simulation 41

2.4 Control parameter tuning 47

2.4.1 Linearized dynamics in the set point 47

2.4.2 Characteristic equation 48

2.4.3 Root locus plot 49

2.4.4 Time response simulations 54

2.4.5 Choosing the control parameters 54

2.5 Input and state constraints 57

2.5.1 The input constraint problem 58

2.5.2 The state constraint problem 68

3 Two input PD-control 75

3.1 Feedback law 76

3.2 Closed loop stability analysis 76

3.2.1 Closed loop stability analysis using passivity theory . . 77

3.2.2 Closed loop stability analysis using Liapunov theory . . 78

3.3 Control parameter tuning 78

3.3.1 Root locus analysis of the linearized dynamics 78

3.3.2 Single input PD-control vs two input PD-control 84
3.3.3 Simulation of transients 86
3.4 Phase portrait simulation 93

4 Two input PID-control **99**
4.1 Controller dynamics and stability analysis 100
4.2 Control parameter tuning 104
4.2.1 Linearized dynamics in the set point 105
4.2.2 Root locus analysis of the closed loop dynamics 105
4.2.3 System performance in the presence of disturbances . . 112
4.2.4 Generalizations 123
4.2.5 Simulation results 126
4.3 Stability regions under state constraints 132
4.3.1 Theoretical analysis 132
4.3.2 Simulation results 134

5 Decoupling **141**
5.1 Decoupling of the temperature dynamics 142
5.1.1 Parameter tuning 145
5.1.2 Some remarks 152
5.2 The robustness problem 152

6 Robust single input PD-control **157**
6.1 Controller structure 158
6.2 Stability analysis 160
6.3 Robust design with a finite stability region 163

6.4 Control parameter tuning 167

7 Conclusions **173**
7.1 Summary 174
7.2 Further research 176
7.2.1 Generalizations of the robust PD/PID controller 176
7.2.2 Survey of and comparison with alternative controller design methods 176
7.2.3 Application to real world industrial plants 177

Chapter 1

Introduction

In Chapter 1 we present an introduction to the problem of controlling a nonlinear chemical stirred tank reactor. Section 1.1 contains a description of the continuous stirred tank reactor (CSTR), the control problem, the system's working conditions, the selection of the set point and the problem of stabilization. We describe the system's dynamic equations both in physical and in dimensionless representations. In Section 1.2 we briefly discuss the state of the art describing some existing stabilization methods applied to a CSTR. Subsequently we state the objectives of our work and our personal contribution to the subject. We recall a number of concepts and results from systems and control theory that will be needed for the development of our ideas. Finally we give an overview of the thesis.

1.1 Problem statement

Linear models often do not adequately describe the dynamics of a process to be controlled except near the point at which the model was identified. This fact causes difficulties for processes whose dynamics extend over wide regions in state space, possessing multiple operating points and requiring set point changes based on economic or technical criteria. In these cases, the models used as the basis for control and estimation must be nonlinear to accurately capture the behaviour of the plant in all its probable operating regimes. Nonlinearities are common in chemical processes. They may arise from reactor kinetics, for instance in the relationship between reaction rate and temperature in the Arrhenius equation or they may be the result of higher order reactions.

During the last decades a detailed understanding of the behaviour of nonlinear processes has been developed although methods for their control are still evolving. This thesis studies the design of controllers for a nonlinear CSTR model. Sometimes we use a model of the process linearized about a steady state operating point. In principle the reactor dynamics are globally feedback linearizable. Globally linearizing control (GLC) has been studied by Willis (1994) and McColm (1994). Other popular nonlinear methodologies that have been proposed for use within the chemical and process industries include generic model control (GMC),(James and Peter, 1995) or model predictive control(Clarke,1988), (Muske, 1993). In the present work however, motivated by practical considerations for an industrial environment we prefer to design simple linear time invariant controllers such as the classical PID algorithm. Our design principle is the global asymptotic stabilization of the desired set point using Liapunov methods and passivity/dissipativity theory.

1.1.1 Description of the CSTR

An ideal state reactor is also called a mixed reactor, an ideal continuous stirred tank reactor (CSTR), or a constant flow stirred tank reactor (CFSTR). As its name suggests, it is a reactor in which the contents is well stirred and uniform throughout. Thus, the exit stream from this reactor has the same composition as the fluid within the reactor. Flow reactors, which constitute another type of reactor, are used for greater production rates, when the reaction time is comparatively short, when labor costs are high. Material and energy balances are based on the conservation laws. In the operation of liquid phase reactions at steady state in a CSTR, the input and output flow rates are constant, so the holdup is fixed. Figure 1.1 shows a typical representation of a CSTR.

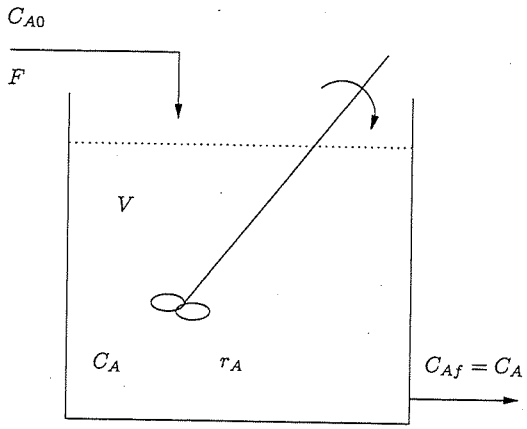

Figure 1.1: Typical representation of a CSTR. V= reactor volume, F= feed flow, C_{A0} =feed concentration, C_A =reactor concentration, C_{Af} =output concentration, r_A =reaction rate.

An important concept when talking about reactors is "Kinetics". We have one or several reactants which combine to produce one or more products. Possibly there is a limited conversion at equilibrium: We can have the possibility that part of the moles are still present as reactants and part of them are being formed as products, this is called intermediate conversion. It is also possible that full conversion is reached in steady state. We can say that thermodynamics tell us about the condition of the reactants once steady state has been reached while kinetics tell us about reaction speed, i.e. how long the reaction takes to reach this condition. An outline of reactor thermodynamics and kinetics can be found in Levenspiel(1999).

Equilibrium constant K_c

This constant tells us about the quality of the conversion. If a moles of species A react with b moles of species B to produce c moles of C and d moles of D then K_c is given by :

$$K_c = \frac{[C]^c_{equil}[D]^d_{equil}}{[A]^a_{equil}[B]^b_{equil}}$$

E.g. $K_c = 10^{-3}$ means that reactants dominate the composition of the equilibrium product and we have limited conversion. If $K_c = 1$ we have intermediate conversion and if K_c has a high value, say $K_c = 10^3$ we have a high conversion.

The following expression shows how K_c is related to the thermodynamic quantities :

$$RTlnK_c = -\Delta G = -\Delta H + T\Delta S$$

where

$$\begin{aligned} T &= \textit{Absolute temperature} \\ R &= \textit{Universal gas constant} \\ K_c &= \textit{Equilibrium constant} \\ \Delta G &= \textit{Gibbs free energy} \\ \Delta S &= \textit{Entropy change} \\ \Delta H &= \textit{Enthalpy change} \end{aligned}$$

ΔH corresponds to the enthalpy change associated with the reaction or the reaction heat. It is the heat (energy) you have to add to or to remove from the system to permit the reaction to occur at constant temperature. If the reaction produces heat (exothermal reaction), it is necessary to remove heat. Then ΔH is negative and (ΔS) is positive. The opposite happens if the reaction is endothermic. In this case the enthalpy change (ΔH) is positive while the entropy change (ΔS) is negative.

The equilibrium conditions depend on temperature. If the temperature changes in the system, all the thermodynamics change. If T increases because we have an exothermic reaction then we will reach a lower conversion. If temperature decreases this results in a higher conversion. Problems occur in the case of abrupt, large temperature variations. In conclusion the temperature affects the thermodynamics and the kinetics of a reaction.

Reaction rate r_A

The reaction rate specifies the speed of a reaction. It is defined as:

$$r_A = \frac{1}{V}\frac{dN_A}{dt}$$

where
N_A=Number of moles of species A
V= Volume of the reactor
N_A is not practical to measure. It is more practical to work with concentrations. Moles and concentration are related by:

$$N_A = VC_A$$

In this way the rate of reaction can be written as:

$$r_A = -\frac{d(C_A)}{dt}$$

A zero order reaction is defined by :

$$r_A = -\frac{d(C_A)}{dt} = K_A$$

For a first order reaction with constant reactor volume:

$$r_A = -\frac{d(C_A)}{dt} = K_A C_A$$

A common way to express the effect of the temperature is given by the Arrhenius relation :

$$K_A = K_0 exp\frac{(-E_0)}{RT}$$

E_0 being the activation energy. For instance when we go from the reactant A to the product B an enthalpy change ΔH occurs. Before reaching B the reaction goes through some intermediate states generating an energy barrier to get to this intermediate from A. This is called "activation energy E_0".

1.1.2 The control problem

There are two major types of reactors, the batch reactor and the continuous reactor. In most of them it is necessary to maintain the values of pressure, temperature and concentration between reasonable limits. Depending on the type of reactor a different control strategy will be needed. In the present

thesis we study the CSTR where clearly a stabilization problem occurs. The two manipulated variables are feed temperature and feed concentration while the controlled variables are reactor concentration and reactor temperature. A typical temperature control scheme for a CSTR is presented in the graph of Figure 1.2.

Here we see that if the input refrigerant temperature T_i changes, then T_r

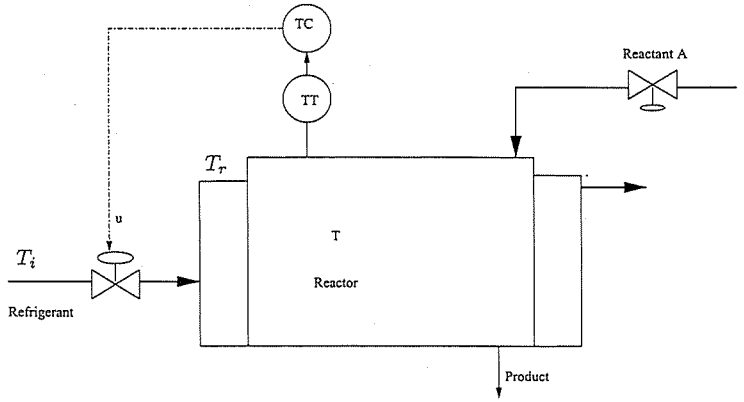

Figure 1.2: Typical reactor temperature control. TT = temperature transmitter, TC= temperature control unit.

(jacket temperature) and T (reactor temperature) will change too. The TC controller will correct this by changing the control signal u. A more detailed diagram including temperature as well as concentration control is presented in Figure 1.3. Here a cascade control strategy is proposed. The temperature can be measured directly in the reactor or in the jacket. With the latter we obtain a correction of the effect of the disturbance T_i on T_r before the latter one affects T in a significant way. The concentration is controlled by first measuring the concentration with the use of an analyzer and then acting over the feed reactant flow valve. In the bottom part of the scheme a single level loop appears which keeps the level of the fluid inside the CSTR in the desired selected value.

In the application at hand the reactor's state space model is of second order. It is written in the form

$$\dot{x} = f(x,u)\,, x \triangleq \begin{bmatrix} T \\ C \end{bmatrix}, u \triangleq \begin{bmatrix} T_0 \\ C_0 \end{bmatrix}$$

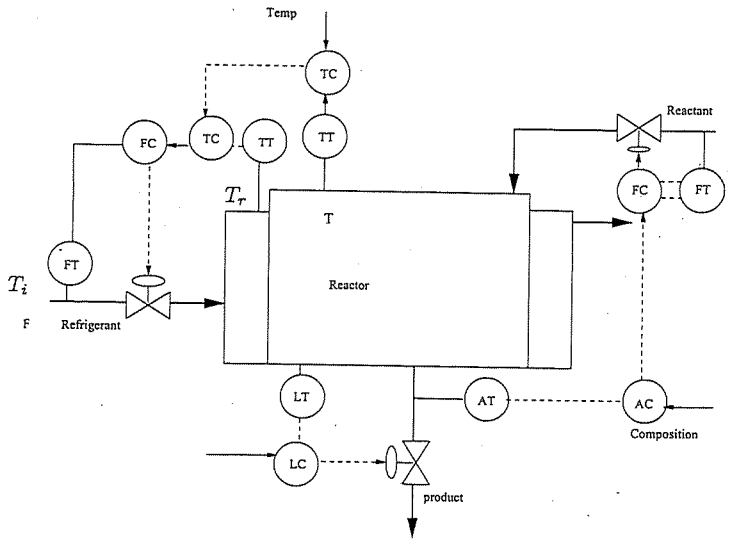

Figure 1.3: General configuration for temperature and concentration control in a CSTR. AC=analysis controller, FC=flow controller, FT= flow transmitter, AT=analysis transmitter, LC= level controller, LT=level transmitter.

As shown in Figure 1.4 we shall design linear time invariant controllers for controlling both the reactor temperature and the reactor concentration by using passivity techniques and Liapunov theory. The algorithms will be tested in two numerical examples. Simulations in both open and closed loop will display the advantages and disadvantages of linear PD or PID controllers for this class of nonlinear processes.
First we will analyze a single feedback loop where the state variables are fed back to the reactor feed temperature as the only input, using a PD-control algorithm. Multivariable control loops which, in addition, use feed concentration as an input and which a.o. apply PID control are discussed later.

For the parameter tuning of the stabilizing controller structure we can rely on classical root locus techniques applied to the linearized closed loop. We present simulations of transients and of the open and closed loop's phase portraits.

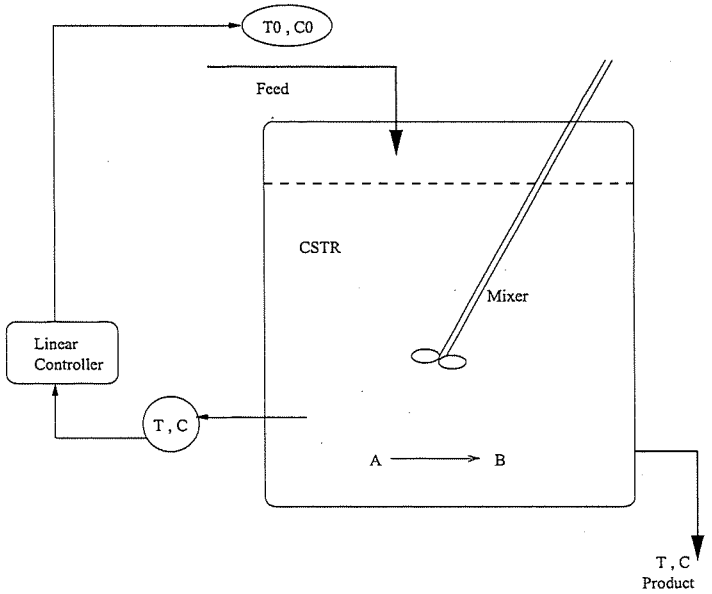

Figure 1.4: CSTR with state variables T =reactor temperature and C =reactor concentration,inputs T_0 =feed temperature and C_0 =feed concentration.

We wish to consider the controller's robustness and to pay attention to the magnitude of the required control inputs and of the resulting state variable **fluctuations.**

1.1.3 Working conditions in an industrial environment

For each unit the operational conditions must be optimized to maximize reaction conversion and to minimize both release of materials to environment and consumption of energy. Safe working conditions should be maintained. From an environmental perspective, reactors are the most important operational units in a chemical process. When heat is added to or removed from the reaction mass, the temperature will change. As the reaction rate is strongly dependent on the temperature (Arrhenius equation), we will get a remarkable change in reaction rate r_A with changing temperature.

The three different thermal operational modes of chemical reactors are : the adiabatic mode, the isothermal mode and the polytropic mode. The first one means that there is no heat exchange with the surroundings. Sometimes the two other modes are integrated in the term "non-adiabatic operational modes". Their common property is that they generate heat exchange with the environment. Isothermal means that the heat exchange is managed in such a way that the reaction mass remains at a constant temperature. This can be done by external temperature control or automatically by the way the process is conducted, for instance in a stationary state where the heat produced by the reaction is exactly carried away by convection. Polytropic means that the temperature of the reaction mass is steered in time and space following some programme.

An important aspect of operating a $CSTR$ is the speed of the reaction. Reactor speed cannot be predicted from basic principles, and is not simple to compute. Therefore it must be measured. Here it is important to know the type of reaction (exothermal or endothermal), because a reactor must operate in a safe way. Optimal process conditions bear on :

- ideal temperature

- ideal pressure

- ideal concentration

- ideal flow rates

In practice ideal operating conditions are not necessarily maximum conversion or the fastest kinetics, that is to produce as fast as possible. For example when we are dealing with an exothermal reaction we have to prevent the temperature from rising to an unacceptable level. What is desired is to have fast kinetics, good thermodynamics but with moderation.

1.1.4 Choice of the set point

Consider a system in which a single first order irreversible exothermal chemical reaction takes place. Depending on the process parameter values there may exist either one or three open loop equilibrium points in the uncontrolled process dynamics as shown in Figures 1.5 and 1.6 for the two numerical examples defined in Chapter 2. The line segments in both diagrams represent the relationships defining equilibrium conditions.

Two of the equilibria, which are located at extremum values of the state variables are stable. The one in the middle is unstable (saddle point, A). Typically in the stable cases reaction temperature will be too high for safety or conversion to the end product will be too low from an economical point of view. The desired set point is the unstable one.

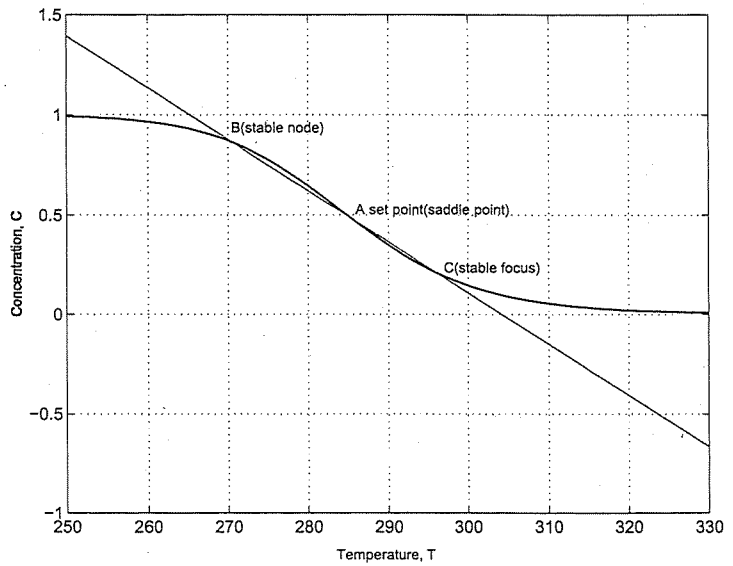

Figure 1.5: Equilibrium points for Example 1(see Chapter 2, page 43).

If the equilibrium temperature increases conversion will be lower but the speed of the reaction will be higher. In this sense the saddle point is the best set point, and the problem is then to stabilize it. We will design the controller

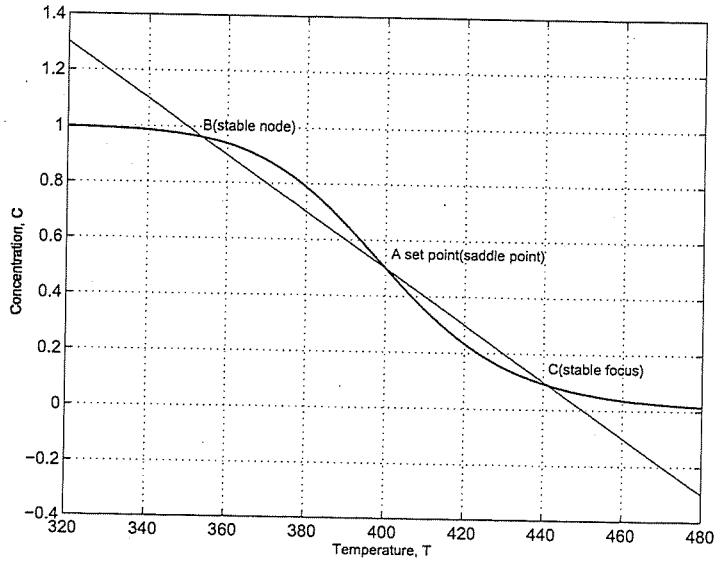

Figure 1.6: Equilibrium points for Example 2(see Chapter 2, page 44).

structure to obtain global stabilization of the set point. Then the parameters of the controller will be adjusted to optimize the loop's transient behaviour.

1.1.5 Stabilization technique

The state equations of the reactor model to be controlled contain a product type nonlinearity in which one factor depends linearly and the other factor depends exponentially on the state variables. Using well established principles from dissipativity and passivity theory sufficient conditions are derived under which the closed loop can be represented as a feedback interconnection of passive components and global stability can be guaranteed. In doing so we shall not try to compensate the complex nonlinearities of the controlled process. Instead, exploiting the special structure of these nonlinearities, simple linear control laws will be synthesized which globally stabilize the selected set point. An interpretation of the obtained stability criteria in terms of Liapunov theory is included. Moreover the proposed technique allows a design with good

robustness properties.

1.1.6 Physical dynamic equations vs dimensionless equations

We compile a list of variables of interest for the analysis of the unsteady-state behaviour and the control of a CSTR.
Consider a reactor in which the reaction $A \rightarrow B$ takes place. The reactor is equipped with a jacket with a heat exchange fluid circulating through the jacket at a high enough rate to keep the temperature of the heat exchange fluid constant.

The temperature of the fluid entering the reactor vessel may change with time, however the volume of the reactor contents and the flow rate of the streams into and out of the reactor remain constant. The concentration of A in the inlet stream may also change with time. We write the unsteady-state balances needed to describe the time dependent behaviour of the reactor. In the situation described above the composition of the material in the CSTR and its temperature will both change with time. Thus it will be necessary to make a material balance and an energy balance of the CSTR. From Fogler's text (See also Luyben, 1990) on reactor design, (Fogler, 2000), for an ideal continuous stirred tank reactor with feed flow F and constant volume V,where a first order irreversible reaction $A \rightarrow B$ takes place, the following equations are obtained:

Material balance

$$V\frac{dC}{dt} = F(C - C_0) - VK_0Cexp(\frac{-E}{RT}) \tag{1.1}$$

Energy balance

$$V\rho c_p\frac{dT}{dt} = F\rho c_p(T_0 - T) - UA(T - T_k) + (-\Delta H)VK_0Cexp(\frac{-E}{RT}) \tag{1.2}$$

In the energy balance the term in the right side of (1.2)is just the enthalpy change that occurs when the feed stream is brought to the temperature inside the reactor. We express this information in terms of volumetric flow rate, density and the specific heat on a mass basis. The coefficient term of the temperature derivative at the left side of (1.2) is the total heat capacity of the reactor contents. We express this in terms of volume, density and specific heat

for our problem.

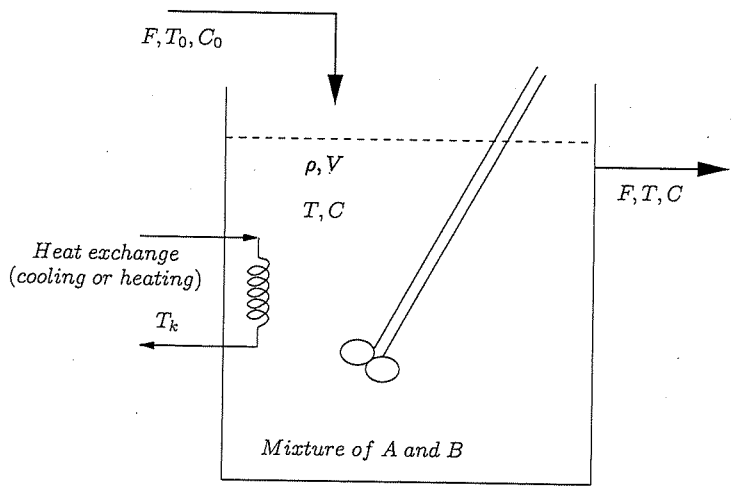

Figure 1.7: CSTR to control.

For a first order reaction the reaction speed per unit of volume $r = f(T, C)$ is given by :

$$r = KC(\tfrac{moles}{m^3 s});\ C = C_A;\ K = K_0 e^{(\frac{-E}{RT})}$$

and where :

C_0 = *feed concentration of the component of interest*
C = *concentration of species of interest inside the reactor*
ρ = *specific mass*
T_0 = *feed temperature*
T = *temperature inside reactor*
$-\Delta H$ = *molar heat of the reaction*, $(\frac{J}{mole})$

UA = *overall heat transfer coefficient times heat exchange area for reactor jacket*
t = *time*
c_p = *heat capacity (may be assumed to be the same for all components)*
V = *reactor volume*
F = *volumetric flow rate of inlet and outlet streams*
ρ = *density (may be assumed to be constant for inlet and outlet streams)*
U = *heat transfer coefficient*
T_c = *cooling temperature*
T_h = *heating temperature*
$K_0 C exp(\frac{-E}{RT})$ = *reaction speed per unit of volume*

$(-\Delta H) > 0$ for an exothermic reaction (needs cooling via $T_k = T_c$) and < 0 for an endothermic reaction (needs heating via $T_k = T_h$).

The block diagram of Figure 1.8 describes the reactor's input-output relations: T_0 or alternatively T_k and eventually C_0 are the manipulated variables, C and

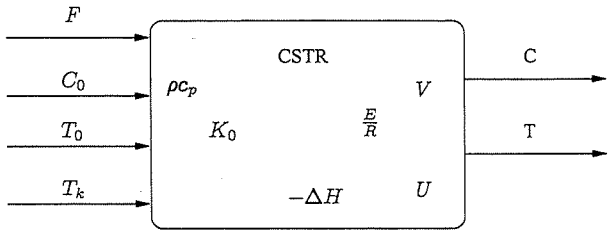

Figure 1.8: Manipulated and control variables in the CSTR.

T are the controlled variables. F can be a disturbance, but we shall assume it is a constant.
A transformation to dimensionless quantities produces the reduced form :

$$\dot{z}_1 = r - (1+\vartheta)z_1 + m_2 z_2 exp(\frac{-10^4}{z_1}) + u_1 \qquad (1.3)$$

$$\dot{z}_2 = 1 - z_2 - m_1 z_2 exp(\frac{-10^4}{z_1}) + u_2 \quad (1.4)$$

The dimensionless inputs are :

$$\begin{aligned} u_1 &\triangleq \frac{10^4 R}{E}\Delta T_0(t) \\ u_2 &\triangleq \frac{1}{C_0}\Delta C_0(t) \end{aligned} \quad (1.5)$$

which represent scaled fluctuations of the feed temperature, with nominal value T_0 (or eventually cooling temperature, with nominal value T_k) and feed concentration C_0

Furthermore

$$z_1 \triangleq \frac{RT}{E}10^4,\ z_2 \triangleq \frac{C}{C_0},\ \vartheta \triangleq \frac{U}{F\rho c_p},$$
$$r \triangleq 10^4\frac{R}{E}\left(T_0 + \frac{UT_k}{F\rho c_p}\right),\ m_1 \triangleq \frac{Vk_0}{F},$$
$$m_2 \triangleq 10^4\frac{(-\Delta H)Vk_0C_0R}{F\rho c_p E}$$

and $f(y) \triangleq exp(\frac{-10^4}{y})$. Time has been rescaled as $\tau \triangleq t/(\frac{V}{F})$.
(1.3), (1.4) can be written in vector form as

$$\dot{z} = Az + k - bf(c'z).g'z + u \quad (1.6)$$

with

$$z \triangleq \begin{bmatrix} z_1 \\ z_2 \end{bmatrix}, A \triangleq \begin{bmatrix} -(1+\vartheta) & 0 \\ 0 & -1 \end{bmatrix},$$
$$k \triangleq \begin{bmatrix} r \\ 1 \end{bmatrix}, b \triangleq \begin{bmatrix} -m_2 \\ m_1 \end{bmatrix}, c \triangleq \begin{bmatrix} 1 \\ 0 \end{bmatrix},$$
$$g \triangleq \begin{bmatrix} 0 \\ 1 \end{bmatrix}, u \triangleq \begin{bmatrix} u_1 \\ u_2 \end{bmatrix},$$

Redefining the state as a deviation variable $x \triangleq z - z_s$, z_s being the system's set point brings (1.6) in the form

$$\dot{x} = Ax - b[f_1(c'x) + f_2(c'x)g'x] + u \quad (1.7)$$

with

$$x \triangleq \begin{bmatrix} x_1 \\ x_2 \end{bmatrix},\ f_1(y) \triangleq [\ f(y + c'z_s) - f(c'z_s)\ ]\ g'z_s,$$

and

$$f_2(y) \triangleq [\ f(y + c'z_s)\ ]$$

1.2 State of the art

In this section we summarize some of the work that has been done in the direction of chemical reactor control and specifically in the direction of CSTR control.

The dynamics and stability of nonlinear models of the uncontrolled CSTR have been studied a.o. by Noldus et al.(1974) and by Loccufier and Noldus(1994). One of the oldest contributions to the stabilization of a CSTR was proposed by R.B.Warden (1964) where the CSTR is analyzed for stability w.r.t. finite perturbations by the direct method of Liapunov. Stephanopoulos and Schuelke (1976) proposed the application of vector Liapunov functions in process design. The peculiarities of dynamic behaviour and stability in the field of chemical engineering were reviewed by Eigenberger (1985).

A nonlinear PID controller based on neural networks was proposed by Tan and Van Cauwenberghe(1999). The idea was to develop a conventional PID adaptive controller based on a nonlinear process model instead of using a controller with fixed parameters designed on the assumption that the process to be controlled is linear. Simulation results show that the neural network based generalized nonlinear PID controller can handle nonlinear processes effectively and the convergence condition for the method provides an effective way for choosing parameters leading to stable and fast convergence.

Some demonstrative examples of the stabilization of unstable reactors have been worked using both linear (LMBPC) and nonlinear model based predictive control (NMBPC). This work has been done by Rawlings,Tenny and Wright(2002). Their goal is to reach and maintain the unstable operating point. Some model based predictive control (MPC) results of unstable reactors show better behaviour when applying NMBPC, reaching and maintaining the set point forever, while some LMBPC approximations show the trajectories escaping from the chosen set point.

The authors conclude that:

- Nonlinear models are necessary for many relevant industrial applications.
- Nonlinear MPC exhibits superior control over linear MPC, even on simple nonlinear examples.
- Nonlinear regulation and estimation methods are computationally efficient and can be solved in real time. However one of the main obstacles of implementation is that the process needs to be well understood: It is important to know what are the main process features that should be modeled. Also greater focus on nonlinear modeling (e.g, subspace identification) efforts should be made.

In another application by Brown and Bordons (1995) a neural network is used to identify a CSTR and to control it by MPC. The potential of model predictive control is discussed where the model of the CSTR is built by a neural network which is continuously adapted to the process.

Dostal and Bobál (2001) deal with the adaptive control of nonlinear processes. A CSTR with first order consecutive exothermic reactions and with a perfectly mixed cooling jacket is considered. The CSTR is approximated by an externally linear model with recursively estimated parameters. The controller design procedure provides the internal properties and stability of the control system.

In a recent publication by Marchand and Alamir (1998) a new state feedback law for the stabilization of a CSTR is presented . This work is based on the generation of open loop trajectories used to design a stabilizing feedback controller and on Liapunov theory to prove the global asymptotic stabilization of the system. Sufficient conditions on the open loop trajectory generator are given such that the proposed feedback asymptotically stabilizes the CSTR.

Some similar applications have been developed in the field of biochemical processes such as the one by Efe et al. (2001) which uses an intelligent approach (applying neural networks) in the design of controllers for a CSTR. It has been shown that the control system exhibits a highly robust behaviour against disturbances and sharp changes in the command signal.

A special field of research is the periodic optimization of chemical processes, where the conversion to the desired end product is improved by periodic excitation around the static optimum, see e.g Noldus (1977), Matsubara et al.

(1973) or Rigopoulos et al. (1988).

A recent book by Bequette (2003) thoroughly discusses the process dynamics and control of a CSTR. The internal model control (IMC) strategy is explained in detail, as well as a procedure to obtain a PID controller based on the computed IMC realization. This methodology is implemented with stable and unstable chemical processes, using a first order model with time delay. The philosophy is extended to tackle the problem of non-measurable disturbances and uncertainty in the process, i.e. the robustness problem.

Advanced control techniques such as MPC are shortly explained and focus on industrial applications. The importance of tuning parameters, stability and the ability of MPC to handle constraints in an optimal way are covered as well.

A full chapter is dedicated to an industrial example (propylene glycol production). Different cascade control strategies are proposed. Steady state solutions for the standard CSTR and for a more detailed model which includes the effect of the cooling jacket dynamics are presented. It is shown that although all of the steady-state input output curves are nonlinear, larger reactors in general exhibit a multiple steady-state behaviour while small reactors exhibit only one stable equilibrium point. Controllers using proportional feedback are designed to stabilize the reactor operation in the case of the open loop unstable CSTR . It must be observed that although general nonlinear models were developed, dynamic simulations were based on linear systems.

An interesting report by Nikolaou (2001) focusses on the application of linear control strategies to nonlinear processes. This paper presents recent developments concerning the quantification of nonlinearity in feedback systems. Some methods are presented within the context of assessing whether (and what) linear control is adequate for certain nonlinear processes (specifically chemical processes are discussed) or whether (and what) nonlinear control is warranted (See also Harris and Seppala, 2001). The problem whether a constrained MBPC should employ a linear or a nonlinear model of a controlled process is discussed as well as whether it is possible to stabilize an unstable nonlinear process by using linear control. Departing from the notion of nonlinearity measures based on the distance (norm of difference) between a nonlinear operator and a suitable linear operator, a number of investigators took different pathways towards quantifying nonlinearity. Guay et al. (1995) proposed to quantify the static nonlinearity of a system in terms of the local geometry of the steady state

locus. Guay (1996) extended these results to the quantification of dynamic nonlinearity.

1.3 Objective of the thesis

The purpose of this thesis is to design simple linear time invariant controllers such as PD or PID- controllers for the stabilization of a nonlinear CSTR model. Although there are several techniques to design nonlinear controllers we do not want to concentrate on these approaches. Instead of compensating or modifying the complex nonlinearities of the process we develop globally stabilizing linear control algorithms.

1.4 Basic concepts and results

In this section we discuss some basic concepts and theorems which will permit the reader to understand the algorithms developed in our work. We first present some important theorems from Liapunov theory. Then some notions on dissipativity and passivity are given. Subsequently we formulate the main lemma of Kalman-Yacubovich-Popov. Finally a brief summary of the root locus technique is presented.

1.4.1 Principles from Liapunov theory

An overview of the principles of Liapunov theory can be found in many text books, for example in Khalil (1996). We recall the main points.

Let $V(x)$ be a real scalar function of the vector x, and let S be a closed bounded region in the x-space, containing the origin.

Definition 1:The function $V(x)$ is positive semi-definite in S if, for all x in S,

(i) $V(x)$ has continuous partial derivatives with respect to the components of the vector x,
(ii) $V(0) = 0$,

(iii) $V(x) \geq 0$

Definition 2:The function $V(x)$ is positive definite in S if, for all x in S,

(i) $V(x)$has continuous partial derivatives with respect to the components of the vector x,
(ii) $V(0) = 0$,
(iii) $V(x) > 0 \quad if\, x \neq 0$

Liapunov stability

Consider the autonomous system

$$\dot{x} = f(x) \tag{1.8}$$

where $f : D \rightarrow R^n$ is a locally Lipschitz map from a domain $D \subset R^n$ into R^n. We suppose that the origin $x = 0$ is an equilibrium point of (1.8), i.e.

$$f(0) = 0$$

Liapunov theory is a fundamental tool for the stability analysis of dynamic systems. The following definitions and theorems are used to characterize and study the stability of the origin which will be a concept to be applied throughout this thesis.

Definition 3 : Stability

The equilibrium point $x = 0$ of the system (1.8) is

- stable, if for each $\epsilon > 0$, there is a $\delta(\epsilon) > 0$ such that

$$|x(0)| < \delta \Rightarrow |x(t)| < \epsilon, \forall t \geq 0$$

The following graph illustrates the concept of a stable condition (Figure 1.9): All trajectories which start inside the ball with radius δ, will stay inside the ball with radius ϵ.

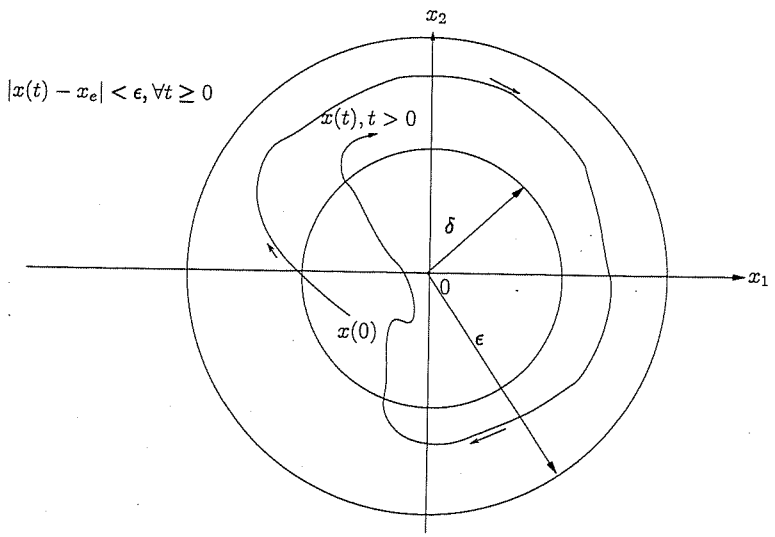

Figure 1.9: Stable equilibrium state $x_e = 0$.

Basically and intuitively stability means the following : If the system has an initial deviation from its equilibrium state, it starts to move. The deviation could be due to a disturbance. The equilibrium state is called stable, if the system does not go far from the equilibrium for small initial deviations.

- unstable, if not stable
- Convergent if there is a $\delta_0 > 0$ such that $|x(0)| < \delta_0 \Rightarrow \lim_{t \to +\infty} x(t) = 0$
- asymptotically stable, if it is stable and convergent

Stability means that if a system is slightly disturbed from its equilibrium state, then the subsequent motions remain in a corresponding small neighbourhood of the equilibrium state. Asymptotic stability requires in addition that after a small perturbation all subsequent motions return to the equilibrium.

The above definitions correspond to local properties of the system around the equilibrium point. The stability concepts become global when the corresponding conditions are satisfied for any initial state:

- asymptotically stable in the large, or globally asymptotically stable, if it is stable, and if every motion converges to the equilibrium state as $t \to +\infty$

The direct method of Liapunov

In general it is not possible to find the solutions of a nonlinear system equation, except numerically. Therefore, methods have been developed to obtain information on the stability behaviour of dynamic systems without requiring analytical expressions of the solutions. Such a technique is the direct method of Liapunov.

Definition 4: Liapunov function

$V(x)$ is called a Liapunov function for the system (1.8) if, in a ball B containing the origin, $V(x)$ is positive definite and if its time derivative along the solutions of (1.8) is negative semi-definite, i.e.

$$\dot{V}(x) = (\frac{\partial V}{\partial x})' f(x) \leq 0$$

The following theorems can be used for the local and global stability analysis of an equilibrium point.

Theorem 1 : Local stability

The equilibrium point $x = 0$ of system (1.8) is (asymptotically) stable if there exist a scalar function $V(x)$ and a ball B containing the origin such that $V(x)$ is positive definite and $\dot{V}(x)$ is negative semi-definite(negative definite) in B.

Theorem 2: Global stability

The equilibrium point $x = 0$ of system (1.8) is globally asymptotically stable if there exists a scalar function $V(x)$ such that over the entire state space $V(x)$ is positive definite, $\dot{V}(x)$ is negative definite and $V(x)$ is radially unbounded, i.e.

$$V(x) \rightarrow +\infty \; as \; |x| \rightarrow \infty$$

Krasovskii-LaSalle's results extend the stability conditions of the previous theorems to the case where $\dot{V}(x)$ is only negative semi-definite. They read as follows:

Invariant set

A set S is an invariant set for a dynamic system if every trajectory starting in S remains in S for all $t \in (-\infty, +\infty)$.
Invariant sets include equilibrium points, limit cycles, as well as any complete trajectory of the system.

LaSalle's invariance principle

Let Ω be a compact (closed and bounded) set with the property that every solution of the system (1.8) that starts in Ω remains in Ω for all future time. Let $V : \Omega \rightarrow R$ be a continuously differentiable function such that $\dot{V}(x) \leq 0$ in Ω.

Let E be the set of all points in Ω where $\dot{V}(x) = 0$. Let M be the largest invariant set in E. Then, every solution starting in Ω approaches M as $t \rightarrow +\infty$.

The following two colloraries extend Theorems 1 and 2.

Collorary 1 : Barbachin-LaSalle

Let $x = 0$ be an equilibrium point for (1.8). Let $V : D \rightarrow R$ be a positive definite function on a neighborhood D of $x = 0$, such that $\dot{V}(x) \leq 0$ in D. Let $S = \{x \in D | \dot{V}(x) = 0\}$, and suppose that no solution can stay in S forever, other than the trivial solution. Then, the origin is asymptotically stable.

Collorary 2 : Krasovskii-LaSalle

Let $x = 0$ be an equilibrium point for (1.8). Let $V : R^n \rightarrow R$ be a radially unbounded, positive definite function such that $\dot{V}(x) \leq 0 \; \forall x \in R^n$. Let $S = \{x \in R^n | \dot{V}(x) = 0\}$, and suppose that no solution can stay in S forever, other other than the trivial solution. Then, the origin is globally asymptotically stable.

When $\dot{V}(x)$ is negative definite then $S = \{0\}$ and Colloraries 1 and 2 coincide with Theorems 1 and 2, respectively.

In discussing the concepts of stability and asymptotic stability, we only assumed that there is some small region about the equilibrium position in which the conditions on $V(x)$ hold.

1.4.2 The linearization principle

It is expected that the stability criteria for linear systems could be applied to nonlinear systems if the deviations from the equilibrium state remain sufficiently small, so that the nonlinearity has only a minor effect. This leads to the linearization principle. For autonomous systems we have (Vidyasagar, 1993), (Willems, 1970) :

Theorem 1: The null solution of the nonlinear system

$$\dot{x} = Ax + h(x) \tag{1.9}$$

with $h(0) = 0$, is asymptotically stable if:

1. $\lim_{|x|\to 0} \frac{|h(x)|}{|x|} = 0$

2. The null solution of the linear system

$$\dot{x} = Ax \tag{1.10}$$

is asymptotically stable, i.e. A is Hurwitz matrix.
(1.10) is called the equation of the first approximation of (1.9) about the origin. The vector function $h(x)$ is the sum of the higher-order terms with respect to $|x|$. If the nonlinear system equation is

$$\dot{x} = f(x) \tag{1.11}$$

with $f(0) = 0$, **then its equation of the first approximation about the** origin is

$$\dot{x} = [\frac{\partial f(x)}{\partial x}]_{x=0} x \tag{1.12}$$

where $\partial f(x)/\partial x$ denotes the Jacobian matrix

$$\frac{\partial f(x)}{\partial x} = \begin{pmatrix} \frac{\partial f_1}{\partial x_1} & \frac{\partial f_1}{\partial x_2} & \cdots & \frac{\partial f_1}{\partial x_n} \\ \frac{\partial f_2}{\partial x_1} & \frac{\partial f_2}{\partial x_2} & \cdots & \frac{\partial f_2}{\partial x_n} \\ \vdots & \vdots & & \\ \frac{\partial f_n}{\partial x_1} & \frac{\partial f_n}{\partial x_2} & \cdots & \frac{\partial f_n}{\partial x_n} \end{pmatrix} \tag{1.13}$$

System (1.12) is also called the linearized system of (1.11) about the origin.

1.4.3 Principles from dissipativity and passivity

For background information on this material we refer to Lozano et al. (2000). The main concepts were developed a.o. by J.C.Willems (1972) and by Hill and Moylan (1976,1980). Consider the nonlinear system

$$\dot{x} = f(x) + g(x)u \tag{1.14}$$
$$y = h(x) + p(x)u \tag{1.15}$$

$x \in R^n$; $u,y \in R^m$; f,g,h,p are smooth, i.e. they are continuous with continuous partial derivatives w.r.t. the components of x. $f(0) = h(0) = 0$. Let us call $w = w(u,y)$ the supply rate, such that $\forall u$, $\forall x(0)$ and $\forall t \geq 0$

$$\int_0^t |w(u(s),y(s))|ds < \infty$$

i.e. $w(u,y)$ is locally integrable.

Definition 1: Dissipative system

The system (1.14), is said to be dissipative if there exists a so called storage function $V(x) \geq 0$, $\forall x$ such that $\forall u$, $\forall x(0)$

$$V(x(t)) - V(x(0)) \leq \int_0^t w(u(s),y(s))ds$$

The latter relationship is called a dissipation inequality. It means that the value of the storage function $V(x(t))$ at a future time t is not larger than the sum of the available $V(x(0))$ at an initial time 0 plus the total energy $\int_0^t w(u(s),y(s))ds$ supplied to the system from the external sources in the interval $[0,t]$. There is no internal generation of energy.
Passive systems represent an important subset of dissipative systems.

Definition 2: Passive system

A system with input u and output y where $u(t), y(t) \in R^m$ is passive if there is a constant β such that

$$\int_0^T y'(t)u(t)dt \geq \beta \tag{1.16}$$

for all input functions $u(t)$ and all $T \geq 0$. If, in addition, there are constants $\delta \geq 0$ and $\epsilon \geq 0$ such that

$$\int_0^T y'(t)u(t)dt \geq \beta + \delta \int_0^T u'(t)u(t)dt + \epsilon \int_0^T y'(t)y(t)dt \tag{1.17}$$

for all input functions $u(t)$ and all $T \geq 0$, then the system is input strictly passive if $\delta > 0$, output strictly passive if $\epsilon > 0$, and very strictly passive if $\delta > 0$ and $\epsilon > 0$.

Obviously $\beta \leq 0$ as the inequality is to be valid for all functions $u(t)$ and in particular the control $u(t) = 0$ for all $t \geq 0$, which gives $0 = \int_0^T y'(t)u(t)dt \geq \beta$.

Theorem 1

Assume that there is a continuous function $V(t) \geq 0$ such that

$$V(T) - V(0) \leq \int_0^T y'(t)u(t)dt - \delta \int_0^T u'(t)u(t)dt - \epsilon \int_0^T y'(t)y(t)dt \quad (1.18)$$

for all input functions $u(t)$ and for all $T \geq 0$. Then, the system is input strictly passive if $\delta > 0$, output strictly passive if $\epsilon > 0$, and very strictly passive if $\delta > 0$ and $\epsilon > 0$.

Consider a real scalar function $f(t)$ which satisfies $f(t) \equiv 0$ for $t < 0$. Define the truncated function

$$\begin{aligned} f_T(t) &= f(t); t \leq T \\ &= 0 \quad ; t > T \end{aligned}$$

where $T > 0$. Let

$$\|f_T\| \triangleq [\int_0^T f^2(t)dt]^{\frac{1}{2}}$$

and let $\mathcal{L}_e$ be the space of functions $f(.)$ for which

$$\|f_T\| < \infty \, ; \, \forall T > 0$$

Definition 3: Finite-gain stability

A system with input $u(.) \in \mathcal{L}_e$ and output $y(.) \in \mathcal{L}_e$ is finite-gain stable if there exists a $k > 0$ such that for all inputs $u(.)$

$$\|y_T\| \leq k\|u_T\|$$

The concept of finite-gain stability is related to the controller design method of H_∞-control for linear systems, which uses the norm

$$\|G(s)\|_\infty \triangleq \max_{u(t) \neq 0} \frac{\|y_T\|}{\|u_T\|}$$

(Skogestad and Postlethwaite, 1996).

There exists an extensive theory on input-output stability of feedback systems (see Glad and Lyung,(2003) and Khalil(1996)) . One result reads as follows :

Theorem 2

Consider the single input-single output feedback loop of Figure 1.10, with forward path and feedback path operators H_1 and H_2. The loop is finite-gain stable, i.e.

$$\|y_T\| \leq k\|u_T\| \; for \; some \; k > 0$$

if either H_1 is passive and H_2 is input strictly passive, or if H_1 is output

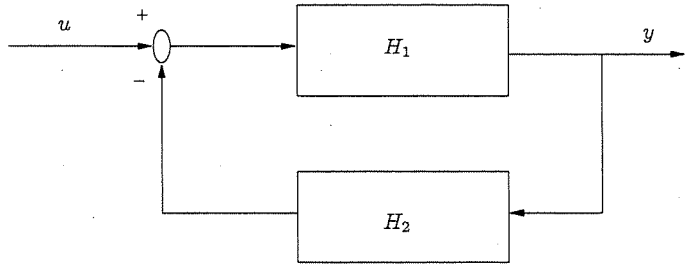

Figure 1.10: A single input-single output feedback system.

strictly passive and H_2 is passive.
The relationship between finite-gain stability and asymptotic stability has been studied by Hill and Moylan (1980).

1.4.4 The Kalman-Yacubovich-Popov main lemma

The Kalman-Yacubovich-Popov (KYP) lemma is a cornerstone in modern control theory. Its significance in linear-quadratic optimization and nonlinear stability theory has been exposed in many papers and textbooks, e.g. in J.C. Willems (1971), Vidyasagar(1993), Lozano et al.(2000). The lemma establishes an equivalence between conditions in the frequency domain on certain

matrix functions related to the dynamical behaviour of systems, and certain input-output relationships of the system in the time domain, and conditions on the matrices describing the state space representation of the system.

We will use this lemma to prove the existence of Liapunov functions or the validity of passivity properties which ensure the stability of a closed-loop system describing the dynamics of a feedback controlled CSTR.

In this thesis we use the following version of the KYP-lemma :
Assume given :

$A \in R^{n\times n}$; *Hurwitz*
$R \in R^{n\times n}$; $R = R' \geq 0$
$B \in R^{n\times m}$; (A, B) *controllable*; $m \leq n$
$H \in R^{n\times m}$; (A, H') *observable*
$T \in R^{m\times m}$
$\varepsilon \in R$; $\varepsilon \geq 0$
$\gamma \in R$; $\gamma \geq 0$

Consider the system of algebraic equations

$$\begin{aligned} PA + A'P &= -QQ' - \varepsilon I - \gamma R && (1.19)\\ QT &= PB - H && (1.20)\end{aligned}$$

The system (1.19),(1.20) has a real solution $P = P' > 0$, $Q \in R^{n\times m}$, $\varepsilon = 0$, $\gamma = 0$ if

$$T'T + 2He[H'(j\omega I - A)^{-1}B] > 0, \ \forall \omega \in R \qquad (1.21)$$

The system (1.19),(1.20) has a real solution $P = P' > 0$, $Q \in R^{n\times m}$, $\varepsilon > 0$, **and sufficiently small,** $\gamma = 0$ if in addition to (1.21) :

$$lim_{\omega\to\infty}\omega^2\{T'T + 2He[H'(j\omega I - A)^{-1}B]\} > 0 \qquad (1.22)$$

The system (1.19),(1.20) has a real solution $P = P' > 0$, $Q \in R^{n\times m}$, $\varepsilon = 0$, $\gamma > 0$ if

$$T'T + 2He\{H'(j\omega I - A)^{-1}B - \gamma B'[(j\omega I - A)^{-1}]^* R(j\omega I - A)^{-1}B\}$$

$$> 0 \ for\ all\ real\ \omega \qquad (1.23)$$

Notations :

$P = P' \geq 0$: **symmetric, positive semidefinite**
$P = P' > 0$: **symmetric positive definite**
$\bar{A}$: complex conjugate of A
A' : transpose of A
$A^* = \bar{A}'$ (conjugate transpose)
He A : Hermitian part of A : $HeA = \frac{1}{2}(A + A^*)$
Re A= real part of A : $ReA = \frac{1}{2}(A + \bar{A})$

Special case: m=1

The system (1.19),(1.20) becomes :

$$\begin{aligned} PA + A'P &= -qq' - \varepsilon I - \gamma R; \quad q \in R^n \\ qt &= Pb - h; \quad t \in R; b \in R^n; h \in R^n; \end{aligned}$$

The frequency conditions (1.21),(1.22) and (1.23) become :

$$t^2 + 2Re[h'(j\omega I - A)^{-1}b] > 0, \ \forall \omega \in R \qquad (1.24)$$

$$lim_{\omega\to\infty}\omega^2\{t^2 + 2Re[h'(j\omega I - A)^{-1}b]\} > 0 \qquad (1.25)$$

$$t^2 + 2Re\{h'(j\omega I - A)^{-1}b - \gamma b'[(j\omega I - A)^{-1}]^* R(j\omega I - A)^{-1}b\} > 0 \ for\ all\ real\ \omega \qquad (1.26)$$

1.5 Overview and personal contribution

We give a short overview of the different chapters of the thesis. In Chapter 1 we discuss the problem statement, we present a description of the CSTR, **define the control problem and formulate the problem of stabilization.** We describe the dynamic equations of the process to be controlled. **We briefly survey** the state of the art of the research problem at hand describing some existing stabilization methods applied to a CSTR.

In each one of the Chapters 2 to 6 we discuss the stabilization of the CSTR using Liapunov and/or passivity theory, we compute stability regions under state

or input constraints, we set the parameters of the controller using root locus techniques and we make simulations of transients for the linearized and for the nonlinear dynamics. In Chapters 2-4 we subsequently design single input PD-controllers and two input PD-and PID-controllers. Chapters 5-6 present modified approaches putting more emphasis on the robustness of the solution. In Chapter 7 we give some concluding comments. A flowchart for the thesis is given in Figure 1.11.

One of the main features of some of our algorithms is that they do not require the exact knowledge of the process parameters although the exact knowledge of the dynamical structure is needed. We focus on simplicity, linearity and robustness of the design. The basic objective is the global asymptotic stabilization of the set point. We study both single input and two input control systems. To prove stability we rely on the theories of dissipativity, passivity and of Liapunov. The latter technique allows us to compute stability regions in state space under input and state variable constraints. Parameter tuning is achieved using standard root locus procedures.

Our controller design methods strongly rely on the stability analysis of the closed loop. Stability is the most important condition to be imposed on a control system : Indeed, an unstable control system cannot work. The Kalman-Yacubovich-Popov lemma allows us to express the stability conditions in terms of a frequency domain criterion on the controller's linear component. This approach naturally places the design method in a frequency domain setting, similar to a number of clasical controller design methods such as the Nyquist theorem approach for linear systems and the circle and Popov theorem technique for certain nonlinear systems.

We have recently published most of our results in the scientific literature . We believe the contents of the following six chapters is fully original.

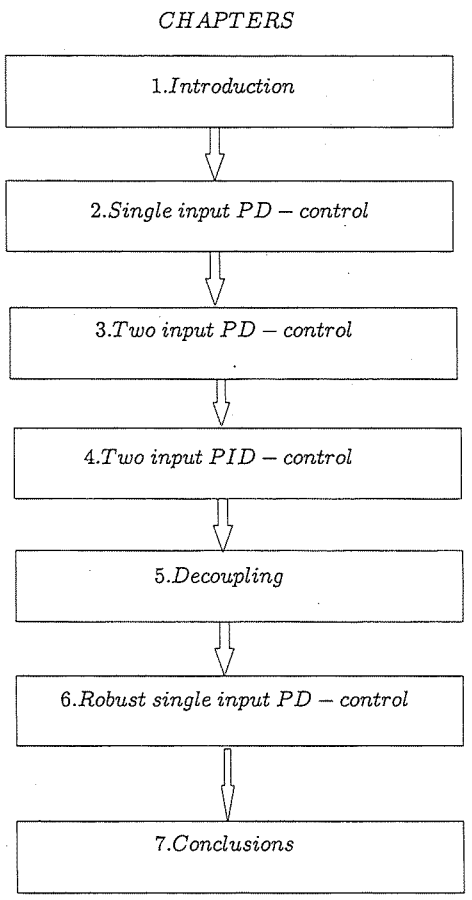

Figure 1.11: Flow chart for the thesis.

Chapter 2

Single input PD-control

In this chapter the stabilization of the chemical stirred tank reactor is investigated using feed temperature (or eventually cooling temperature) as the only input. Stabilization is achieved using linear dynamic output feedback control, ***more specifically PD-control. Conditions are derived under*** *which the closed loop can be modelled as a feedback interconnection of passive components, which allows the design of a simple globally stabilizing feedback law. The control parameters are tuned using a root locus analysis of the linearized system and simulations of the closed loop transients and phase portraits. Besides dissipativity and passivity theory the underlying modelling technique relies on concepts from the direct method of Liapunov. Constraints on the input and states will be taken into account as well. The results are new and have been published in* ***(Muñoz, Loccufier and Noldus, 2003a)***

2.1 Open loop process dynamics and control law

As has been explained in Chapter 1, the problem we are discussing is the design of a multivariable process control system. The two inputs are proportional to feed temperature and feed concentration respectively while the two outputs are given by the reactor temperature and the concentration of the product inside the reactor.

First we will control the CSTR using only the feed temperature $\Delta T_0(t)$ as the **input, setting the feed concentration variations** $\Delta C_0(t)$ equal to zero in our **analysis** ($\Delta C_0(t)$ can also be taken as a disturbance).

In this chapter a PD controller for the CSTR is tuned. Good values for the PD controller parameters are determined and tested in closed loop simulations with both the nonlinear plant and the linearized version. We **have redefined** the state variables as deviations from the set point values (See (1.6), (1.7)) where x_1 and x_2 correspond to deviation variables, while z_{1s} and z_{2s} are the set point's equilibrium values corresponding to the input $u(t) \equiv 0$. When the system is in the stationary condition there are no deviations, so, $x_1 = x_2 = 0$, and $\dot{x}_1 = \dot{x}_2 = 0$. Letting $u_2 = \frac{\Delta C_0(t)}{C_0} \equiv 0$ the reactor equations look as :

$$\dot{x} = Ax - b\left[f_1(c'x) + f_2(c'x)g'x\right] + du_1 \tag{2.1}$$

with

$$x \triangleq \begin{bmatrix} x_1 \\ x_2 \end{bmatrix}, A \triangleq \begin{bmatrix} -(1+\vartheta) & 0 \\ 0 & -1 \end{bmatrix},$$
$$b \triangleq \begin{bmatrix} -m_2 \\ m_1 \end{bmatrix}, c = d \triangleq \begin{bmatrix} 1 \\ 0 \end{bmatrix},$$
$$g \triangleq \begin{bmatrix} 0 \\ 1 \end{bmatrix},$$

$f_1(y) \triangleq [f(y + c'z_s) \;\; -f(c'z_s)]\, g'z_s$ and $f_2(y) \triangleq f(y + c'z_s)$,
with $f(y) \triangleq exp(-\frac{10^4}{y})$

From the state equations (2.1) we obtain:

$$m_1\dot{x}_1 + m_2\dot{x}_2 = -m_1(1+\vartheta)x_1 - m_2x_2 + m_1u_1 \tag{2.2}$$

Let us apply a control law given by

$$\begin{aligned} u_1(t) &= \frac{1}{m_1}[(m_1 + m_1\vartheta + \alpha)x_1 + (m_1 + \beta)\dot{x}_1 + m_2\dot{x}_2] \\ &= (1 + \vartheta + \frac{\alpha}{m_1})x_1 + (1 + \frac{\beta}{m_1})\dot{x}_1 + \frac{m_2}{m_1}\dot{x}_2 \end{aligned} \tag{2.3}$$

α and β are the controller parameters which will be adjusted in order to obtain good closed loop stability properties, i.e. good transient responses or interesting regions of attraction in state space. This special control structure is proposed in order to fulfil the passivity requirements of the system. That is because passivity theory is used in the controller design. In other words this control law is used with the purpose of obtaining a controller which guarantees a forward and feedback passive system.

For practical implementation it is needed to measure the states x_1 and x_2. The temperature (x_1) can be measured easily, however most of the time the concentration (x_2) cannot be measured. Then it could be necessary to design an observer. For the set point being globally asymptotically stable it will be necessary to select $\alpha > 0$ and $\beta > 0$.

2.2 Closed loop stability analysis

We are studying the equilibrium point $x = 0$ of (2.1) and (2.3) instead of the original set point $z = z_s$.
Substituting (2.3) into (2.2) yields:

$$\beta\dot{x}_1 + \alpha x_1 - m_2 x_2 = 0 \tag{2.4}$$

while the second equation of (2.1) becomes

$$\dot{x}_2 = -x_2 - m_1[f_1(c'x) + f_2(c'x)g'x] \tag{2.5}$$

Combining (2.4) and (2.5) then produces the closed loop dynamics:

$$\dot{x} = A_0 x - b_0\left[\hat{f}_1(c'x) + \hat{f}_2(c'x)c'\dot{x}\right] \tag{2.6}$$

where

$$A_0 \triangleq \begin{bmatrix} -\frac{\alpha}{\beta} & \frac{m_2}{\beta} \\ 0 & -1 \end{bmatrix}, \; b_0 \triangleq \begin{bmatrix} 0 \\ 1 \end{bmatrix} c \triangleq \begin{bmatrix} 1 \\ 0 \end{bmatrix}$$

$\hat{f}_1(y) \triangleq m_1 z_{2s}[f(y + z_{1s}) - f(z_{1s})] + \frac{m_1\alpha}{m_2} y f(y + z_{1s})$
$\hat{f}_2(y) \triangleq \frac{m_1\beta}{m_2} f(y + z_{1s})$

2.2.1 Closed loop stability analysis using passivity theory

The system (2.6) can be represented by the block diagram of Figure 2.1a which, for any $\alpha_0 \geq 0$ is equivalent to the diagram of Figure 2.1b.

The component in the forward path is linear with transfer function:

$$H(s) = c'(sI - A_0)^{-1}b_0 = \frac{m_2}{(\beta s + \alpha)(s + 1)} \tag{2.7}$$

Note that (A_0, b_0, c) is a controllable and observable triple. Now it is readily

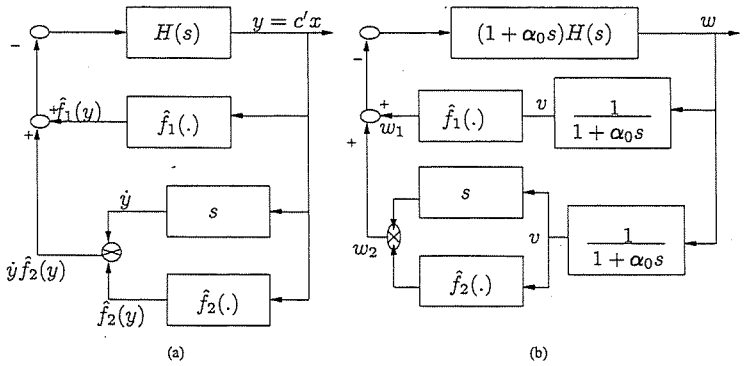

Figure 2.1: Block diagram of the system (2.6).

verified that $(1 + \alpha_0 s)H(s)$ is strictly positive real (Lozano et al.,2000), i.e. A_0 is Hurwitz,

$$\mathrm{Re}(1 + \alpha_0 j\omega)H(j\omega) > 0 \quad ; \quad \forall\omega \in R \tag{2.8}$$

and

$$\lim_{\omega^2 \to \infty} \omega^2 \mathrm{Re}(1 + \alpha_0 j\omega)H(j\omega) > 0 \tag{2.9}$$

if $\alpha > 0$, $\beta > 0$ and α_0 is selected such that $\alpha_0 \geq \beta/(\alpha + \beta)$. Hence the forward path in the feedback loop of Figure 2.1b is output strictly passive. The feedback

path is a parallel connection of two passive components if

$$y\hat{f}_1(y) > 0 \quad ; \quad \forall y \in R, \quad y \neq 0 \tag{2.10}$$

and

$$\hat{f}_2(y) > 0 \quad ; \quad \forall y \in R \tag{2.11}$$

Indeed, for every input $w(t) = v(t) + \alpha_0 \dot{v}(t)$ applied to these components at $t = 0$,

$$\begin{aligned} \int_0^{+\infty} w_1(t)w(t)dt &= \\ \int_0^{+\infty} \hat{f}_1(v)(v + \alpha_0 \dot{v})dt &\geq 0 \end{aligned} \tag{2.12}$$

$$\begin{aligned} \int_0^{+\infty} w_2(t)w(t)dt &= \\ \int_0^{+\infty} \hat{f}_2(v)\dot{v}(v + \alpha_0 \dot{v})dt &\geq 0 \end{aligned} \tag{2.13}$$

The finite gain stability of the closed loop then results from Theorem 2, p.28-29 (Fantoni and Lozano (2002)). Note that in the chemical reactor model $\hat{f}_1(y)$ and $\hat{f}_2(y)$ satisfy the conditions (2.10), (2.11).

2.2.2 Closed loop stability analysis using Liapunov theory

Alternatively the global asymptotic stability of the equilibrium state $x = 0$ in state space can be verified using a candidate Liapunov function of the form :

$$\begin{aligned} V(x) \triangleq\ & x'Px + \alpha_0 \int_0^{c'x} \hat{f}_1(\theta)d\theta \\ & + \int_0^{c'x} \hat{f}_2(\theta)\theta d\theta \end{aligned} \tag{2.14}$$

Rewrite the closed loop as:

$$\dot{x} = A_0 x - b_0 f_0(x, \dot{x}) \tag{2.15}$$

with

$$f_0(x, \dot{x}) \triangleq \hat{f}_1(c'x) + \hat{f}_2(c'x)c'\dot{x}$$

The derivative of (2.14)) along the solutions of (2.6) is

$$\dot{V}(x) = \dot{x}'Px + x'P\dot{x} + \alpha_0 \hat{f}_1(c'x)c'\dot{x} + \hat{f}_2(c'x)c'xc'\dot{x} \tag{2.16}$$

Taking into account that

$$\begin{aligned} \dot{x}'Px &= [\ x'A_0' - b_0' f_0(x, \dot{x})\ ]Px = x'A_0'Px - x'Pb_0 f_0(x, \dot{x}) \\ x'P\dot{x} &= x'P[\ A_0 x - b_0 f_0(x, \dot{x})\ ] = x'PA_0 x - x'Pb_0 f_0(x, \dot{x}) \\ \alpha_0 \hat{f}_1(c'x)c'\dot{x} &= \alpha_0 [\ f_0(x, \dot{x}) - \hat{f}_2(c'x)c'\dot{x}\ ]c'[\ A_0 x - b_0 f_0(x, \dot{x})\ ] \end{aligned}$$

we find

$$\begin{aligned} \dot{V}(x) \ =\ & x'[PA_0 + A_0'P]x - x'[2Pb_0 - A_0'c\alpha_0]f_0(x, \dot{x}) \\ & -\alpha_0 c'b_0 f_0^2(x, \dot{x}) - \alpha_0 \hat{f}_2(c'x)(c'\dot{x})^2 + \hat{f}_2(c'x)c'xc'\dot{x} \end{aligned} \tag{2.17}$$

Rewrite (2.17) in the simpler form

$$\begin{aligned} \dot{V}(x) &= -[q'x + tf_0(x, \dot{x})]^2 - c'x\hat{f}_1(c'x) - \alpha_0 \hat{f}_2(c'x)(c'\dot{x})^2 && (2.18) \\ &= -[q'x + tf_0(x, \dot{x})][q'x + tf_0(x, \dot{x})] - c'x\hat{f}_1(c'x) \\ &\quad -\alpha_0 \hat{f}_2(c'x)(c'\dot{x})^2 \\ &= -x'qq'x - 2x'qtf_0(x, \dot{x}) - t^2 f_0^2(x, \dot{x}) - c'x\hat{f}_1(c'x) - \\ &\quad \alpha_0 \hat{f}_2(c'x)(c'\dot{x})^2 && (2.19) \\ &= -x'qq'x - x'[2qt + c]f_0(x, \dot{x}) - t^2 f_0^2(x, \dot{x}) \\ &\quad -\alpha_0 \hat{f}_2(c'x)(c'\dot{x})^2 + \hat{f}_2(c'x)c'x(c'\dot{x}) && (2.20) \end{aligned}$$

Comparing (2.17) and (2.20) we obtain the conditions

$$\begin{aligned} t^2 &= \alpha_0 c'b_0 && (2.21) \\ PA_0 + A_0'P &= -qq' && (2.22) \\ 2Pb_0 - A_0'c\alpha_0 &= 2qt + c && (2.23) \end{aligned}$$

By an application of the KYP-lemma the system (2.21)→(2.23) has a real solution $P = P' > 0$, $q \in R^2$, $t \in R$ if

$$\alpha_0 c'b_0 + Re(c' + \alpha_0 c'A_0)(j\omega I - A_0)^{-1}b_0 > 0;\ \forall \omega \in R$$

Using the identity

$$sc'(sI - A_0)^{-1}b_0 \equiv c'b_0 + c'A_0(sI - A_0)^{-1}b_0$$

this can be transformed to the condition (2.8) which is satisfied for $\alpha > 0, \beta > 0$ and $\alpha_0 \geq \frac{\beta}{\alpha+\beta}$.

Note that for the present application $c'b_0 = 0$, hence t=0. Now $V(x)$ is positive definite and radially unbounded while $\dot{V}(x)$ is negative semidefinite. Furthermore because of the observability of A_0, c the largest invariant subset of the closed loop state space where $\dot{V}(x) \equiv 0$ consists of the set point $x = 0$. By Collorary 2, p.25 (Fantoni and Lozano (2002)), the origin is globally asymptotically stable.

Now we compute the Liapunov function $V(x)$ which will be used later on to find regions of attraction for the system under control and/or state constraints.

Let

$$P = \begin{bmatrix} p_1 & p_2 \\ p_2 & p_3 \end{bmatrix}, \; q = \begin{bmatrix} q_1 \\ q_2 \end{bmatrix},$$

Note that

$$Pb_0 = \begin{bmatrix} p_2 \\ p_3 \end{bmatrix}, \; A_0'c\alpha_0 + c = \begin{bmatrix} -\frac{\alpha}{\beta}\alpha_0 + 1 \\ \frac{m_2}{\beta}\alpha_0 \end{bmatrix}$$

From these expressions we can compute p_2 and p_3:

$$p_2 = 1/2[1 - \frac{\alpha}{\beta}\alpha_0] \tag{2.24}$$

$$p_3 = \frac{m_2}{2\beta}\alpha_0 \tag{2.25}$$

To compute p_1 (2.22) is expanded as

$$\begin{bmatrix} p_1 & p_2 \\ p_2 & p_3 \end{bmatrix}\begin{bmatrix} -\frac{\alpha}{\beta} & \frac{m_2}{\beta} \\ 0 & -1 \end{bmatrix} + \begin{bmatrix} -\frac{\alpha}{\beta} & 0 \\ \frac{m_2}{\beta} & -1 \end{bmatrix}\begin{bmatrix} p_1 & p_2 \\ p_2 & p_3 \end{bmatrix} = -\begin{bmatrix} q_1^2 & q_1q_2 \\ q_2q_1 & q_2^2 \end{bmatrix} \tag{2.26}$$

Equating the corresponding terms in (2.26) we get

$$-\frac{2\alpha}{\beta}p_1 = -q_1^2 \tag{2.27}$$

$$\frac{m_2}{\beta}p_1 - (1 + \frac{\alpha}{\beta})p_2 = -q_1q_2 \tag{2.28}$$

$$-\frac{2m_2}{\beta}p_2 - 2p_3 = -q_2^2 \tag{2.29}$$

Combining (2.24), (2.25) and (2.29) we obtain

$$q_2^2 = \frac{m_2}{\beta}\left[\; \alpha_0 + \tfrac{\alpha}{\beta}\alpha_0 - 1 \;\right] \geq 0 \tag{2.30}$$

In order to satisfy (2.30) we need the relationship between the controller tuning parameters:

$$\alpha_0(1 + \frac{\alpha}{\beta}) \geq 1 \Rightarrow \alpha_0 \geq \frac{\beta}{(\alpha+\beta)} \tag{2.31}$$

Note that if $q = \begin{bmatrix} q_1 \\ q_2 \end{bmatrix}$ satisfies the equation (2.22) then $q = \begin{bmatrix} -q_1 \\ -q_2 \end{bmatrix}$ also satisfies (2.22). Therefore without loss of generality we take

$$q_2 = \sqrt{\frac{m_2}{\beta}[\alpha_0(1 + \frac{\alpha}{\beta}) - 1]} \tag{2.32}$$

Finally from (2.27) and (2.28) we can compute q_1 and p_1. Remember that we must have $P = P' > 0$, hence

$$p_1 > 0 \quad ; \quad p_1p_3 - p_2^2 > 0$$

Therefore take

$$q_1 = -\sqrt{\frac{\alpha}{m_2}}[\sqrt{\frac{\alpha}{\beta}[\alpha_0(1 + \frac{\alpha}{\beta}) - 1]} \mp 1] \tag{2.33}$$

$$p_1 = \frac{\beta}{2m_2}[\sqrt{\frac{\alpha}{\beta}[\alpha_0(1 + \frac{\alpha}{\beta}) - 1]} \mp 1]^2 \tag{2.34}$$

We have two values for p_1. So we must verify if both values satisfy $p_1p_3 - p_2^2 > 0$

Using (2.24), (2.25) and (2.34) we get

$$p_1p_3 - p_2^2 = \alpha_0[\sqrt{\frac{\alpha}{\beta}[\alpha_0(1 + \frac{\alpha}{\beta}) - 1]} \pm 1]^2 - [1 - \frac{\alpha}{\beta}\alpha_0]^2 > 0 \tag{2.35}$$

$$\alpha_0^2\frac{\alpha}{\beta} + \underbrace{[\alpha_0(1 + \frac{\alpha}{\beta}) - 1]}_{\geq 0} \pm 2\alpha_0\sqrt{\frac{\alpha}{\beta}\underbrace{[\alpha_0(1 + \frac{\alpha}{\beta})}_{\geq 1} - 1]} > 0 \tag{2.36}$$

or

$$\left[\alpha_0 \sqrt{\tfrac{\alpha}{\beta}} \pm \sqrt{\alpha_0(1+\tfrac{\alpha}{\beta})-1} \right]^2 > 0 \qquad (2.37)$$

which is satisfied. In this way we have proved that both p_1-values fulfill the requirement. The Liapunov function (2.14) can be expressed as

$$V(x) = p_1 x_1^2 + 2p_2 x_1 x_2 + p_3 x_2^2 + \alpha_0 \int_0^{x_1} \hat{f}_1(\theta) d\theta + \int_0^{x_1} \hat{f}_2(\theta)\theta d\theta \qquad (2.38)$$

with the parameter values as obtained above.

Direct correlations between the frecuency response and the corresponding transient response characteristics are somewhat tenuous, so we have systematically used the frequency domain approach. We have used some design criteria that will normally result in a satisfactory transient response. Specifically we have used the frequency domain conditions resulting from the Kalman-Yacubovich-Popov Lemma and from passivity theory. But at the end we evaluate the controllers's yield by examining the time characteristics. Also we decided to use the root locus technique as a performance analysis tool because of its simplicity.

As a conclusion every PD-controller of the form (2.3) globally stabilizes the system's set point if the design parameters α and β are chosen positive. The feedback law (2.3) endows the controller with some robustness since the ratio $\frac{m_2}{m_1} = 10^4(-\Delta H)C_0 R/\rho c_p E$ is the only model parameter that must be accurately known. The robustness issue will be further examined in Chapters 5→ 7.

2.3 Phase portrait simulation

In this section we make some computer simulations of both the uncontrolled and the controlled system for two reactors examples taken from the literature (Loccufier and Noldus, 1994), (Genesio, Tartaglia and Vicino, 1985). In each case the uncontrolled reactor possesses three equilibrium points : a stable node z_n, a saddle point z_s and a stable focus z_f. The diagrams of Figures 2.2 and 2.3 show a phase portrait of the uncontrolled(open loop) dynamics in the state plane.

After the PD-controller has been designed, satisfactory choices for α and

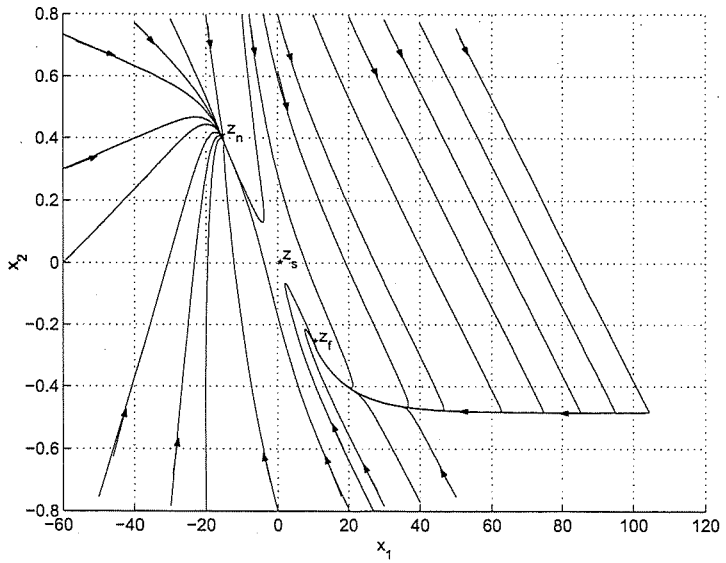

Figure 2.2: Example 1: phase portrait of an uncontrolled reactor model (Loccufier and Noldus, 1994) with parameters values : $m_1 = 1.7685.10^{15}$, $m_2 = 7.8041.10^{16}$, $r = 301.2696$, $\vartheta = 0.1356$.

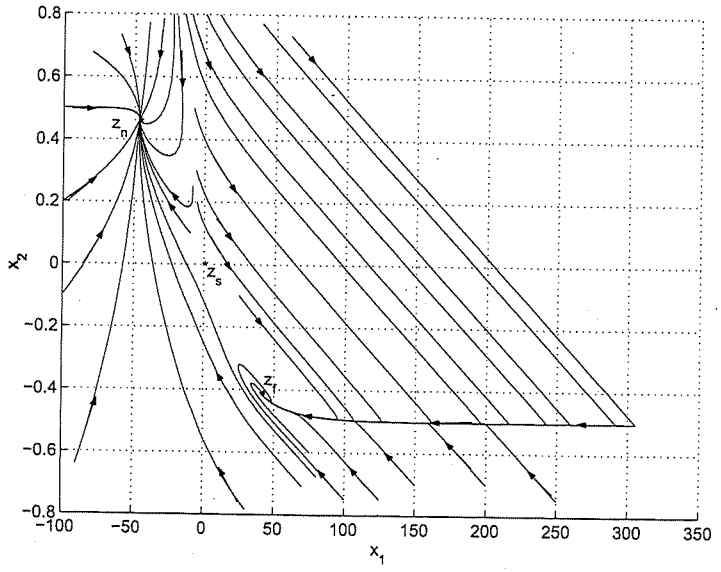

Figure 2.3: Example 2: phase portrait of an uncontrolled reactor model (Genesio, Tartaglia and Vicino, 1985) with parameters values : $m_1 = e^{25}$, $m_2 = 200e^{25}$, $r = 700$, $\vartheta = 1$.

β lead us to the corresponding closed loop phase portraits displayed in Figures 2.4a and 2.4b. The controller stabilizes the equilibrium point z_s while

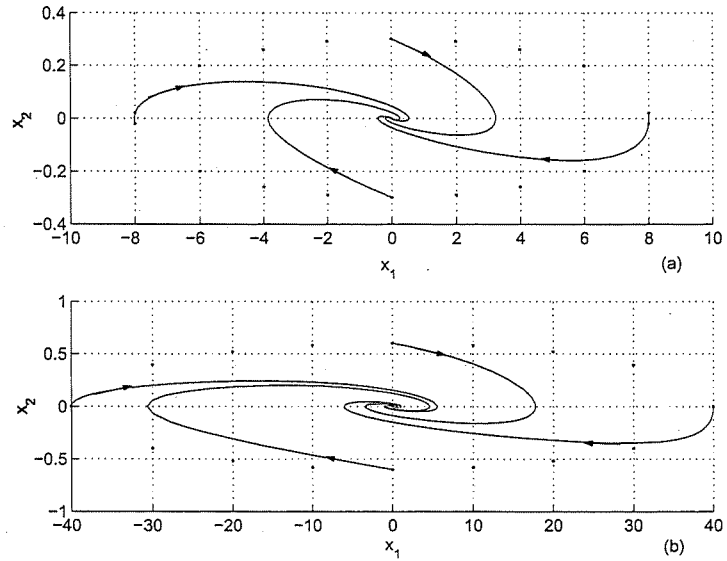

Figure 2.4: Phase portrait of the controlled reactor in deviation variables. (a) Example 1: $\alpha = 1.08.10^{12}$, $\beta = 2.10^{15}$. (b) Example 2: $\alpha = 9.44.10^{7}$, $\beta = 1.10^{11}$

the equilibria z_n and z_f disappear in closed loop. After closing the loop the selected set point z_s becomes globally asymptotically stable.

Below we present computer simulations of the closed loop dynamics for the two examples. The behaviour of the nonlinear transients are shown in Figure 2.5 and Figure 2.6 which represent step response diagrams resulting from a change of set point. At $t = 0$ the reactor is in equilibrium at the initial point $x(0)$. For $t > 0$ the reactor moves from this equilibrium point to the new set point $x = 0$. Since the system is nonlinear the transients will vary in shape when the magnitude of the input step changes.

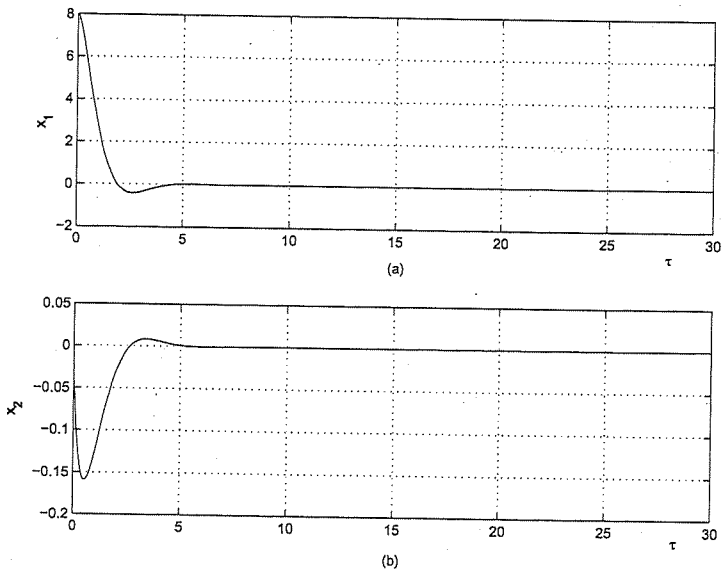

Figure 2.5: Transient response of the controlled reactor of Example 1, for initial values $x_1(0) = 8$; $x_2(0) = 0$: (a) Reactor temperature response; (b)Reactor concentration response.

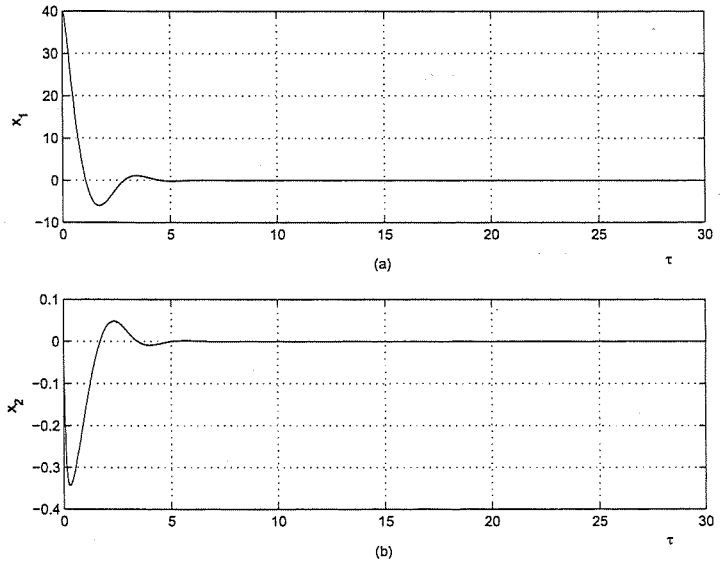

Figure 2.6: Transient response of the controlled reactor of Example 2, for initial values $x_1(0) = 40$; $x_2(0) = 0$: (a) Reactor temperature response; (b)Reactor concentration response.

Choosing various initial states $x(0)$ on ellipses around the set point reveals that the response becomes strongly nonlinear for initial states with $|x_1|_{max} > 4$; $|x_2|_{max} > 0.15$ in Example 1 and $|x_1|_{max} > 8$; $|x_2|_{max} > 0.2$ in Example 2.

2.4 Control parameter tuning

In this section we illustrate the technique used for tuning the PD-controller. First, the system is represented in its linearized version and the characteristic equation is obtained. Then the root locus technique is applied for parameter tuning. Finally we show some simulations in closed loop for each of the examples.

2.4.1 Linearized dynamics in the set point

Using a Taylor series expansion the linearization of (2.4) and (2.5) about the set point yields :

$$\dot{x}_1 = -\frac{\alpha}{\beta}x_1 + \frac{m_2}{\beta}x_2 \tag{2.39}$$

$$\dot{x}_2 = -a_0 x_1 - (1 + b_{0l})x_2 \tag{2.40}$$

with

$$a_0 \triangleq m_1 \frac{df_1(\sigma)}{d\sigma}|_{\sigma=0} = m_1 x_{2s} \frac{10^4}{x_{1s}^2} e^{\frac{-10^4}{x_{1s}}} > 0; \tag{2.41}$$

$$b_{0l} \triangleq m_1 f_2(0) = m_1 e^{\frac{-10^4}{x_{1s}}} > 0$$

In vector form we have:

$$\dot{x} = A_c x \tag{2.42}$$

$$A_c \triangleq \begin{bmatrix} -\frac{\alpha}{\beta} & \frac{m_2}{\beta} \\ -a_0 & -(1 + b_{0l}) \end{bmatrix} \tag{2.43}$$

Now we can see the difference between the linearized and the nonlinear system. The nonlinear closed loop version of the system is represented by

$$\dot{x} = A_c x + \begin{bmatrix} 0 \\ 1 \end{bmatrix} \hat{f}_0(x_1, x_2) \tag{2.44}$$

where the nonlinear term $\hat{f}_0(x_1, x_2)$ corresponds to terms of higher degree in $|x|$:

$$\hat{f}_0(x_1, x_2) \triangleq \begin{matrix} -m_1 f_1(x_1) + a_0 x_1 \\ -m_1 f_2(x_1)x_2 + b_{0l}x_2 \end{matrix} \tag{2.45}$$

If we divide the modulus of the nonlinear part by the modulus of the linear one it is possible to establish if the nonlinearities are important enough or not for the response: Consider the maximum of

$$\frac{|\hat{f}_0(x_1, x_2)|}{|A_c x|} \tag{2.46}$$

on the perimeter C of an ellipse around the equilibrium. If this value does not exceed say 1% the conclusion is that the nonlinearities have a small effect on the total response and the system behaves as a linear system in the interior of the ellipse(Glad and Lyung, 2003). In this way we can expect the nonlinear system to have almost the same phase plane as the linear part close to the equilibrium, since $f_0(x_1, x_2)$ is very small compared to $A_c x$ there. This can be observed in Figures 2.19 and Figure 2.20.

2.4.2 Characteristic equation

There are several methods to tune an industrial PID controller, among them the Ziegler-Nichols method which permits to find suitable controller gains when we know the model of the process. In our case we have designed a globally stabilizing PD controller of the form (2.3) using a nonlinear process model. Below a method based on root locus theory (See Ogata, 1998) is proposed for tuning the parameters α and β.

From (2.43) the characteristic roots of the system are found putting

$$det(sI - A_c) = det \begin{bmatrix} s + \frac{\alpha}{\beta} & -\frac{m_2}{\beta} \\ a_0 & s + 1 + b_{0l} \end{bmatrix} = 0 \tag{2.47}$$

Solving the determinant we get the characteristic equation:

$$\beta s^2 + (\beta + \beta b_{0l} + \alpha)s + \alpha(1 + b_{0l}) + a_0 m_2 = 0 \tag{2.48}$$

For the two examples from the literature the physical parameters are.

	m_1	m_2	r	ϑ	a_0	b_{0l}
Example1	$1.7685.10^{15}$	$7.8041.10^{16}$	301.2696	0.1356	0.0634	1.0672
Example2	e^{25}	$200e^{25}$	700	1	0.0313	1

Let the characteristic roots be $s = \lambda_1$, $s = \lambda_2$. Then

$$\lambda_1\lambda_2 = \frac{\alpha(1+b_{0l}) + a_0 m_2}{\beta} > 0$$

$$\lambda_1 + \lambda_2 = -\frac{(\beta + \beta b_{0l} + \alpha)}{\beta} < 0$$

Hence both of the roots lie in the open left half plane :

$$Re(\lambda_1) < 0 \quad ; \quad Re(\lambda_2) < 0$$

2.4.3 Root locus plot

Let us write (2.48) as :

$$\beta s^2 + (\beta + \beta b_{0l})s + a_0 m_2 + \alpha(s + 1 + b_{0l}) = 0 \qquad (2.49)$$

$$0 < \alpha < +\infty \qquad (2.50)$$

We examine the root locus plots of (2.49), (2.50) for some positive values of β using both examples. This allows us to study the influence of α on the closed loop eigenvalue spectrum of the linearized dynamics. (2.49), (2.50) is seen as the characteristic equation of the linear system represented in the graph of Figure 2.7:
Next we write (2.48) as :

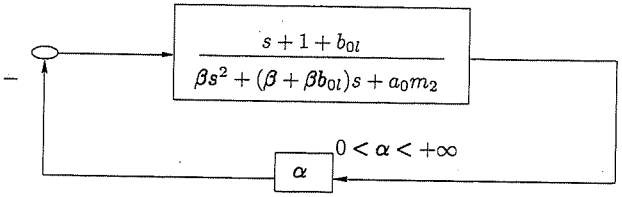

Figure 2.7: Effect of the parameter α on the location of the closed loop poles

$$s^2 + (1 + b_{0l})s + \frac{1}{\beta}[\alpha s + \alpha(1 + b_{0l}) + a_0 m_2] = 0 \qquad (2.51)$$

$$0 < \frac{1}{\beta} < +\infty \qquad (2.52)$$

We repeat the same procedure as before for some fixed positive values of α. So we can study the influence of β on the closed loop eigenvalue spectra of the linearized dynamics. A block diagram representing this case is presented in Figure 2.8. By analyzing the different spectrums for the two examples we can

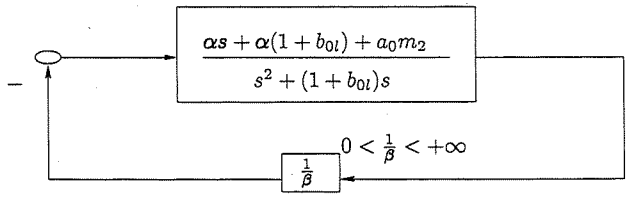

Figure 2.8: Effect of the parameter $\frac{1}{\beta}$ on the location of the closed loop poles

adjust the values for the parameters α and β to give the best behaviour of the closed loop response.

Finally we can use these values for the simulation of both the linearized and the nonlinear process.

Still another approach is to write (2.48) as:

$$(s + \frac{\alpha}{\beta})(s + 1 + b_{0l}) + \frac{m_2}{\beta} a_0 = 0 \qquad (2.53)$$

where $a_0 > 0$, $b_{0l} > 0$ and $m_2 > 0$ are process parameters while $\frac{\alpha}{\beta}$ and $\frac{1}{\beta}$ are the control parameters. We consider the root locus of (2.53) for a given value of $\frac{\alpha}{\beta}$ and for $0 < \frac{1}{\beta} < +\infty$:
The system has two closed loop poles. Each of them approaches an asymptote as $\frac{1}{\beta} \to +\infty$. The system shows stability for all positive values of the gain $\frac{1}{\beta}$(see Figures 2.9, 2.10). The break point can be computed as:

$$\frac{1}{s + \frac{\alpha}{\beta}} + \frac{1}{s + 1 + b_{0l}} = 0$$

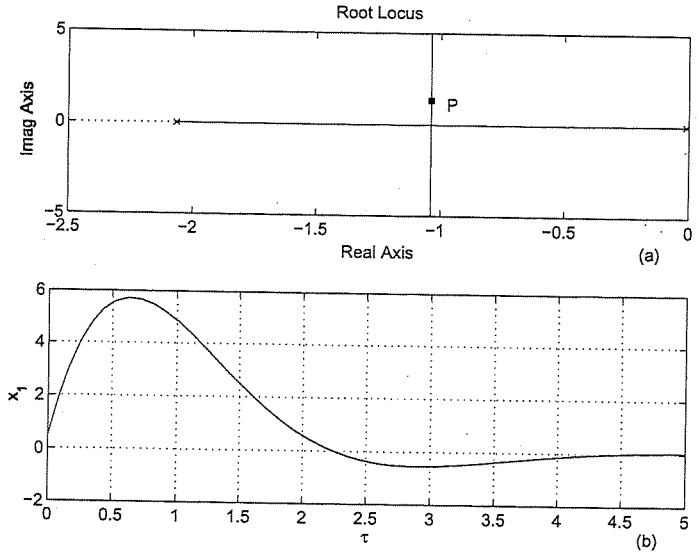

Figure 2.9: Influence of $1/\beta$ on the closed loop characteristic values for Example 1. $\frac{\alpha}{\beta} = 0.01$, $\frac{1}{\beta} = 6.10^{-16}$, break point at $s = -1.04$

$$\Rightarrow s = -\frac{1}{2}[\frac{\alpha}{\beta} + 1 + b_{0l}]$$

We can write the characteristic equation as :

$$s^2 + [1 + b_{0l} + \frac{\alpha}{\beta}]s + \frac{\alpha}{\beta}(1 + b_{0l}) + \frac{m_2}{\beta}a_0 = 0 \qquad (2.54)$$

The linearized system dynamics we are working with correspond to a second order system. The transfer function of such a system has the form.

$$G(s) = \frac{k\omega_n^2}{s^2 + 2\zeta\omega_n s + \omega_n^2}$$

where the meaning of the symbols is :
k : static gain
ω_n: undamped natural frequency.

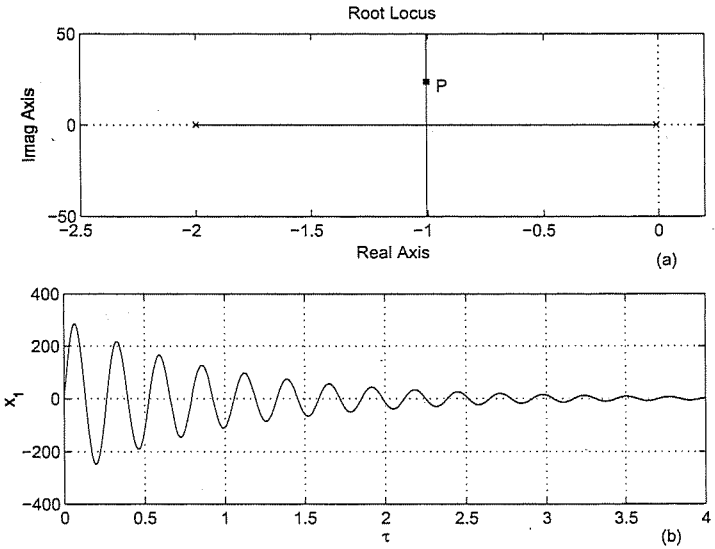

Figure 2.10: Influence of $1/\beta$ on the closed loop characteristic values for Example 2. $\frac{\alpha}{\beta} = 0.01$, $\frac{1}{\beta} = 1.2529.10^{-9}$, break point at $s = -1$

ζ:damping factor.

For $\zeta < 1$ the transient response to the initial conditions (Golten and Verwer, 1999) has the form :

$$y(t) = y_0 e^{-\zeta\omega_n t} cos(\omega_d t + \theta) \qquad (2.55)$$

where $\omega_d \triangleq \sqrt{1-\zeta^2}\omega_n$ is the damped natural frequency.

The decay ratio is the ratio of two consecutive positive/negative peaks :

$$\text{decay ratio} = e^{\frac{-2\pi\zeta}{\sqrt{1-\zeta^2}}}$$

The absolute exponent of this expression is called the logarithmic decrement.

The percentage overshoot is related to the above expression :

$$overshoot = 100e^{\frac{-\pi\zeta}{\sqrt{1-\zeta^2}}}$$

The settling time is the time for the exponential envelope to decay to within a set tolerance band. This is directly related to the exponential decay factor in the transient response:

$$e^{\sigma t} = e^{-\zeta\omega_n t}$$

Similar to the case of a first order system the 5% settling time is:

$$t_s \approx 3\tau = \frac{3}{-\sigma} = \frac{3}{\zeta\omega_n}$$

Comparison with the standard second order characteristic equation for a second order system yields:

$$s^2 + 2\zeta\omega_n s + \omega_n^2 = 0 \qquad (2.56)$$

$$\omega_n = \sqrt{\frac{\alpha}{\beta}(1+b_{0l}) + \frac{m_2}{\beta}a_0}$$

$$\zeta = \frac{1}{2}\frac{[1+b_{0l}+\frac{\alpha}{\beta}]}{\sqrt{\frac{\alpha}{\beta}(1+b_{0l})+\frac{m_2}{\beta}a_0}}$$

This gives us the following properties of the closed loop behaviour :

- Oscillatory response if $\zeta < 1$

$$[1+b_{0l}+\frac{\alpha}{\beta}] < 2[\sqrt{\frac{\alpha}{\beta}(1+b_{0l})+\frac{m_2}{\beta}a_0}]$$

which is equivalent with

$$\frac{1}{\beta} > \frac{1}{4a_0m_2}[1+b_{0l}-\frac{\alpha}{\beta}]^2 \qquad (2.57)$$

- Non-oscillatory response if,

$$\frac{1}{\beta} < \frac{1}{4a_0m_2}[1+b_{0l}-\frac{\alpha}{\beta}]^2 \qquad (2.58)$$

2.4.4 Time response simulations

Figure 2.11 and Figure 2.12 show the effect on the transient shapes for both linearized examples for two particular values of $\frac{\alpha}{\beta}$ (variations of reactor temperature and concentration). It can be concluded that when we increase this parameter the transient response is less oscillatory and dies out faster.

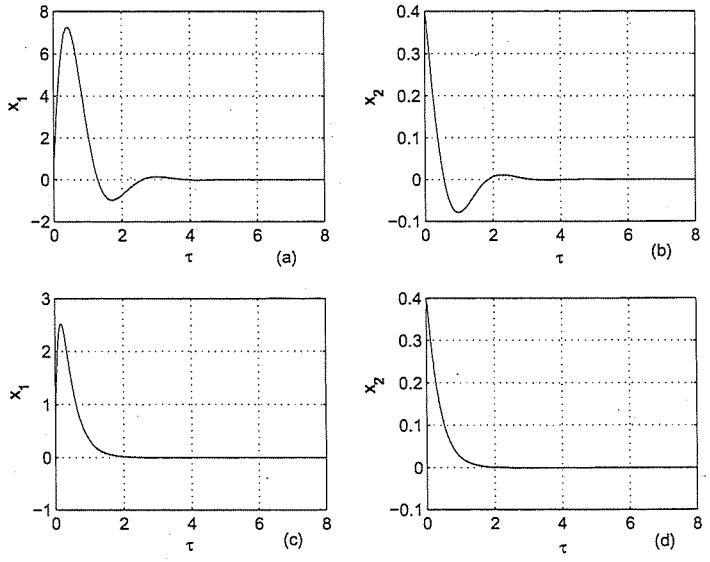

Figure 2.11: Influence of $\frac{\alpha}{\beta}$ on the transients for Example 1. $\frac{1}{\beta} = 1.22.10^{-15}$. (a) and (b): $\frac{\alpha}{\beta} = 1$; (c) and (d): $\frac{\alpha}{\beta} = 10$.

Figure 2.13 and Figure 2.14 show the same effect on the transient response when β is increased.

Other simulations for different parameter values can be found in (Muñoz, Loccufier and Noldus, 2002).

2.4.5 Choosing the control parameters

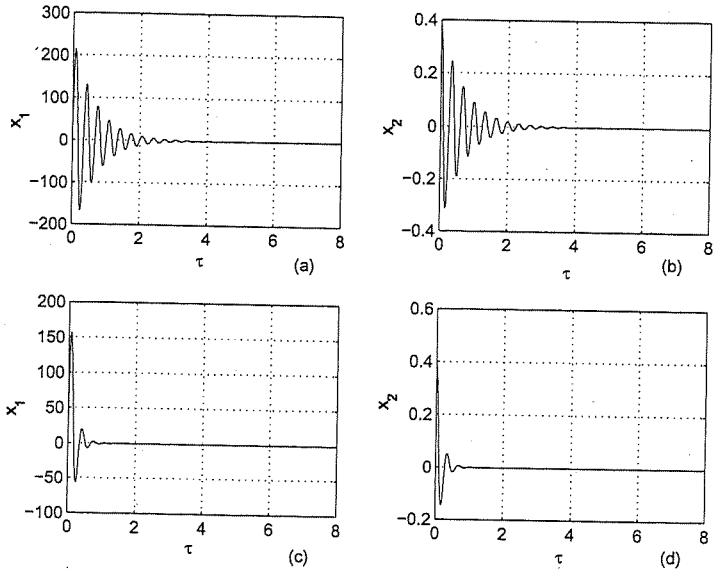

Figure 2.12: Influence of $\frac{\alpha}{\beta}$ on the transients for Example 2. $\frac{1}{\beta} = 7.98.10^{-10}$. (a) and (b): $\frac{\alpha}{\beta} = 1$; (c) and (d): $\frac{\alpha}{\beta} = 10$.

When selecting the controller parameters, the following conclusions should be taking into account:

- Assume that (2.57) holds. Then the undamped natural frequency ω_n increases for increasing $\frac{\alpha}{\beta}$ and for increasing $\frac{1}{\beta}$.
- The response dies out faster for increasing $\frac{\alpha}{\beta}$. The rate of decay of the response is determined by the maximum of the real part of the system's eigenvalues. As a measure of the rate of decay of the response we define :

$$\nu \triangleq -max_{i=1...n} Re(p_i)$$

where p_i, i=1...n are the eigenvalues of a system of order n.

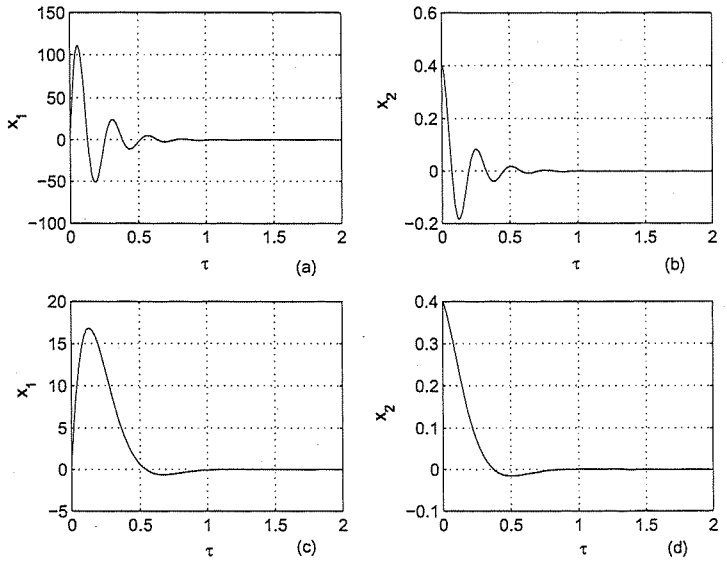

Figure 2.13: Influence of $\frac{1}{\beta}$ on the transients for Example 1. $\frac{\alpha}{\beta} = 10$. (a) and (b) $\frac{1}{\beta} = 1.2531.10^{-13}$; (c) and (d) $\frac{1}{\beta} = 1.10^{-14}$

In the present case the maximum rate of decay is reached if

$$\frac{1}{\beta} = \frac{1}{4a_0 m_2}[1 + b_{0l} - \frac{\alpha}{\beta}]^2$$

It is given by

$$\nu_{max} = \frac{1}{2}[\frac{\alpha}{\beta} + 1 + b_{0l}] \tag{2.59}$$

- The closed loop eigenvalues can be arbitrarily assigned in the half plane $\{Res \leq -(1 + b_{0l})\}$.

Figure 2.15 shows the variation of the parameter ζ with the change of the controller parameters $\frac{1}{\beta}$ and $\frac{\alpha}{\beta}$. We conclude that good transient responses are found for very small values of $\frac{\alpha}{\beta}$ while the curve becomes almost flat and

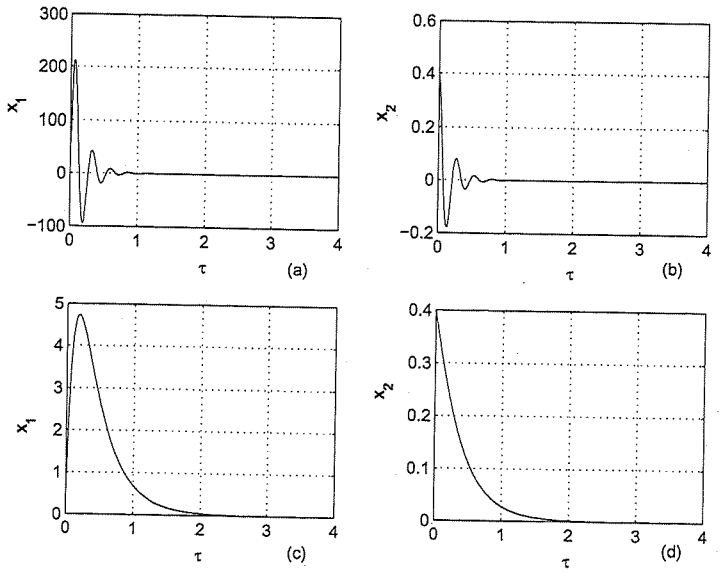

Figure 2.14: Influence of $\frac{1}{\beta}$ on the transients for Example 2. $\frac{\alpha}{\beta} = 10$. (a) and (b) $\frac{1}{\beta} = 1.2529.10^{-9}$; (c) and (d) $\frac{1}{\beta} = 1.2529.10^{-11}$

represents an overdamped system for very high values of this parameter. Also it can be noted that for a fixed value of the parameter $\frac{1}{\beta}$, the value of ζ increases when increasing $\frac{\alpha}{\beta}$.

2.5 Input and state constraints

This section is dedicated to the design of a PD-controller for the one input CSTR, subject to constraints on the plant input (control variable) as well as on the states(output variables). Most applications in control engineering involve hard constraints on the plant input (eg a flow rate in a valve). Unfortunately there are only a few design procedures which deal with such constraints. In practical usage this has led to ad-hoc methods (or, in the worst case, wait-

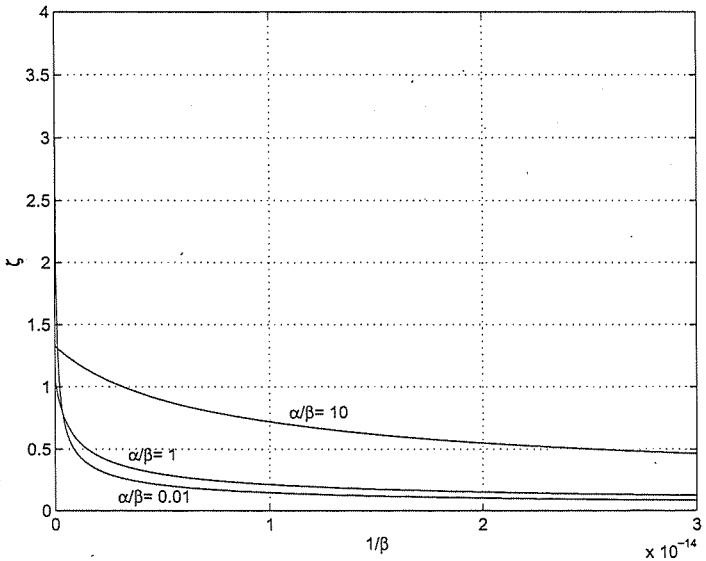

Figure 2.15: Influence of $\frac{1}{\beta}$ and $\frac{\alpha}{\beta}$ on the damping factor ζ for Example 1.

and-see-what-happens methods) which have little theoretical justification. The approach used in the present application is to avoid saturation , i.e. we look for the operating conditions under which the control signal generated by the PD-controller and the state values remain smaller in amplitude than some prescribed values.

Specifically using the Liapunov function that arises from the closed loop stability analysis we compute regions of initial states from which the controller drives the system to its set point while satisfying such constraints. These regions indeed show to what extent the set point is stabilized under practical industrial operating conditions.

2.5.1 The input constraint problem

The first problem we discuss is related to the constraints on control input amplitudes. We compute a region of attraction Ω of the set point in state space under an input constraint $u_1 < a$.

Let

$$u_1(t) \equiv a > 0 \tag{2.60}$$

Then (2.3) becomes:

$$[(m_1 + m_1\vartheta + \alpha)x_1 + (m_1 + \beta)\dot{x}_1 + m_2\dot{x}_2] = m_1 a \tag{2.61}$$

In closed loop we have

$$\begin{aligned} \beta\dot{x}_1 + \alpha x_1 - m_2 x_2 &= 0 && (2.62)\\ \dot{x}_2 &= -x_2 - m_1[f_1(x_1) + f_2(x_1)x_2] && (2.63) \end{aligned}$$

Substituting (2.62) and (2.63) into (2.61) we get

$$(1 + \vartheta - \frac{\alpha}{\beta})x_1 + \frac{m_2}{\beta}x_2 - m_2[f_1(x_1) + f_2(x_1)x_2] = a \tag{2.64}$$

Equation (2.64) represents the points in the state plane where the control law is constant ($u_1 = a$).

Next we look for the point on the curve (2.64) where $\dot{u}_1 = 0$. Taking the derivative with respect to time we obtain:

$$\begin{aligned} [1 + \vartheta - \frac{\alpha}{\beta} - m_2(\frac{df_1(x_1)}{dx_1} + \frac{df_2(x_1)}{dx_1}x_2)]\dot{x}_1 \\ +[\frac{m_2}{\beta} - m_2 f_2(x_1)]\dot{x}_2 = 0 \end{aligned} \tag{2.65}$$

After introducing the derivatives from the dynamical system (2.62),(2.63) and some further substitutions we get

$$\begin{aligned} &[1 + \vartheta - \frac{\alpha}{\beta} - m_2(z_{2s} + x_2)\frac{10^4}{(z_{1s} + x_1)^2}e^{\frac{-10^4}{z_{1s}+x_1}}]\frac{(m_2 x_2 - \alpha x_1)}{\beta} \\ &+[\frac{m_2}{\beta} - m_2 e^{\frac{-10^4}{z_{1s}+x_1}}][-x_2 - m_1 z_{2s}(e^{\frac{-10^4}{z_{1s}+x_1}} - e^{\frac{-10^4}{z_{1s}}}) - m_1 x_2 e^{\frac{-10^4}{z_{1s}+x_1}}] = 0 \end{aligned} \tag{2.66}$$

The solution of (2.64), (2.66) corresponds to the point where $\dot{u}_1 = 0$ and $u_1 = a$. Let

$$x_a \triangleq \begin{bmatrix} x_{1a} \\ x_{2a} \end{bmatrix}$$

be the point of the curve (2.64) where (2.66) holds. We can make a similar calculation with $u_1 \equiv -b < 0$.

Figures 2.16 and 2.17 schematically illustrate the situation when we make the following constraint on the control input : $-b < u_1(t) < a$, for some given $a, b > 0$.

Ω_a and Ω_b correspond to regions of attraction of the set point $x = 0$ with the constraints $u_1 < a$ and $u_1 > -b$. Ω_a is the intersection of the sets $\{V(x) < V(x_a)\}$ and $\{u_1 < a\}$ while Ω_b is the intersection of the sets $\{V(x) = V(x_b)\}$ and $\{u_1 > -b\}$. Note that the Liapunov function must be evaluated at the points x_a and x_b respectively. That is $V(x_a) \triangleq c_a$ and $V(x_b) \triangleq c_b$

The intersection of the sets Ω_a and Ω_b in Figures 2.16 and 2.17 corresponds to the estimated region of attraction for the proposed constraints. The shaded area in Figure 2.18 shows the intersection $\Omega \triangleq \Omega_a \bigcap \Omega_b$. This is a region of attraction of the set point with the control input constraint

$$-b < u_1(t) < a$$

A proof of this property for the more general case of a three dimensional state space is presented in Chapter 4. A formal proof for the two-dimensional state space of a PD-controlled reactor can be found in (Muñoz, Loccufier and Noldus, 2003a). The applied technique was inspired by a procedure originally developed by J.L.Willems (1969) involving the use of open Liapunov surfaces.

Let us examine the calculation of the stability region Ω_a in more detail. We start with the curve $u_1 = a$

From (2.64) we have:

$$x_2 = \frac{a - (1 + \vartheta - \frac{\alpha}{\beta})x_1 + m_2 z_{2s}(e^{\frac{-10^4}{z_{1s}+x_1}} - e^{\frac{-10^4}{z_{1s}}})}{m_2[\frac{1}{\beta} - e^{\frac{-10^4}{z_{1s}+x_1}}]} \tag{2.67}$$

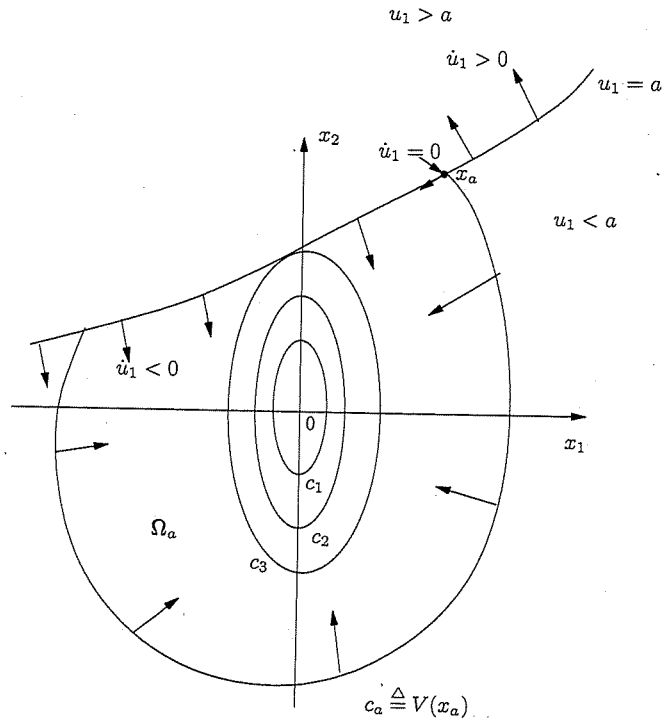

Figure 2.16: Region of attraction under control constraint($u_1 < a$).The closed curves represent the level sets $V(x) = c_i, i = 1, 2, 3...$

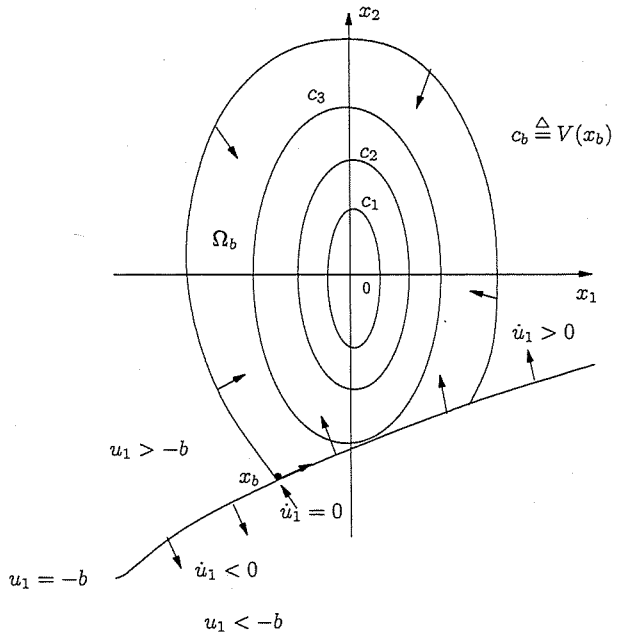

Figure 2.17: Region of attraction under control constraint ($u_1 > -b$).The closed curves represent the level sets $V(x) = c_i, i = 1, 2, 3...$

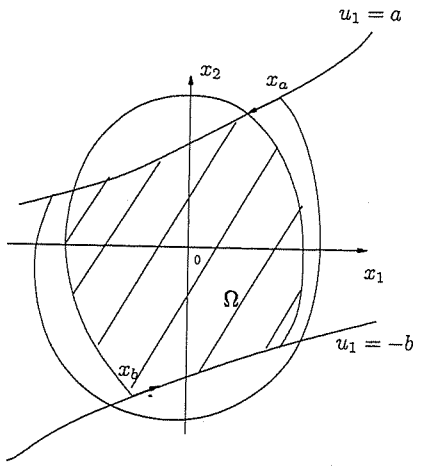

Figure 2.18: Total estimated region of attraction Ω under control constraints $-b < u_1(t) < a$.

From (2.67) we compute the point x_1 where the state x_2 goes to ∞.

Let

$$\frac{1}{\beta} - e^{\frac{-10^4}{z_{1s}+x_1}} = 0$$

Then

$$x_1 = -z_{1s} + \frac{10^4}{ln\beta}$$

It follows that for every value of a the curve $u_1 = a$ has the same vertical asymptote in the $x_1 - x_2$ plane. This curve consists of two branches : one to the left and one to the right of the asymptote. We wish to select $\alpha > 0$ and $\beta > 0$ such that for given initial deviations from the set point $x = 0$, the variations of the control $|u_1(t)|$ remain as small as possible.

Figure 2.19 displays the lines of constant control force in the state plane of both reactor examples, for a given choice of the controller parameters α and β.

Now we calculate the value x_a, the point along the curve $u_1 = a$ where $\dot{u}_1 = 0$.

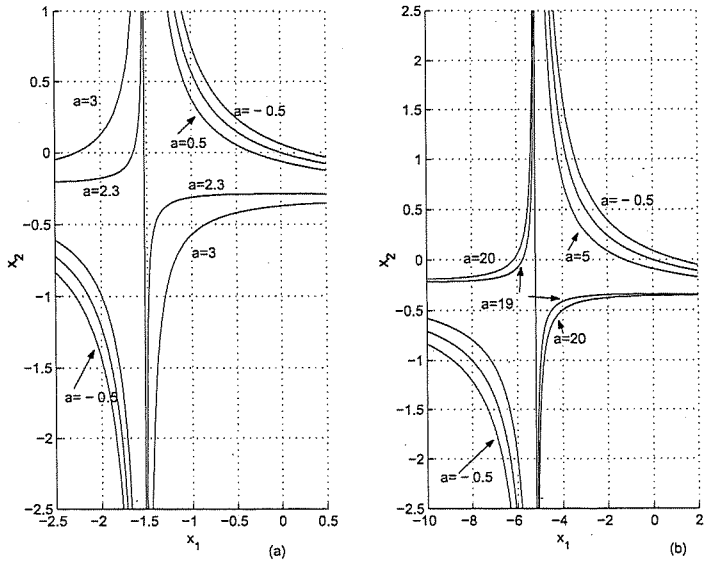

Figure 2.19: Curves of constant control force $u_1 = a$ in the state plane of the non-linear reactor system. (a) Example 1, $\alpha = 10^{13}$, $\beta = 2.10^{15}$; z_s=(285.3567, 0.4837). All curves have the same vertical asymptote : At the critical value $a_{crit} = 2.3$ the curves switch from $dx_2/dx_1 < 0$ to $dx_2/dx_1 > 0$. (b) Example 2, $\alpha = 9.44.10^7$, $\beta = 10^{11}$; z_s=(400, 0.5); $a_{crit} = 19.0$

In the system's nonlinearities we can discard the quadratic and higher degree terms if

$$|\frac{x_1}{z_{1s}}| << 1 \text{ and } |\frac{x_1}{z_{1s}}\frac{10^4}{z_{1s}}| << 1$$

which is approximately satisfied if $|x_1| << 1$. Then (2.64) can be written approximately as:

$$\mu_1 x_1 - \mu_2 x_2 - \mu_3 x_1 x_2 = a \qquad (2.68)$$

where after some calculations we find

$$\mu_1 \triangleq 1+\vartheta-\frac{\alpha}{\beta}-\frac{m_2 z_{2s}}{z_{1s}}e^{\frac{-10^4}{z_{1s}}}\frac{10^4}{z_{1s}} \quad (2.69)$$

$$\mu_2 \triangleq m_2 z_{2s}e^{\frac{-10^4}{z_{1s}}}-\frac{m_2}{\beta} \quad (2.70)$$

$$\mu_3 \triangleq \frac{m_2}{z_{1s}}e^{\frac{-10^4}{z_{1s}}}\frac{10^4}{z_{1s}} \quad (2.71)$$

This gives us the curves of constant control $u_1 = a$ in the state plane, in the neighbourhood of the set point. They have been displayed in Figure 2.20. Comparing Figures 2.19, 2.20 we can see that they both have a similar representation of the system in the neigboorhood of the origin.

For $u_1 = a = -\frac{\mu_1\mu_2}{\mu_3}$, (2.68) becomes:

$$[\mu_3 x_1+\mu_2][\mu_1-\mu_3 x_2]=0 \quad (2.72)$$

or

$$x_1 = -\frac{\mu_2}{\mu_3}$$
$$x_2 = \frac{\mu_1}{\mu_3}$$

So the horizontal and the vertical lines in Figure 2.20 correspond to the control input level $a = -\frac{\mu_1\mu_2}{\mu_3}$.

Next we find a quadratic approximation for the Liapunov function in the neighbourhood of the origin:

Some calculations yield:

$$V(x) = (p_1+\frac{\alpha_0 V_1}{2}+\frac{V_2}{2})x_1^2+2p_2x_1x_2+p_3x_2^2 \quad (2.73)$$

where

$$V_1 = \frac{m_1 z_{2s}}{z_{1s}}e^{\frac{-10^4}{z_{1s}}}\frac{10^4}{z_{1s}}+\frac{m_1}{m_2}\alpha e^{\frac{-10^4}{z_{1s}}}$$
$$V_2 = \frac{m_1}{m_2}\beta e^{\frac{-10^4}{z_{1s}}}$$

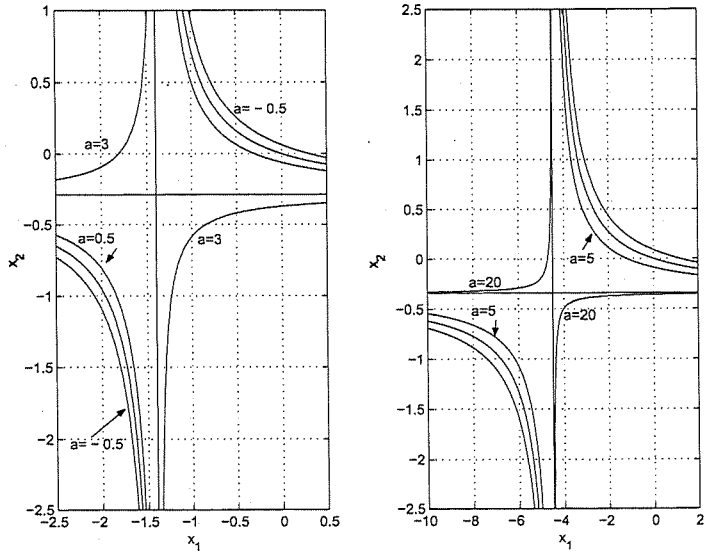

Figure 2.20: Curves of constant control force $u_1 = a$ in the neighbourhood of the set point. (a) Example 1, $\alpha \doteq 10^{13}$, $\beta = 2.10^{15}$. All curves have the same vertical asymptote: At the critical value $a_{crit} = 2.3$ the curves switch from $dx_2/dx_1 < 0$ to $dx_2/dx_1 > 0$. (b) Example 2, $\alpha = 9.44.10^7$, $\beta = 10^{11}$; $a_{crit} = 19.0$

Linearization of the curves $u_1 = a$ and $\dot{u}_1 = 0$ gives

$$\lambda_1 x_1+\lambda_2 x_2 = a \quad (2.74)$$
$$\lambda_3 x_1+\lambda_4 x_2 = 0 \quad (2.75)$$

with

$$\lambda_1 = \mu_1$$
$$\lambda_2 = -\mu_2$$
$$\lambda_3 = -\frac{\alpha\mu_1}{\beta}+\mu_2[m_1\frac{z_{2s}}{z_{1s}}e^{\frac{-10^4}{z_{1s}}}\frac{10^4}{z_{1s}}]$$

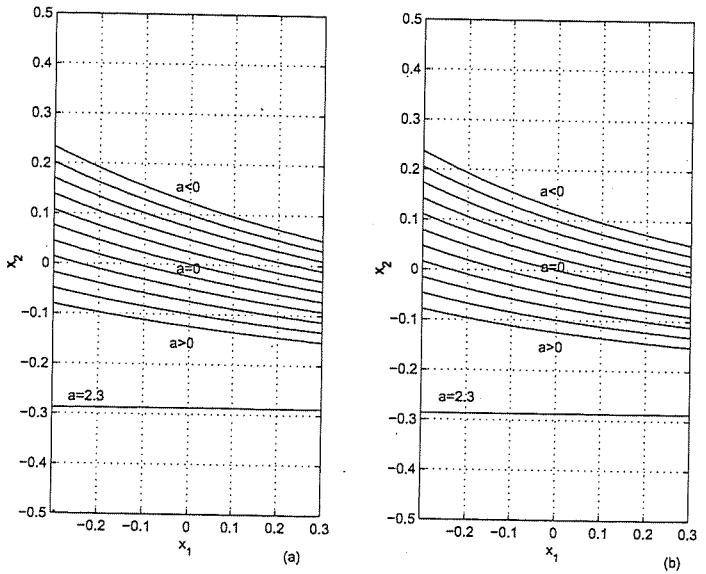

Figure 2.21: Curves of constant control force $u_1 = a$ in the state plane of the reactor system for Example 1. $\alpha = 10^{13}$, $\beta = 2.10^{15}$.(a)Nonlinear system. Asymptotes at the critical value $a_{crit} = 2.3$ (b) approximation (2.71).

$$\lambda_4 = \frac{m_2\mu_1}{\beta} + \mu_2[1 + m_1 e^{\frac{-10^4}{x_{1s}}}]$$

By solving (2.74), (2.75) we can find the state state point where $u_1 = a$ and $\dot{u}_1 = 0$:

$$x_1 = \frac{a\lambda_4}{\lambda_1\lambda_4 - \lambda_2\lambda_3} \triangleq x_{1a}$$
$$x_2 = -\frac{a\lambda_3}{\lambda_1\lambda_4 - \lambda_2\lambda_3} \triangleq x_{2a}$$

A similar analysis applies to the case of a lower bound on the input $u_1 > -b$. Figures 2.22 and 2.23 display computed stability regions Ω_a under the constraint $u_1 < a = 0.1$ for Examples 1 and 2, using the approximations (2.73), (2.74), (2.75). All these linearizations have been done in order to avoid numerical problems and save time during simulations. So under some mathematical restrictions this approach can be used to obtain regions of attractions of the set point.

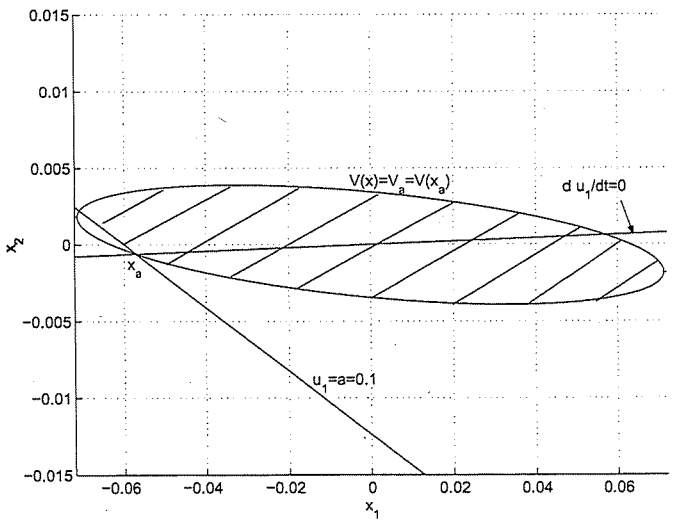

Figure 2.22: Stability region Ω_a with $u_1 < a = 0.1$ for Example 1; $\alpha_0 = \frac{\alpha}{\alpha+\beta}$, $\alpha = 10^{13}$, $\beta = 2.10^{15}$. For p_1, equation (2.34), the best choice has been made.

The Liapunov function parameter has been selected as $\alpha_0 = \frac{\beta}{\alpha+\beta} \triangleq \alpha_{0min}$. A better estimate of the true stability region under the given control input constraint is obtained by taking the union of the sets Ω_a over all $\alpha_0 \geq \frac{\beta}{\alpha+\beta}$. However comparing the results for $\alpha_0 = \alpha_{0min}$ and $\alpha_0 = +\infty$ shows that little is gained in this way(Figures 2.24, 2.25, 2.26).

2.5.2 The state constraint problem

In this section we estimate a region of attraction of the set point $x = 0$ in state space under constraints on a state variable. As an example consider a reactor temperature constraint $x_1 < a$.

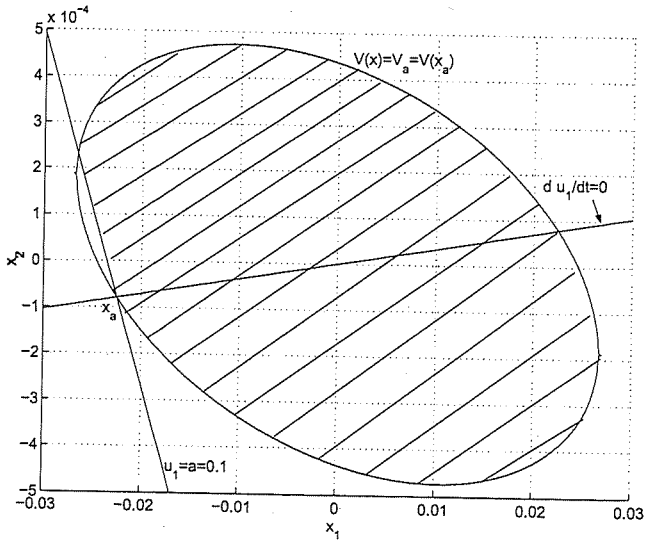

Figure 2.23: Stability region Ω_a with $u_1 < a = 0.1$ for Example 2; $\alpha_0 = \frac{\alpha}{\alpha+\beta}$. $\alpha = 10^6$, $\beta = 10^6$

Let

$$x_1 = a$$

By (2.4) we have in closed loop:

$$\begin{aligned} \dot{x}_1 &= 0 \Rightarrow \\ x_2 &= \frac{\alpha x_1}{m_2} = \frac{\alpha a}{m_2} \end{aligned}$$

Let

$$x_b \triangleq \begin{bmatrix} a \\ \frac{\alpha a}{m_2} \end{bmatrix} \triangleq \begin{bmatrix} x_{1b} \\ x_{2b} \end{bmatrix}$$

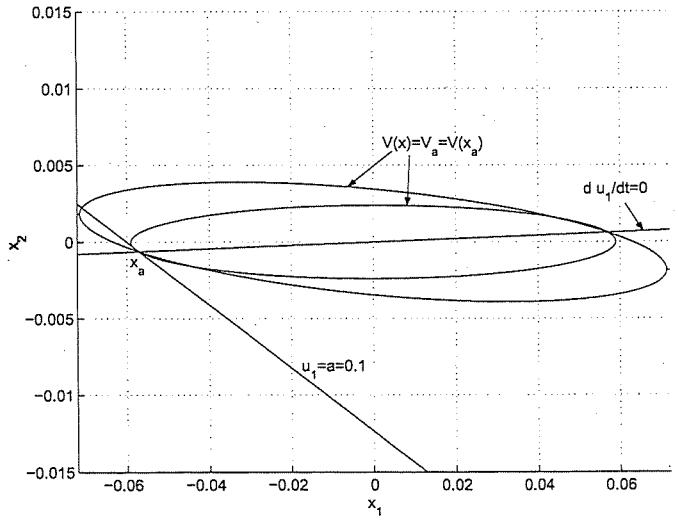

Figure 2.24: Stability region Ω_a with $u_1 < a = 0.1$ for Example 1; $\alpha_0 = \alpha_{0min}$ (exterior curve) versus $\alpha_0 = +\infty$(interior curve).

By a similar analysis as in the previous section the set $\Omega_c = \{V(x) < V(x_b); x_1 < a\}$ is a region of attraction of the set point under the state constraint $x_1 < a$ (see Figure 2.27). A similar analysis applies to constraints on x_2. Let

$$x_2 = a;\ \dot{x}_2 = 0$$

From (2.5) we find after some calculations:

$$x_b \triangleq \begin{bmatrix} -z_{1s} + \frac{10^4}{ln(\eta)} \\ a \end{bmatrix}$$

where

$$\eta \triangleq \frac{z_{2s}+a}{z_{2s}e^{\frac{-10^4}{z_{1s}}} - \frac{a}{m_1}}$$

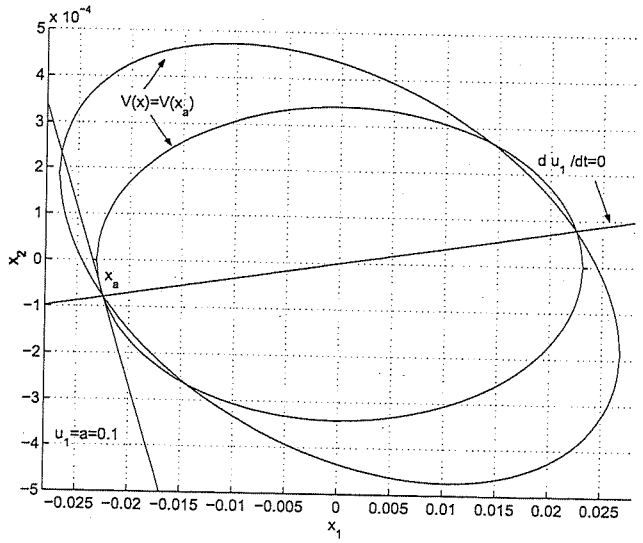

Figure 2.25: Stability region Ω_a with $u_1 < a = 0.1$ for Example 2; $\alpha_0 = \alpha_{0min}$(exterior curve) versus $\alpha_0 = +\infty$(interior curve).

For sufficiently small values of $|a|$ we have that $\eta > 0$.

Now $\Omega_d = \{V(x) < V(x_b); x_2 < a\}$ is a region of attraction of the set point under the constraint $x_2 < a$.

Some examples of stability regions under state constraints have been computed in (Muñoz, Loccufier and Noldus, 2003a).

As a conclusion, we have discussed the global asymptotic stabilization of a chemical CSTR model using single input linear time invariant PD-control. Regions of asymptotic stability for the system's set point in state space have been computed where the control and/or state variable fluctuations satisfy a priori given upper bounds. Simulations indicate that tuning the controller parameters may require a trade-off between maximizing these stability regions and optimizing the controlled system's transients during convergence to the

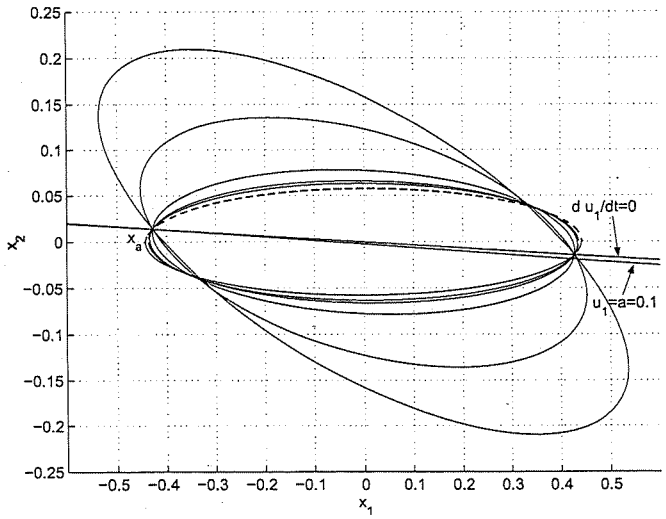

Figure 2.26: Stability region Ω_a with $u_1 < a = 0.1$ for Example 1; $\alpha = 1.08.10^{14}$, $\beta = 2.10^{16}$, Computation of $\bigcup \Omega_a$ over α_{0min}(exterior curve) $\leq \alpha_0 < +\infty$(interior dotted curve).

set point.

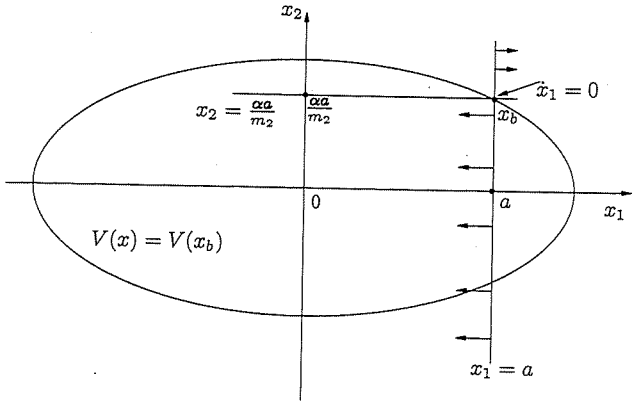

Figure 2.27: Region of attraction with constraint on the state variable x_1

Chapter 3

Two input PD-control

In this chapter we explain how the stabilization of the chemical stirred tank reactor can be achieved using multivariable feedback control, in particular PD-control using the two available inputs u_1 and u_2. Conditions are derived under which the closed loop can be modelled as a feedback interconnection of passive components, which allows the design of a globally stabilizing feedback law. Concepts from the direct method of Liapunov are also used. The control parameters are tuned in the same way as in Chapter 2, using simulations of the closed loop transients and phase portraits. Some results are published in (Muñoz, Loccufier and Noldus, 2003)

3.1 Feedback law

We extend the design presented in Chapter 2 to the case where the full input vector $u = \begin{bmatrix} u_1 \\ u_2 \end{bmatrix}$ is used to control the system. That is, instead of fitting u_2 to zero, this signal is used as another PD-generated control input with a new parameter β_1 which should also be tuned. Define

$$u_0 \triangleq m_1 u_1 + m_2 u_2 \tag{3.1}$$

and, generalizing (2.3), choose

$$u_0 = [m_1(1+\vartheta)+\alpha]x_1 + [m_1+\beta]\dot{x}_1 + m_2\dot{x}_2 \tag{3.2}$$

$$u_2 = -\beta_1 w \quad ; \quad w = x_1 + \alpha_0 \dot{x}_1$$

Now the control law can be written as:

$$u_1 = [1+\vartheta+\frac{\alpha}{m_1}+\frac{m_2}{m_1}\beta_1]x_1 + [1+\frac{\beta}{m_1}+\frac{m_2}{m_1}\beta_1\alpha_0]\dot{x}_1 + \frac{m_2}{m_1}\dot{x}_2 \tag{3.3}$$

$$u_2 = -\beta_1(x_1+\alpha_0\dot{x}_1) \tag{3.4}$$

3.2 Closed loop stability analysis

The closed loop equations with a second input u_2 read:

$$\beta\dot{x}_1 + \alpha x_1 - m_2 x_2 = 0 \tag{3.5}$$

$$\dot{x}_2 = -x_2 - m_1[f_1(c'x) + f_2(c'x)g'x] + u_2 \tag{3.6}$$

Reorganizing (3.5) and (3.6) we obtain:

$$\dot{x} = A_0 x - b_0\left[\hat{f}_1(c'x) + \hat{f}_2(c'x)c'\dot{x} - u_2\right] \tag{3.7}$$

where $\hat{f}_1(y)$ and $\hat{f}_2(y)$ are defined as in Section(2.2) and where

$$A_0 \triangleq \begin{bmatrix} -\frac{\alpha}{\beta} & \frac{m_2}{\beta} \\ 0 & -1 \end{bmatrix}, \; b_0 \triangleq \begin{bmatrix} 0 \\ 1 \end{bmatrix}$$

In (3.6) and in (3.7) u_2 is given by (3.4). (3.7) generalizes (2.5).

3.2.1 Closed loop stability analysis using passivity theory

The system (3.4), (3.7) can be represented by the block diagram of Figure 3.1a which, for any $\alpha_0 \geq 0$ is equivalent to the diagram of Figure 3.1b. W.r.t. the

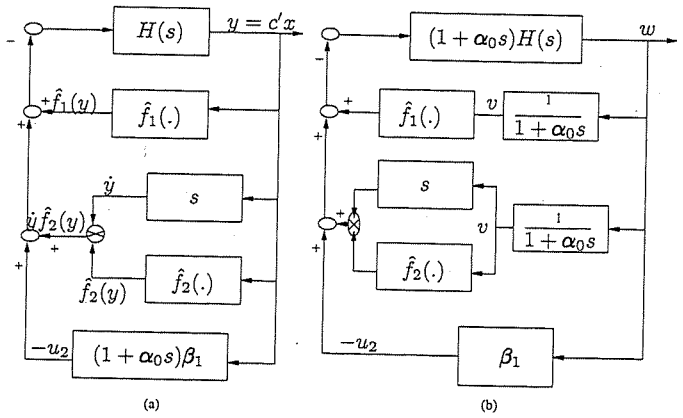

Figure 3.1: Block diagram of the system (3.4), (3.7).

forward path component and the first and the second feedback path components in Figure 3.1b we introduce the same conditions as in the case of the single input PD-controller (Section 2.2).

The only added requirement is that $\beta_1 > 0$, i.e. the third feedback path component is passive:

$$\int_0^{+\infty} \beta_1 w(t) w(t) dt = \int_0^{+\infty} \beta_1 w^2(t) dt \geq 0 \tag{3.8}$$

Now the feedback path in the diagram of Figure 3.1b is a parallel connection of three passive components. The finite gain stability of the closed loop then results from standard passivity theory as before (Lozano et al., 2000). In summary, the design parameters should be selected such that :

$$\alpha > 0 \quad ; \beta > 0 \quad ; \quad \alpha_0 \geq \frac{\beta}{(\alpha+\beta)} \quad ; \quad \beta_1 > 0$$

3.2.2 Closed loop stability analysis using Liapunov theory

The same philosophy as in Chapter 2 is applied when using two inputs to control the system.

The candidate Liapunov function has the form :

$$\begin{aligned} V(x) &\triangleq x'Px + \alpha_0 \int_0^{c'x} \hat{f}_1(\theta) d\theta \\ &\quad + \int_0^{c'x} \hat{f}_2(\theta)\theta d\theta \end{aligned} \tag{3.9}$$

Then

$$\begin{aligned} \dot{V}(x, u_2) &= -(q'x)^2 - c'x\hat{f}_1(c'x) \\ &\quad -\alpha_0 \hat{f}_2(c'x)(c'\dot{x})^2 + wu_2 \end{aligned} \tag{3.10}$$

As a negative feedback from w to u_2 is used through a passive component with gain β_1, it stabilizes the set point. We obtain :

$$\begin{aligned} \dot{V}(x) &= -(q'x)^2 - c'x\hat{f}_1(c'x) \\ &\quad -\alpha_0 \hat{f}_2(c'x)(c'\dot{x})^2 - \beta_1 w^2 \leq 0 \end{aligned} \tag{3.11}$$

$\dot{V}(x) \equiv 0$ implies $x_1(t) \equiv \dot{x}_1(t) \equiv 0$, hence in view of (3.5), $x_2(t) \equiv 0$, so $x(t) \equiv 0$. From Collorary 2, p.24 it follows that the closed loop set point $x_s = 0$ is globally asymptotically stable.

3.3 Control parameter tuning

In this section we illustrate the tuning of the PD-controller with two inputs u_1 and u_2. We follow the same procedure as in Chapter 2. At the end we show some simulations in closed loop for each of the examples.

3.3.1 Root locus analysis of the linearized dynamics

The closed loop linearized state equations are:

$$\dot{x}_1 = -\frac{\alpha}{\beta} x_1 + \frac{m_2}{\beta} x_2 \tag{3.12}$$

$$\dot{x}_2 = -a_0 x_1 - (1 + b_{0l})x_2 + u_2 \quad (3.13)$$

u_2 is given by (3.4) where, according to the stability analysis, β_1 should be positive. a_0 and b_{0l} are process parameters which have been defined in Section 2.4.1.

Introducing the second feedback law into the dynamical system we get:

$$\dot{x}_2 = -a_0 x_1 - (1 + b_{0l})x_2 - \beta_1 x_1 - \beta_1 \alpha_0 [-\frac{\alpha}{\beta} x_1 + \frac{m_2}{\beta} x_2] \quad (3.14)$$

$$= x_1[-a_0 - \beta_1 + \frac{\beta_1 \alpha_0 \alpha}{\beta}] + x_2[-1 - b_{0l} - \frac{\beta_1 \alpha_0 m_2}{\beta}] \quad (3.15)$$

In matrix notation (3.12), (3.15) is represented by:

$$\begin{bmatrix} \dot{x}_1 \\ \dot{x}_2 \end{bmatrix} = \begin{bmatrix} -\frac{\alpha}{\beta} & \frac{m_2}{\beta} \\ -a_0 - \beta_1 + \frac{\beta_1 \alpha_0 \alpha}{\beta} & -1 - b_{0l} - \frac{\beta_1 \alpha_0 m_2}{\beta} \end{bmatrix} \begin{bmatrix} x_1 \\ x_2 \end{bmatrix}$$

The corresponding characteristic equation is:

$$(s + \frac{\alpha}{\beta})(s + 1 + b_{0l} + \frac{\beta_1 \alpha_0 m_2}{\beta}) + (a_0 + \beta_1 - \frac{\beta_1 \alpha_0 \alpha}{\beta})\frac{m_2}{\beta} = 0 \quad (3.16)$$

To fulfill the stability conditions the control parameters are restricted to:

$$\frac{\alpha}{\beta} > 0, \frac{1}{\beta} > 0, \alpha_0 \geq \frac{1}{1 + \frac{\alpha}{\beta}}, \beta_1 > 0$$

(3.16) is written in a standard way suitable for a root locus analysis :

$$(s + \frac{\alpha}{\beta})(s + 1 + b_{0l}) + \frac{m_2 \beta_1 \alpha_0}{\beta}(s + \frac{a_0 + \beta_1}{\beta_1 \alpha_0}) = 0 \quad (3.17)$$

Now we can analyze how the spectrum of the characteristic values is shifted when a change in the parameter $\frac{1}{\beta}$ occurs :

If

$$a \triangleq \frac{\alpha}{\beta}, b \triangleq (1 + b_{0l}), c \triangleq m_2 \beta_1 \alpha_0, q_1 \triangleq -\frac{a_0 + \beta_1}{\beta_1 \alpha_0}$$

(3.17) becomes:

$$(s + a)(s + b) + c\frac{1}{\beta}(s - q_1) = 0 \quad (3.18)$$

The following diagrams reveal the dependence of the spectrum on the process and the control parameters:
Changing the values of α , β and/or α_0, $\beta_1$we can move the points -a or q_1 to

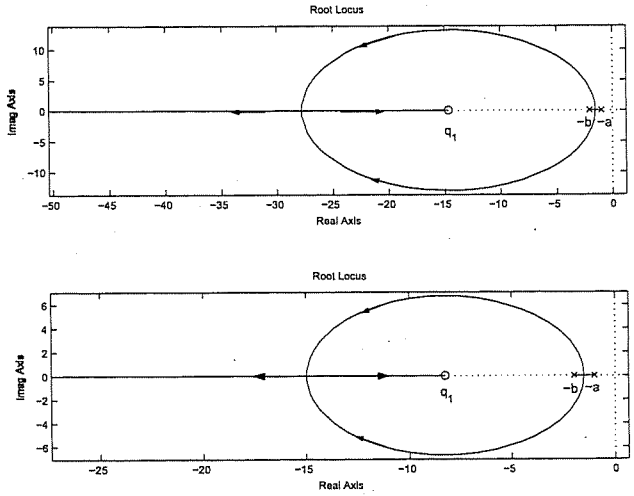

Figure 3.2: Root locus for $0 < \frac{1}{\beta} < +\infty$. (a) Example 1, (b)Example 2

the left which will cause the full spectrum to move to the left. Specifically, increasing $|q_1|$-values will move the spectrum away from the imaginary axis. We can make the closed loop system response oscillatory as well as non-oscillatory depending on the choice of the controller parameters.

The break points in the root locus plot can be computed as follows (Ogata, 1998) :

$$\frac{1}{s + \frac{\alpha}{\beta}} + \frac{1}{s + 1 + b_0} - \frac{1}{s - q_1} = 0 \quad (3.19)$$

or

$$s^2 - 2q_1 s + \gamma = 0 \quad (3.20)$$

where

$$\gamma \triangleq -q_1(1+b_0+\tfrac{\alpha}{\beta}) - \tfrac{\alpha}{\beta}(1+b_0)$$

(3.20) yields:

$$s = q_1 \pm \sqrt{q_1^2 - \gamma}$$

where

$$q_1^2 - \gamma = (q_1 + \tfrac{\alpha}{\beta})(q_1 + 1 + b_0) > 0$$

if

$$-q_1 > max[\frac{\alpha}{\beta}, (1+b_0)] = max(a,b) \qquad (3.21)$$

For given $\frac{\alpha}{\beta}$ and $\alpha_0 \geq \frac{1}{1+\frac{\alpha}{\beta}}$, we choose $\beta_1 > 0$ and sufficiently small such that (3.21) holds. The break points are then:

$$s = q_1 \pm \sqrt{(q_1 + \frac{\alpha}{\beta})(q_1 + 1 + b_0)}$$

Now there is an interval of values for $\frac{1}{\beta}$ where the response is oscillatory :

$$\tfrac{1}{\beta_a} < \tfrac{1}{\beta} < \tfrac{1}{\beta_b}$$

For the values $\frac{1}{\beta} < \frac{1}{\beta_a}$ and $\frac{1}{\beta} > \frac{1}{\beta_b}$ the response is non-oscillatory.

Below we display some root locus diagrams to show the effect of different parameters on the eigenvalue spectrum.

Figure 3.3 displays the effect of the parameter $\frac{\alpha}{\beta}$ on the root locus plot. If $\frac{\alpha}{\beta}$ increases the entire diagram is shifted to the left side of the s-plane. In this way we obtain a substantial increase of the rate of decay of the transient reponse.

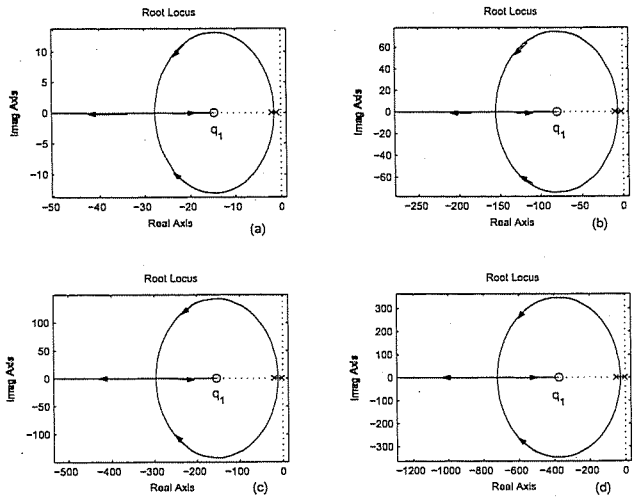

Figure 3.3: Effect of $\frac{\alpha}{\beta}$ on the eigenvalue spectrum for Example 1. (a)$\frac{\alpha}{\beta} = 1$, (b)$\frac{\alpha}{\beta} = 10$, (c) $\frac{\alpha}{\beta} = 20$, (d)$\frac{\alpha}{\beta} = 50$; $\beta_1 = 0.01$; $\alpha_0 = 0.5, 0.0901, 0.0476, 0.0196$ respectively.

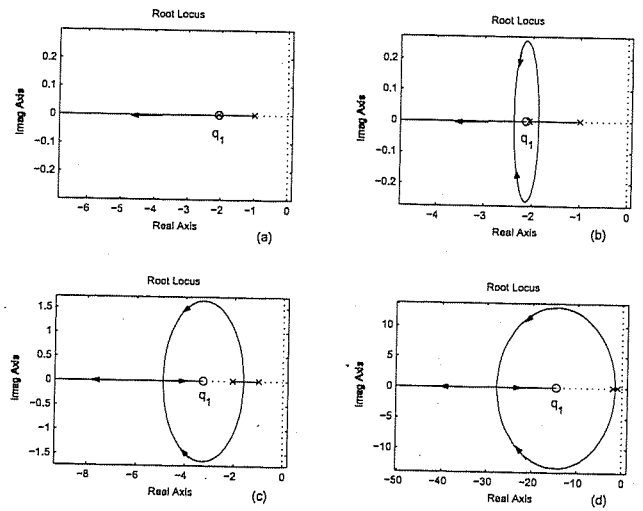

Figure 3.4: Effect of β_1 on the eigenvalue spectrum for Example 1. (a) $\beta_1 = 2$,(b) $\beta_1 = 1$, (c) $\beta_1 = 0.1$, (d) $\beta_1 = 0.01$; $\frac{\alpha}{\beta} = 1$; $\alpha_0 = 0.5$

Figure 3.4 shows different shapes of the root locus for variations in the β_1 parameter. If β_1 decreases a better damped system is obtained again, as the rate of decay grows with decreasing β_1.

In the present application the maximum rate of decay of the response is achieved for $\frac{1}{\beta} \to \infty$:

$$\sigma \to -q_1 = \frac{1}{\alpha_0}(1 + \frac{\alpha_0}{\beta_1})$$

In order to maximize σ, let $\alpha_0 = \frac{1}{1+\frac{\alpha}{\beta}}$ and let $\beta_1 \to 0$. Under this conditions however the system is overdamped.

3.3.2 Single input PD-control vs two input PD-control

For the purpose of studying the effect of adding another control action to the dynamical system we discuss the following figures :

Figures 3.6 and 3.9 represent the transient response, phase portrait and controller response for Example 1, while Figures 3.8 and 3.10 represent the same curves for Example 2, each time using first a single input u_1, then both inputs u_1 and u_2

Figure 3.5 shows the behaviour of the PD-controller and the process under the action of a constant disturbance d_1. The D-action is proportional to the speed changes in the variables x_1 and x_2. If the states's values decrease rapidly, then the D-action is strong and the value of the control action decreases. By adding D-action to the P-controller, a strong action is exerted on the states changes. The D-action is stronger in the minimum and maximum values of u.

In this way the D-action controls the incoming deviation. This allows us to select a bigger amplification for the P-controller avoiding oscillations. Also the remanent deviation will decrease.

When the disturbance's value increases above $d_1 = 0.001$, the effect of the disturbance on the response is greater.

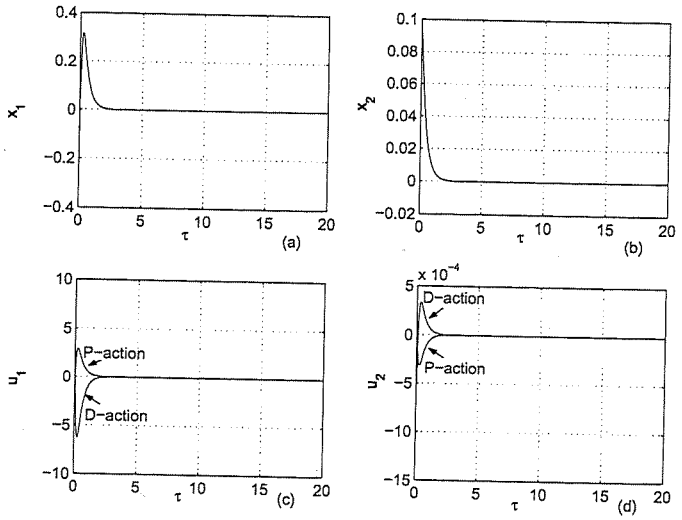

Figure 3.5: Transient response and PD-control signals for Example 1. $\alpha = 1.428.10^{15}; \beta = 1.428{\cdot}10^{15}; \alpha_0 = 0.5; \beta_1 = 0.001$; (a) Temperature response, (b) Concentration response,(c) Control law u_1,(d) Control law u_2

The two input PD-controller produces smoother transients in both of the responses (temperature as well as concentration). Specifically there is a highly oscillatory effect in the temperature response of the CSTR, which is slowly attenuated when adding the second PD-controller u_2.

Furthermore smaller oscillations in the control signal u_1 are observed in both cases.

In both examples the strongest control effort to reach the controlled variables's set points stems from the first control action u_1. The signal with smaller amplitudes corresponds to the case of the two input controller.

In conclusion, if a PD-controller with only one input is used we will have system responses with approximately the same settling time as in the two input case, but with a larger overshoot in the transient. When we connect two inputs better transient characteristics will be found and less energy consumption to generate the control action.

In the closed loop system the position of the poles changes as $\frac{1}{\beta}$ varies. This affects both the response in the time and in the frequency domains. The system can be made to respond faster, but if we are not careful we could make it poorly damped. Increasing $\frac{1}{\beta}$ could give us better accuracy but we run the risk of going near the instability condition.

With the two input PD-controller we can get a better damping in the range

$$\frac{1}{\beta_a} < \frac{1}{\beta} < \frac{1}{\beta_b}$$

compared to the case when we have only one input, as illustrated in Figure 3.11. Figures 3.7 and 3.3.2 shows the evolution of the parameter ζ for different changes in the controller parameters α and β, and for the case of using one input or two inputs respectivelly. These diagrams were used for the controller parameter tuning optimization. Influence of $\frac{1}{\beta}$ and $\frac{\alpha}{\beta}$ on the damping factor ζ for Example 2 (using two inputs).

3.3.3 Simulation of transients

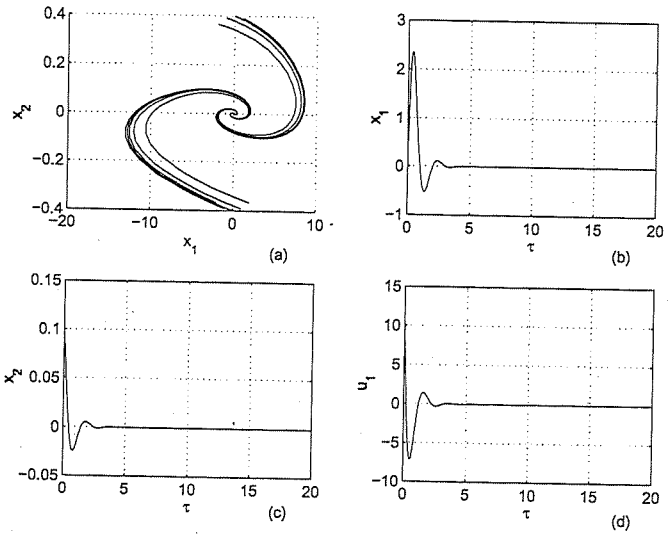

Figure 3.6: Transient response and PD-control signal for Example 1. $\alpha = 5.10^{14}; \beta = 5.10^{14}; \alpha_0 = 0.5$; (a) Phase portrait,(b) Temperature response,(c) Concentration response,(d) Control law u_1 (Single input control)

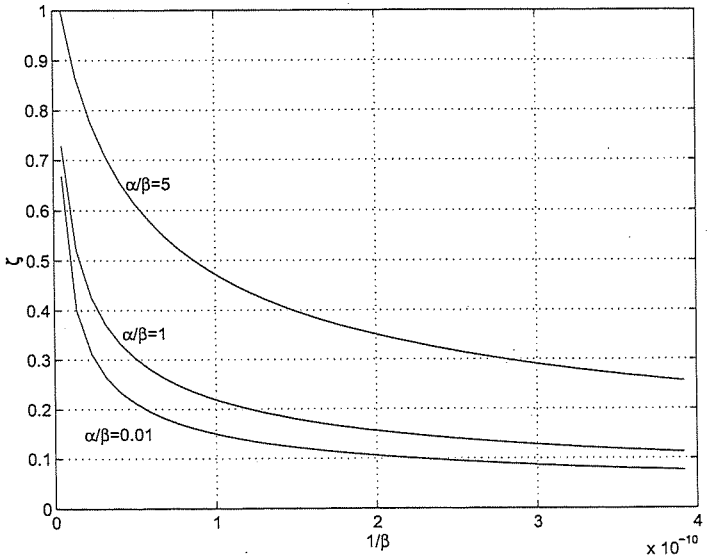

Figure 3.7: Influence of $\frac{1}{\beta}$ and $\frac{\alpha}{\beta}$ on the damping factor ζ for Example 2 (using one input).

Many control system design procedures use step response performance criteria to evaluate the quality of the controller.

The step response criteria are related to the position of the poles on the s-plane. To illustrate the quality of the system response we display some diagrams in the time domain for the linearized system representation of Example1. Similar results are found for Example 2.

Figure 3.12 shows transients responses for both state variables corresponding to an oscillatory and a non-oscillatory behaviour. Figure 3.13 shows the effect of increasing the parameter $\frac{\alpha}{\beta}$. For a larger value of this parameter both the overshoot and the settling time increase. Figure 3.14 shows the opposite effect: When the parameter β_1 is increased both the overshoot and the settling

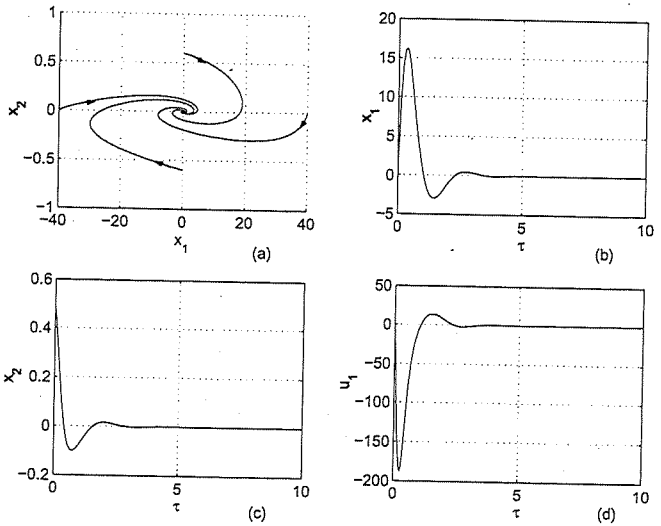

Figure 3.8: Transient response and PD-control signal for Example 2. $\alpha = 6.66.10^{10}; \beta = 6.66.10^{10}$; (a) Phase portrait,(b) Temperature response,(c) Concentration response,(d) Control law u_1 (Single input control)

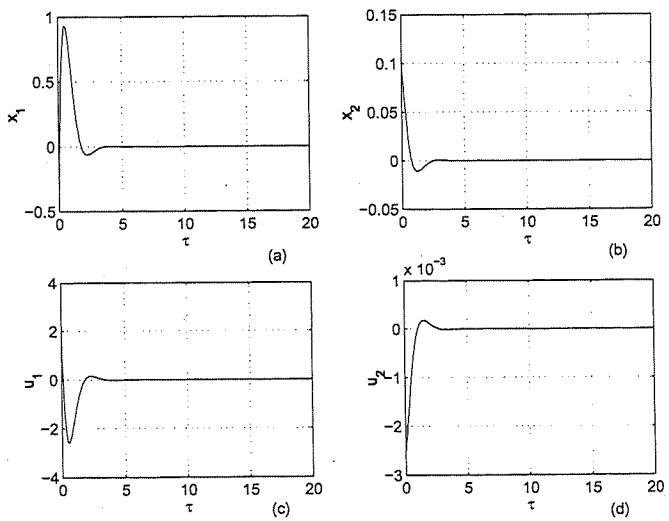

Figure 3.9: Transient response and PD-control signals for Example 1. $\alpha = 1.428.10^{15}; \beta = 1.428.10^{15}; \alpha_0 = 0.5; \beta_1 = 0.001$; (a) Temperature response, (b) Concentration response,(c) Control law u_1,(d) Control law u_2

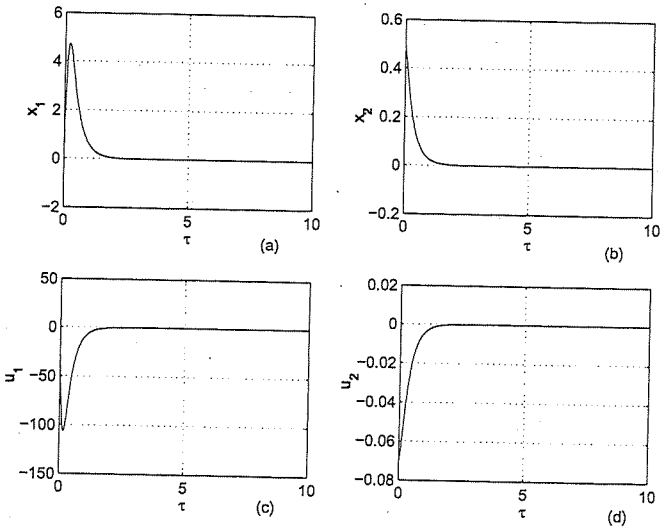

Figure 3.10: Transient response and PD-control signals for Example 2. $\alpha = 10^{11}; \beta = 10^{11}; \alpha_0 = 0.099; \beta_1 = 0.01$; (a) Temperature response, (b) Concentration response,(c) Control law u_1,(d) Control law u_2

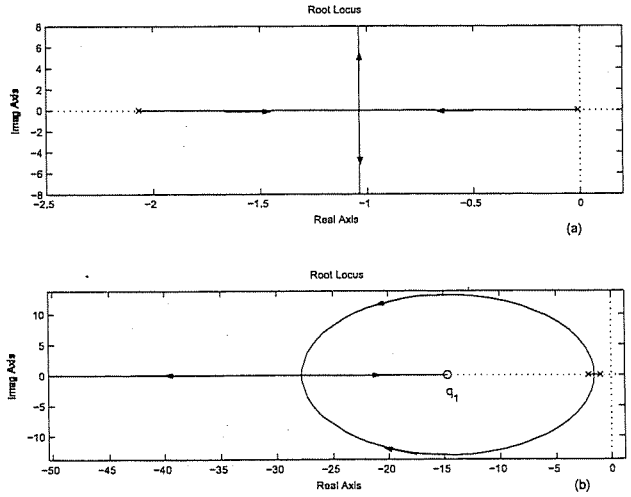

Figure 3.11: Root locus diagram with PD-control. (a) Single input PD-control, (b)Two input PD-control

time decrease. Also the oscillations disappear for a high value of this parameter.

The controllers parameters have been optimized as explained in Chapter 2 (2.4.5).

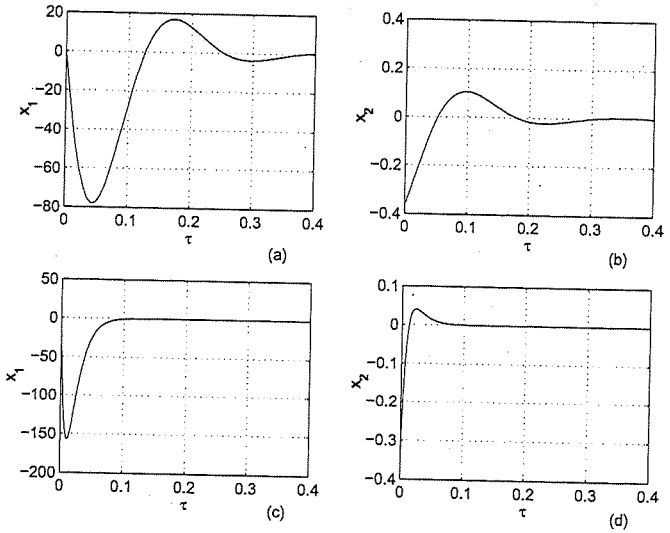

Figure 3.12: Step response with the two input PD-controller for Example 1; $\beta_1 = 0.01$; $\frac{\alpha}{\beta} = 0.5$. (a),(b) oscillatory response : $\frac{1}{\beta} = 2.94.10^{-13}$; $\alpha = 3.78.10^{13}$; (c), (d) non-oscillatory response : $\frac{1}{\beta} = 1.42.10^{-12}$; $\alpha = 3.52.10^{12}$

3.4 Phase portrait simulation

Here we illustrate the different shapes of the phase portrait diagrams for different selections of the control parameters. Figure 3.15 displays an oscillatory response for a number of initial conditions. The arrows show the direction of the states along the trajectories for increasing time t.

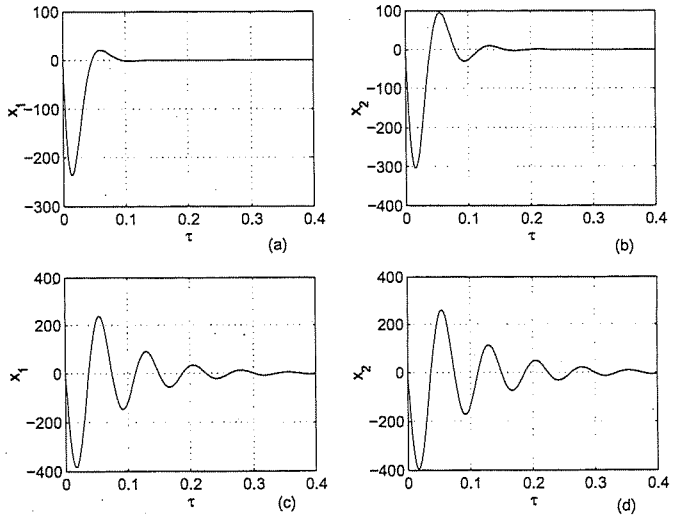

Figure 3.13: Step response with the two input PD-controller for Example 1; $\beta_1 = 0.001$, $\frac{1}{\beta} = 1.42.10^{-12}$; (a) $\frac{\alpha}{\beta} = 0.1$, (b) $\frac{\alpha}{\beta} = 1$, (c) $\frac{\alpha}{\beta} = 5$, (d) $\frac{\alpha}{\beta} = 10$

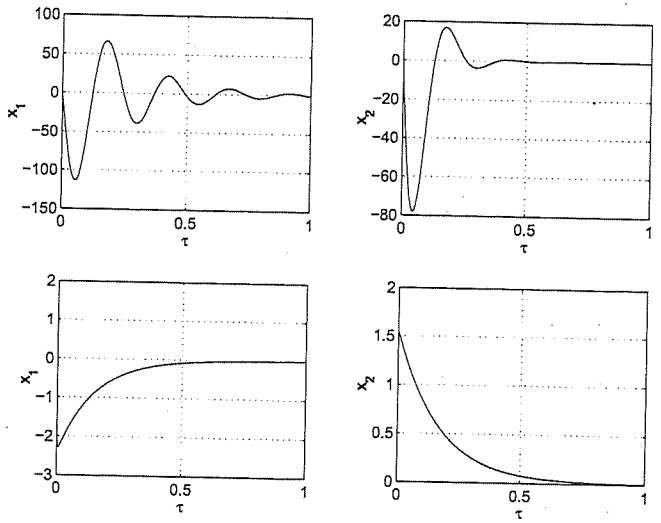

Figure 3.14: Step response with the two input PD-controller for Example 1; $\frac{\alpha}{\beta} = 5$, $\frac{1}{\beta} = 2.94.10^{-13}$ (a)$\beta_1 = 0.001$, (b)$\beta_1 = 0.01$, (c) $\beta_1 = 0.5$, (d)$\beta_1 = 5$

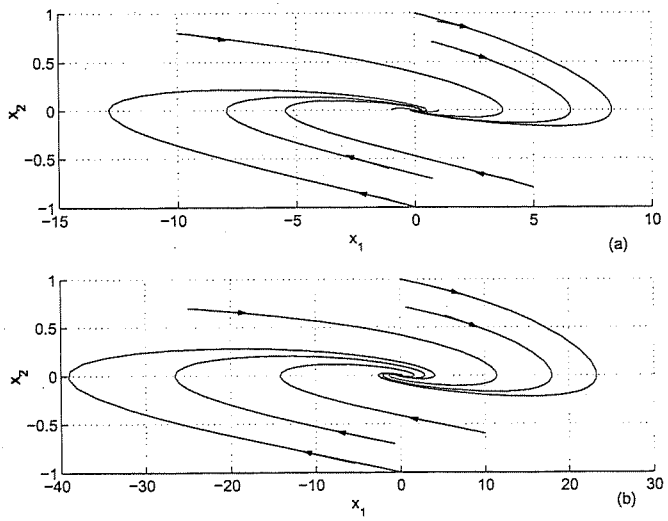

Figure 3.15: Phase portrait with the two input PD-controller; (a) Example 1; $\alpha = 1.08.10^{12}$, $\beta = 2.10^{15}$, $\alpha_0 = 0.99$, $\beta_1 = 0.01$; (b) Example 2; $\alpha = 9.44.10^{7}$, $\beta = 1.10^{11}$, $\alpha_0 = 0.5$, $\beta_1 = 0.01$

The phase portrait in Figure 3.16 corresponds to the simulations shown in Figures 3.9 and 3.10 where we see a non-oscillatory response.

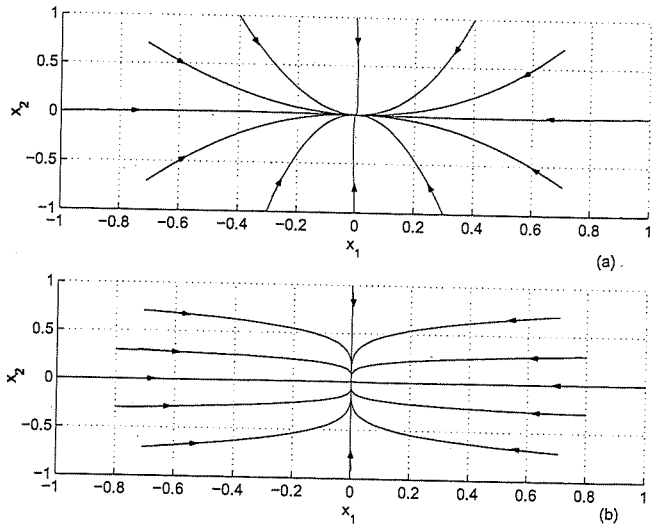

Figure 3.16: Phase portrait with the two input PD-controller; (a) Example 1; $\alpha = 2.87.10^{18}$, $\beta = 2.87.10^{18}$, $\alpha_0 = 0.5$, $\beta_1 = 0.001$; (b) Example 2; $\alpha = 9.44.10^{19}$, $\beta = 10^{19}$, $\alpha_0 = 0.5$, $\beta_1 = 0.001$

Chapter 4

Two input PID-control

In this chapter we discuss the global asymptotic stabilization of the CSTR by means of a multivariable linear time invariant PID-controller with full state feedback. In Section 4.1 we show the controller dynamics and we discuss stability conditions based on dissipativity concepts and Liapunov theory. Section 4.2 explains how the controller parameters are tuned using a root locus analysis of the linearized closed loop dynamics. Here we discuss how the system reacts when disturbances are added to the system and we investigate a more general two input PID-control strategy. The last section explains how to find stability regions in state space under given bounds on the admissible variations of the states and control inputs. Simulation results are shown for both the controller tuning and for the computation of stability regions. New contributions are made in (Muñoz, Loccufier and Noldus, 2003b)

4.1 Controller dynamics and stability analysis

In this section we explain how it is possible to stabilize the selected set point z_s designing first a PD-controller and then, in a second step, introducing the integral action to finally get a PID-controller. We proceed along the same lines as in Chapter 3, replacing the proportional feedback from w to u_2 by an integral feedback.

As before the system equation (1.7) implies that

$$\begin{aligned} m_1\dot{x}_1 + m_2\dot{x}_2 &= -m_1(1+\vartheta)x_1 \\ &\quad -m_2x_2 + u_0 \end{aligned} \tag{4.1}$$

where

$$u_0 \triangleq m_1u_1 + m_2u_2$$

We choose u_0 such that in closed loop $m_2g'x = \alpha c'x + \beta c'\dot{x}$, or

$$m_2x_2 = \alpha x_1 + \beta\dot{x}_1; \quad \alpha > 0, \beta > 0 \tag{4.2}$$

This permits to obtain dissipativity of the system with respect to the input u_2, and is achieved using a PD-control law :

$$\begin{aligned} u_0 &= (m_1(1+\vartheta)+\alpha)\,x_1 + (m_1+\beta)\,\dot{x}_1 \\ &\quad +m_2\dot{x}_2 \end{aligned} \tag{4.3}$$

Combining (4.1) with the second equation of (1.7) yields :

$$\dot{x} = A_0x - b_0\left[\hat{f}_1(c'x) + \hat{f}_2(c'x)c'\dot{x} - u_2\right] \tag{4.4}$$

where $A_0 \triangleq \begin{bmatrix} -\frac{\alpha}{\beta} & \frac{m_2}{\beta} \\ 0 & -1 \end{bmatrix}$, $b_0 \triangleq \begin{bmatrix} 0 \\ 1 \end{bmatrix}$, while $\hat{f}_1(\theta)$ and $\hat{f}_2(\theta)$ are defined as in Section 2.2. Let $f_0(x,\dot{x}) \triangleq \left[\hat{f}_1(c'x) + \hat{f}_2(c'x)c'\dot{x}\right]$

Now we prove dissipativity of the system (4.4) with input u_2 and output

$$w \triangleq [c'x + \alpha_0c'\dot{x}] \tag{4.5}$$

where α_0 is a design parameter. Let

$$H(s) \triangleq c'(sI - A_0)^{-1}b_0 = \frac{m_2}{(\beta s + \alpha)(s+1)} \tag{4.6}$$

be the transfer function of the linear part of the system (4.4) as discussed in Chapter 2. In $H(s)$ there are no pole-zero cancellations, or equivalently the triple (A_0, b_0, c) is controllable and observable. Furthermore A_0 is a Hurwitz matrix.

As in (3.12) let

$$V(x) \triangleq x'Px + \alpha_0 \int_0^{c'x} \hat{f}_1(\theta)d\theta + \int_0^{c'x} \hat{f}_2(\theta)\theta d\theta \quad (4.7)$$

Along the solutions of (4.4),

$$\begin{aligned} \dot{V}(x,u_2) &= \dot{x}'Px + x'P\dot{x} + \alpha_0\hat{f}_1(c'x)c'\dot{x} \\ &\quad + \hat{f}_2(c'x)c'xc'\dot{x} \\ &= x'(PA_0 + A_0'P)x - \\ &\quad x'(2Pb_0 - A_0'c\alpha_0)f_0(x,\dot{x}) - \\ &\quad \alpha_0\hat{f}_2(c'x)(c'\dot{x})^2 + \hat{f}_2(c'x)c'xc'\dot{x} \\ &\quad + 2x'Pb_0u_2 \end{aligned}$$

where we use the fact that $c'b_0 = 0$. This can be written in the form :

$$\begin{aligned} \dot{V}(x,u_2) &= -(q'x)^2 - c'x\hat{f}_1(c'x) \\ &\quad -\alpha_0\hat{f}_2(c'x)(c'\dot{x})^2 + wu_2 \end{aligned} \quad (4.8)$$

where

$$\begin{aligned} w &\triangleq c'x + \alpha_0 c'A_0x \\ &= c'x + \alpha_0 c'\dot{x} \end{aligned}$$

if

$$PA_0 + A_0'P = -qq' \quad (4.9)$$

$$2Pb_0 = A_0'c\alpha_0 + c \quad (4.10)$$

Observe that u_2 appears in (4.4) as the only input, while u_1 is defined in terms of u_2 by the control law (4.3). Below we shall close the loop by feeding back u_2 to w, through a passive component in order to stabilize the system.

By an application of the Kalman-Yacubovich-Popov lemma (Lozano et al., 2000), the Riccati equation (4.9), (4.10) has a real solution $P = P' > 0$, q if

$$\mathrm{Re}(c' + \alpha_0 c'A_0)(j\omega I - A_0)^{-1}b_0 > 0; \quad \forall\omega \in R \quad (4.11)$$

Using the identity $sc'(sI - A_0)^{-1}b_0 \equiv c'b_0 + c'A_0(sI - A_0)^{-1}b_0$, (4.11) can be transformed to

$$\mathrm{Re}(1 + \alpha_0 j\omega)H(j\omega) > 0 \quad ; \quad \forall\omega \in R \quad (4.12)$$

(4.12) is satisfied for $\alpha > 0, \beta > 0$ and $\alpha_0 \geq \frac{\beta}{\alpha+\beta}$. Since in the system's state space $x_1\hat{f}_1(x_1) > 0$ for all $x_1 \neq 0$ and $\hat{f}_2(x_1) > 0$ for all x_1, it follows that

$$\dot{V}(x,u_2) \leq wu_2 \quad (4.13)$$

(4.13) means that (4.4) is dissipative with storage function $V(x)$ and supply rate wu_2. Figure 4.1 represents the partially closed loop in a block diagram form with passive components in the forward path and in two parallel feedback paths. If in addition to (4.12) we require that

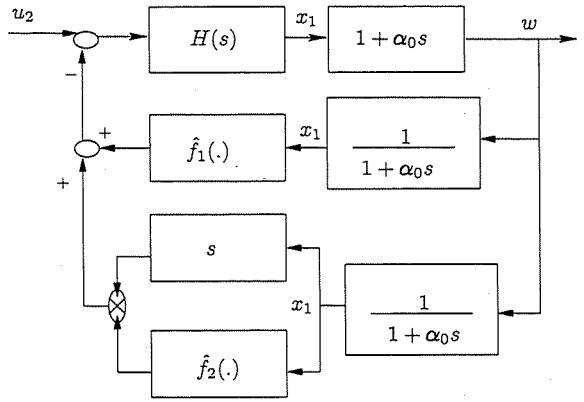

(b)

Figure 4.1: Partially closed feedback loop.

$$lim_{\omega\to\infty}\omega^2 Re(1 + \alpha_0 j\omega)H(j\omega) > 0 \quad (4.14)$$

then the forward path component in Figure 4.1 becomes output strictly passive and any negative feedback of w to u_2 through a passive dynamic component with finite gain stabilizes the loop. The choice

$$u_2(t) = -\beta_0 \left[\int_0^t w(\theta) d\theta \right]; \quad \beta_0 > 0 \tag{4.15}$$

or, in state representation,

$$\dot{y} = w \tag{4.16}$$

$$u_2 = -\beta_0 y \tag{4.17}$$

where $y(0) = u_2(0) = 0$ satisfies that condition. Alternatively we can prove global asymptotic stability in the sense of Liapunov. The closed loop state vector is $x_c \triangleq \begin{bmatrix} x_1 \\ x_2 \\ y \end{bmatrix}$. Let $W(x_c) \triangleq V(x) + \frac{\beta_0}{2} y^2$, which is positive definite and radially unbounded in x_c.

Then $wu_2 + \beta_0 y\dot{y} \equiv 0$ and

$$\begin{aligned} \dot{W}(x_c) &= -(q'x)^2 - c'x\hat{f}_1(c'x) \\ &\quad -\alpha_0 \hat{f}_2(c'x)(c'\dot{x})^2 \leq 0; \forall x_c \in R^3 \end{aligned}$$

Furthermore $\dot{W}(x_c) \equiv 0$ implies $x_1(t) \equiv \dot{x}_1(t) \equiv 0$, hence in view of (4.2), $x_2(t) \equiv 0$ and in view of (4.4),(4.17), $u_2(t) \equiv y(t) \equiv 0$, so $x_c(t) \equiv 0$. From basic Liapunov theory it follows that the closed loop set point $x_c = 0$ is globally asymptotically stable. (4.15), (4.16) can also be written as

$$u_2(t) = -\beta_0 \left[\int_0^t [c'x(\theta) + \alpha_0 c' A_0 x(\theta)] \, d\theta \right] \tag{4.18}$$

The relations (4.3), (4.18) define a linear globally asymptotically stabilizing multivariable PID-controller with controller parameters $\alpha > 0$, $\beta > 0$, $\alpha_0 \geq \frac{\beta}{\alpha+\beta}$, $\beta_0 > 0$.
A more general PID-controller is obtained replacing (4.17) by

$$u_2 = -\beta_0 y - \beta_1 w; \quad \beta_0 > 0, \beta_1 \geq 0 \tag{4.19}$$

It can be proved that using this control law we obtain a globally asymptotically stable closed loop.

Indeed (4.19) introduces an additional nonpositive term $-\beta_1 w^2$ in the expression of $\dot{W}(x_c)$

In conclusion we have the following linear globally asymptotically stabilizing multivariable PID-controller:

$$\begin{aligned} m_1 u_1 + m_2 u_2 &= (m_1(1+\vartheta) + \alpha) x_1 + (m_1 + \beta) \dot{x}_1 \\ &\quad + m_2 \dot{x}_2 \end{aligned} \tag{4.20}$$

where

$$u_2 = -\beta_0 \left[\int_0^t [(1 - \frac{\alpha_0 \alpha}{\beta}) x_1(\theta) + \frac{\alpha_0 m_2}{\beta} x_2(\theta)] d\theta \right]$$

The closed loop can be represented by the block diagram in Figure 4.2a and Figure 4.2b which are equivalent for a any value of $\alpha_0 \geq 0$.

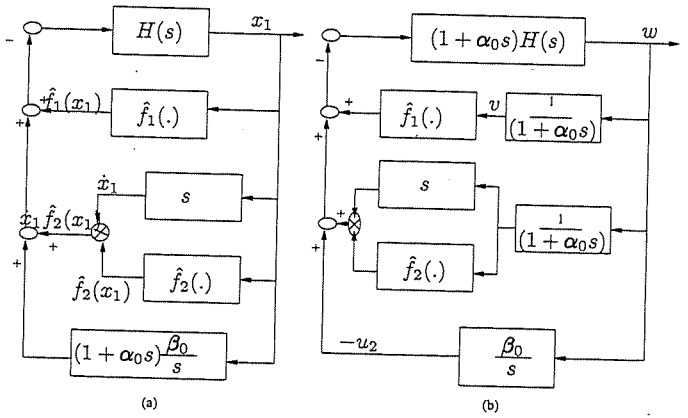

Figure 4.2: Block diagram of the system (4.4).

4.2 Control parameter tuning

In this section we apply the same technique as in Chapter 2 for tuning the PID-controller. Again, the system is represented in its linearized version and the

characteristic equation is obtained. Then the root locus technique is applied for parameter tuning. Finally we show some simulations in closed loop and compare the results with the PD-controller.

4.2.1 Linearized dynamics in the set point

Using a Taylor series expansion the linearization of (4.4), (4.16), (4.17) about the set point yields :

$$\dot{x}_1 = -\frac{\alpha}{\beta}x_1 + \frac{m_2}{\beta}x_2 \tag{4.21}$$

$$\dot{x}_2 = -a_0 x_1 - (1+b_{0l})x_2 - \beta_0 y \tag{4.22}$$

$$\dot{y} = (1-\frac{\alpha_0\alpha}{\beta})x_1 + \frac{\alpha_0 m_2}{\beta}x_2 \tag{4.23}$$

with a_0, b_{0l} given by (2.41).

In vector form we have:

$$\dot{x} = A_c x \tag{4.24}$$

$$A_c \triangleq \begin{bmatrix} -\frac{\alpha}{\beta} & \frac{m_2}{\beta} & 0 \\ -a_0 & -(1+b_{0l}) & -\beta_0 \\ (1-\frac{\alpha_0\alpha}{\beta}) & \frac{\alpha_0 m_2}{\beta} & 0 \end{bmatrix} \tag{4.25}$$

4.2.2 Root locus analysis of the closed loop dynamics

The closed loop characteristic equation for the linearized system becomes :

$$s(s+\frac{\alpha}{\beta})(s+1+b_0) + \frac{m_2(a_0+\beta_0\alpha_0)}{\beta}[s+\frac{\beta_0}{(a_0+\beta_0\alpha_0)}] = 0 \tag{4.26}$$

which can be written as:

$$s(s+c_1)(s+p_1) + \frac{k_1}{\beta}(s-q) = 0 \tag{4.27}$$

where

$$c_1 = \tfrac{\alpha}{\beta}; \quad p_1 = 1+b_0; \quad k_1 = m_2(a_0+\beta_0\alpha_0); \quad q = -\tfrac{\beta_0}{(a_0+\beta_0\alpha_0)}$$

and $\frac{\alpha}{\beta} > 0$, $\frac{1}{\beta} > 0$, $\beta_0 > 0$, $\alpha_0 \geq \frac{1}{1+\frac{\alpha}{\beta}}$ are the control parameters. It is clear that the position of the zero (q) in (4.27) changes from 0 to $-\frac{1}{\alpha_0}$ when β_0 varies from 0 to $+\infty$.

Hence for a proper choice of $\beta_0 > 0$, q can assume all values in the interval :

$$-(1+\tfrac{\alpha}{\beta}) < q < 0$$

irrespective the value of $\frac{1}{\beta}$. Figure 4.3 displays a root locus plot for $0 < \frac{1}{\beta} <$

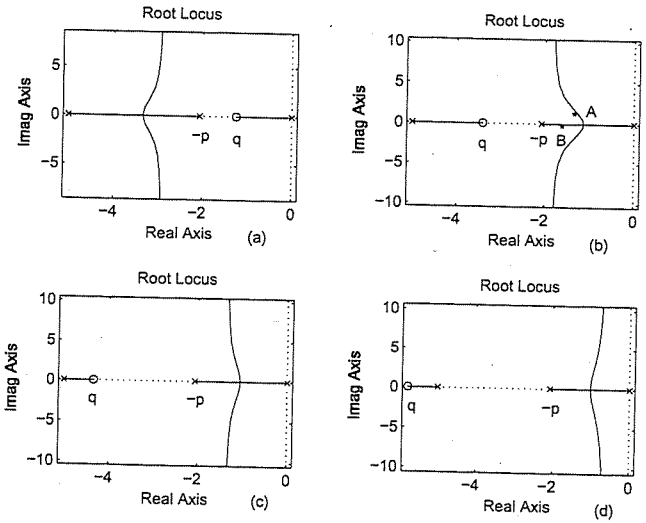

Figure 4.3: Root locus for Example 1, $\frac{\alpha}{\beta} = 5$; $\alpha_0 = 0.1667$; (a) $\beta_0 = 0.1$, (b) $\beta_0 = 0.5$, (c) $\beta_0 = 1$, (d) $\beta_0 = 10$

$+\infty$ and the shift in the eigenvalue spectrum when we change the parameter β_0 from 0.1 to 10.

Observe that the zero q moves further to the left when we increase the value of β_0. The vertical asymptote changes its position to the right according to the

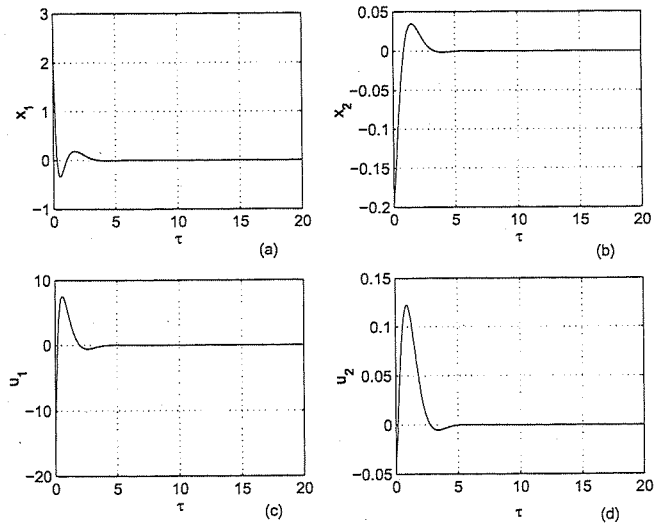

Figure 4.4: Transient response for Example 1, $\frac{\alpha}{\beta} = 5$, $\beta_0 = 0.5$, $\frac{1}{\beta} = 3.7.10^{-16}$, $\alpha_0 = 0.1667$, $x(0) = (3, -0.2, 0.1)$; (a) Temperature deviation, (b) Concentration deviation, (c) Input, u_1, (d) Input, u_2

relation :

$$s = -\frac{[\frac{\alpha}{\beta} + 1 + b_0 + q]}{2} \tag{4.28}$$

Now we display some simulation diagrams to illustrate the way the controller parameters are selected. Figure 4.4 shows the transient response for the linearized dynamical system for specific values of the parameters corresponding to an oscillatory response (see point A in Figure 4.3) while Figure 4.5 shows a non-oscillatory response (point B on the real axis, Figure 4.3). The following

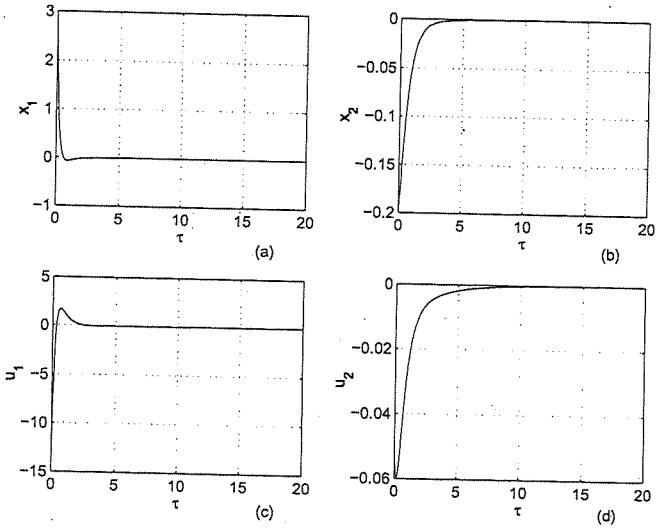

Figure 4.5: Transient response for Example 1, $\frac{\alpha}{\beta} = 5$, $\beta_0 = 0.5$, $\frac{1}{\beta} = 8.72.10^{-17}$, $\alpha_0 = 0.1667$, $x(0) = (3, -0.2, 0.1)$; (a) Temperature deviation, (b) Concentration deviation, (c) Input, u_1, (d) Input, u_2

conclusions can be drawn about the transients' rate of decay. The rate of decay improves if :

- β_0 increases and α_0 decreases: This moves the zero at s=q to the left. Figure 4.6 shows this effect. After α_0 reaches the value 0.019 we do not gain much by further decreasing its value but we note a large shift of the asymptote to the left.

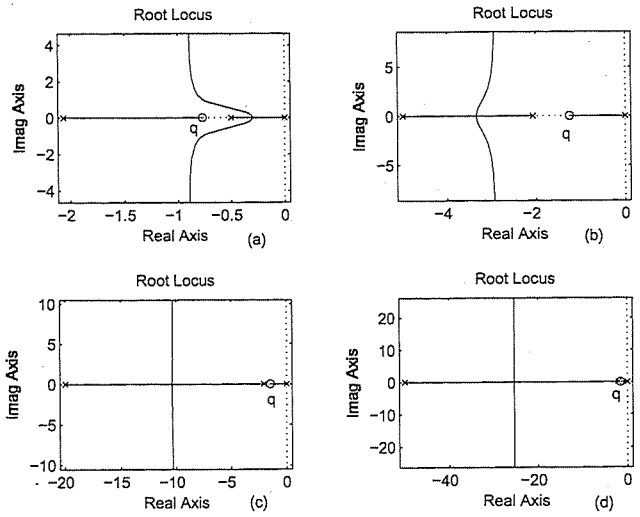

Figure 4.6: Root locus for Example 1, $\frac{\alpha}{\beta} = 5$, $\beta_0 = 0.1$; (a) $\alpha_0 = 0.5$, (b) $\alpha_0 = 5$, (c) $\alpha_0 = 20$, (d) $\alpha_0 = 50$

- $\frac{\alpha}{\beta}$ **increases: This compensates the influence of q on the location** of the asymptote and moves it to the left.

Based on this analysis we choose $\alpha_0 = \frac{1}{1+\frac{\alpha}{\beta}}$ and take $\frac{\alpha}{\beta}$ and β_0 **sufficiently large.**

If $\frac{1}{\beta} \to +\infty$ the rate of decay tends to :

$$\begin{aligned} \nu &\to min\{-q, \frac{1}{2}(\frac{\alpha}{\beta}+1+b_0+q)\} \\ &\leq \frac{1}{2}(\frac{\alpha}{\beta}+1+b_0+q) \\ &< \frac{1}{2}(\frac{\alpha}{\beta}+1+b_0) \end{aligned}$$

Now we **illustrate the main differences between the PD and PID** strategies. Figure 4.7 shows the response of the CSTR using a linear PID controller. We took the same initial condition (x0=-0.4;0.1) as in the case of the PD controller (see Figures 3.6 and 3.9). In the case of PID controller we obtained less overshoot but a bigger settling time (the same ζ factor has been selected for the PD-controller as well as for the PID).

Now we compare the PD-controller and the PID-controller (see Figures 4.8, 4.9 and 4.10) when starting from the same initial condition $((-0.4; 0.1; 0.1))$. The D-action in the PD-controller produces a strong damping to the changes of x_1. The D-action is more active in the maximum and minimum points of the control signal, this is because the D-action is controlling the future deviation. **In this way we can select a bigger amplification for the P-controller** without having oscillations in the control action. Also, after some simulations it was found that the surplus deviation diminishes. Furthermore by increasing α and or β_1 we increase the proportional action and by increasing β, β_1 or α_0 the **D-action effect over the temperature variable is stronger.** It should be noticed that the derivative action over the concentration variable **is fixed and given by** $\frac{m_2}{m_1}$, so in this way the control law u_1 can do nothing to regulate the deviation of x_2. On the other hand, increasing β_1 **gives an amplification of the proportional** gain and makes the derivative action stronger. An additional increase of the parameter α_0 originates a bigger impact on the D-action of the control law u_2.

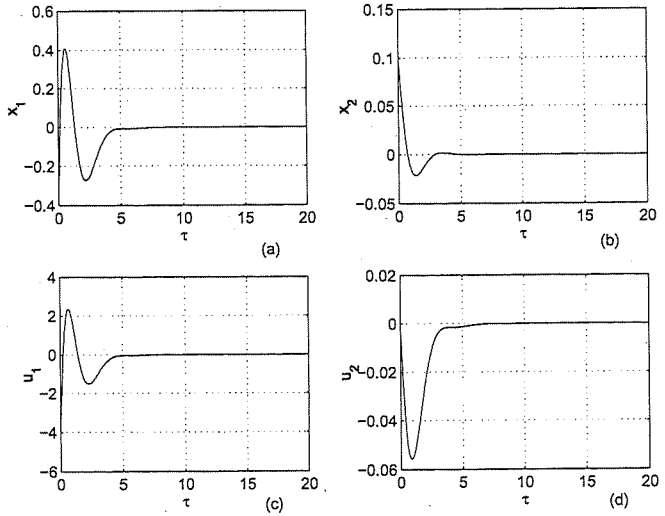

Figure 4.7: Transient response for the nonlinear CSTR Example 1, $\beta_0 = 0.1$, $\frac{1}{\beta} = 3.8.10^{-16}$, $\alpha = 2.63.10^{15}$, $\alpha_0 = 0.5$, $\alpha/\beta = 1$; (a) Temperature deviation, (b) Concentration deviation, (c) Control action u_1, (d) Control action u_2

We now see less overshoot in the temperature response (x_1) in the case of the PD-controller but a bigger settling time with respect to the PID-controller. However in the case of the PD-controller the concentration response (x_2) has no overshoot and a quick response when compared with the PID-controller. Finally less control consumption and time response is observed in the case of PD-control using the two available inputs u_1 and u_2.

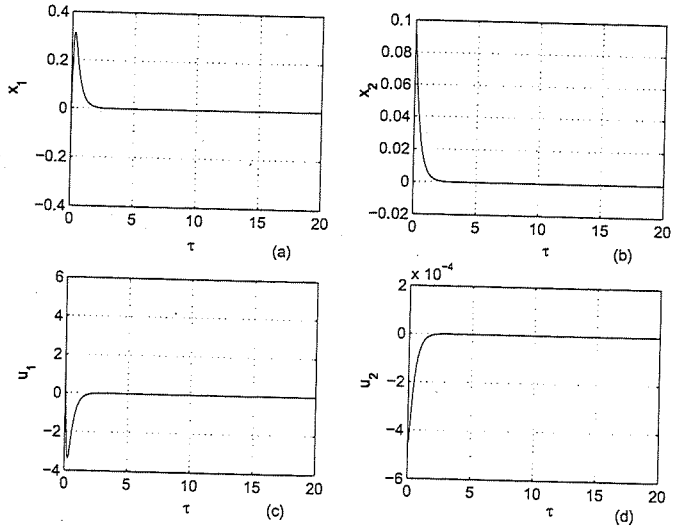

Figure 4.8: Transient response and PD-control signals for Example 1, $\beta_1 = 0.001$, $\alpha = 1.428e^{16}$, $\beta = 1.428e^{15}$, $\alpha_0 = 0.0909$; (a) Temperature deviation, (b) Concentration deviation, (c) Control action u_1, (d) Control action u_2

Until now all the reported simulations do not involve the presence of disturbances, however the PID-controller improves the system's performance in the presence of disturbances as we discuss in the next section.

4.2.3 System performance in the presence of disturbances

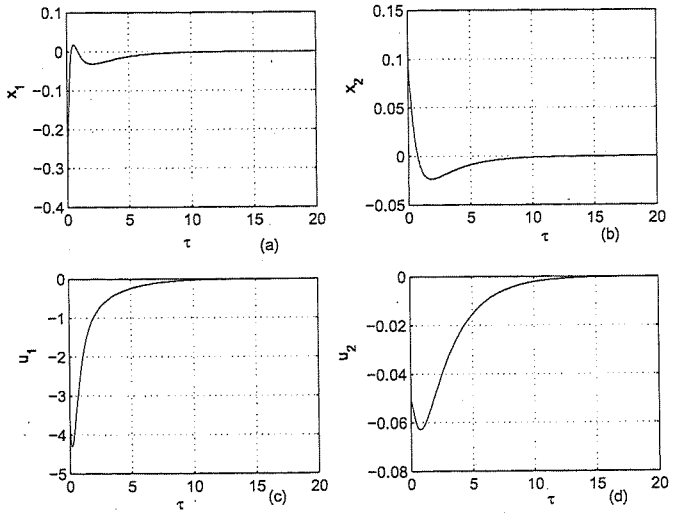

Figure 4.9: Transient response and PID-control signals for Example 1, $\beta_0 = 0.5$, $\alpha = 5.734e^{16}$, $\beta = 1.1468e^{16}$, $\alpha_0 = 0.1667$; (a) Temperature deviation, (b) Concentration deviation, (c) Control action u_1, (d) Control action u_2

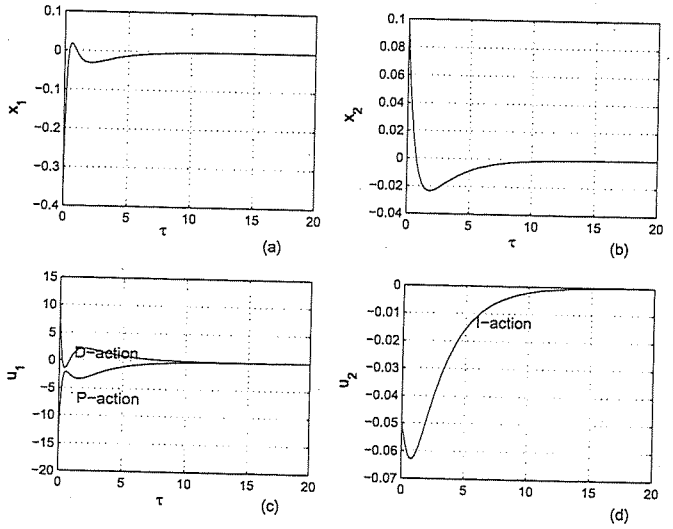

Figure 4.10: Transient response and PID-action signals for Example 1, $\beta_0 = 0.5$, $\alpha = 5.734e^{16}$, $\beta = 1.1468e^{16}$, $\alpha_0 = 0.1667$; (a) Temperature deviation, (b) Concentration deviation, (c) Control action u_1, (d) Control action u_2

Consider the system

$$\dot{z} = f(z) \quad ; \quad z \in R^n \tag{4.29}$$

Let $f(z_s) = 0$ such that $z(t) \equiv z_s$ is an equilibrium solution. Let

$$J(z) \triangleq \frac{\partial f(z)}{\partial z} = \begin{pmatrix} \frac{\partial f_1}{\partial z_1} & \frac{\partial f_1}{\partial z_2} & \cdots & \frac{\partial f_1}{\partial z_n} \\ \frac{\partial f_2}{\partial z_1} & \frac{\partial f_2}{\partial z_2} & \cdots & \frac{\partial f_2}{\partial z_n} \\ \vdots & \vdots & & \\ \frac{\partial f_n}{\partial z_1} & \frac{\partial f_n}{\partial z_2} & \cdots & \frac{\partial f_n}{\partial z_n} \end{pmatrix} \tag{4.30}$$

be the system's Jacobian and assume that $J(z_s)$ is a Hurwitz matrix (all eigenvalues in $Re\{s\} < 0$). Then by the linearization principle $z(t) \equiv z_s$ is a locally asymptotically stable equilibrium. Next consider the system

$$\dot{z} = f(z) + d \quad ; \quad z, d \in R^n \tag{4.31}$$

where d is a constant disturbance. Assume that

$$f(z_d) + d = 0$$

such that $z(t) \equiv z_d$ is an equilibrium solution of the perturbed system. Assume that $z_d \to z_s$ if $d \to 0$. Then $J(z_d) \to J(z_s)$ for $d \to 0$. Hence $J(z_d)$ is a Hurwitz matrix if $|d|$ **is sufficiently small.** So $z(t) \equiv z_d$ is a locally asymptotically stable equilibrium for the perturbed system if $|d|$ **is sufficiently small.**

In the present case the PID-controlled system with a constant disturbance

$$d \triangleq \begin{bmatrix} d_1 \\ d_2 \end{bmatrix}$$

reads, for the forward path system,

$$\begin{aligned} \dot{z}_1 &= r - (1+\vartheta)z_1 + m_2 z_2 f(z_1) + u_1 + d_1 \\ \dot{z}_2 &= 1 - z_2 - m_1 z_2 f(z_1) + u_2 + d_2 \\ \dot{y} &= w = x_1 + \alpha_0 \dot{x}_1 \end{aligned} \tag{4.32}$$

and for the control law,

$$\begin{aligned} u_2 &= -\beta_0 y \\ u_1 &= \frac{u_0 - m_2 u_2}{m_1} \end{aligned} \tag{4.33}$$

$$u_0 = [m_1(1+\vartheta) + \alpha]x_1 + (m_1 + \beta)\dot{x}_1 + m_2\dot{x}_2$$

The state deviations and their derivatives are given by :

$$\begin{aligned} x_1 &= z_1 - z_{1s} \\ x_2 &= z_2 - z_{2s} \\ \dot{x}_1 &= \dot{z}_1 \\ \dot{x}_2 &= \dot{z}_2 \end{aligned} \tag{4.34}$$

$z_s \triangleq \begin{bmatrix} z_{1s} \\ z_{2s} \end{bmatrix}$ is the closed loop set point. If $d_1 = d_2 = 0$, then $z \equiv z_s$ is globally asymptotically stable, so it is certainly locally asymptotically stable. Now assume that $|d_1|$, $|d_2|$ **are sufficiently small and let** z_d be the equilibrium point of the perturbed system, such that

$$z_d \to z_s \quad \text{for} \quad d \to 0$$

We then have that for the perturbed system $z(t) \equiv z_d$ is locally asymptotically stable. In the equilibrium point $z = z_d$ we have :

$$\dot{y} = 0; \quad \dot{x}_1 = 0 \Rightarrow x_1 = 0; z_1 = z_{1s}; \quad \dot{x}_2 = 0 \Rightarrow u_0 = 0$$

$$m_1 r + m_2 - m_1(1+\vartheta)z_1 - m_2 z_2 + m_1 u_1 + m_2 u_2 + m_1 d_1 + m_2 d_2 = 0 \tag{4.35}$$

Without disturbances we have :

$$m_1 r + m_2 - m_1(1+\vartheta)z_{1s} - m_2 z_{2s} = 0 \tag{4.36}$$

Since in (4.35) $u_0 = m_1 u_1 + m_2 u_2 = 0$ **we finally get :**

$$m_2(z_{2s} - z_2) + m_1 d_1 + m_2 d_2 = 0$$

We conclude that for the perturbed system the equilibrium point $z = z_d$ **satisfies** :

$$\begin{aligned} z_{1d} &= z_{1s} \\ z_{2d} &= z_{2s} + \frac{m_1 d_1 + m_2 d_2}{m_2} \end{aligned}$$

A small constant perturbation brings the reactor to a new locally asymptotically stable equilibrium point with the same reactor temperature ($z_{1d} = z_{1s}$)

but with a different reactor concentration ($z_{2d} \neq z_{2s}$).

The reason for this behaviour is that the PID-controller integrates the temperature deviation before feedback.

Figures (4.14 and 4.15) show the transient response for both the non-disturbed and the disturbed system for Example 1. We observed the PID-controller and process behaviour after the constant disturbance. An external disturbance source d_1 influences the process at instant t_0, in such a way that the concentration variable tries to deviate a little bit from its set point. We have used values of the disturbance d_1 only for the first state variable x_1. As we have taken small values for the disturbance, then there are only small deviations in the responses in steady state.

Now we study other disturbances such as a sinusoidal signal with different amplitudes. Figure 4.9 is an illustration of the transient response of the CSTR when applying a constant disturbance d_1 and a PID-controller, while Figures 4.11 and 4.12 show the effect of the sinusoidal signals $d_1 = 0.001 * sin(t)$ and $d_1 = 0.1 * sin(t)$. We conclude that as soon as we increase the amplitude of the disturbance, some oscillations appear on the temperature response as well as on the control actions. The concentration remains stable in the presence of this kind of disturbances.

Figure 4.13 shows how the transients and the control actions remain in a permanent oscillation after the following disturbances appear : $d_1 = e^{-4} + e^{-4} * sin(t)$,$d_2 = e^{-4} + e^{-2} * sin(t)$

As a conclusion we have :

- By tuning the parameters α and β_1 for a well tuned proportional controller, we have small oscillations and then finally a permanent deviation.
- When adding the integral action I, then with the same amplification of the P-controller the control will be a little bit more oscillatory because the I-action makes the P-action to increase.
- Finally, if we add D-action to the PI-controller, then we note a damped movement because the D-action works against the oscillations generated by the I- action, that is works against the quick changes of the state deviations.

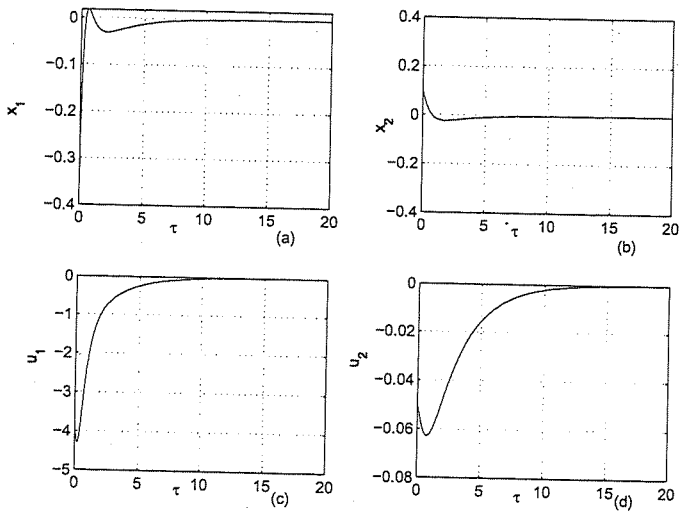

Figure 4.11: Transient response and PID-control signals for Example 1, $\beta_0 = 0.5$, $\alpha = 5.734e^{16}$, $\beta = 1.1468e^{16}$, $\alpha_0 = 0.1667$,$d_1 = e^{-3} * sin(t)$; (a) Temperature deviation, (b) Concentration deviation, (c) Control action u_1, (d) Control action u_2

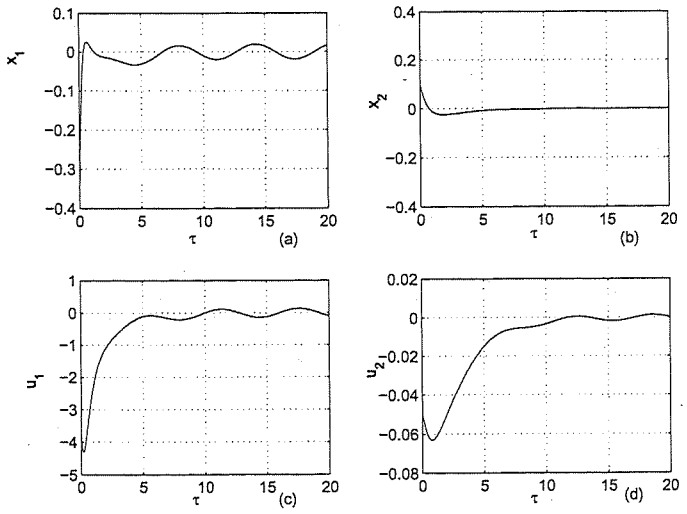

Figure 4.12: Transient response and PID-control signals for Example 1, $\beta_0 = 0.5$, $\alpha = 5.734e^{16}$, $\beta = 1.1468e^{16}$, $\alpha_0 = 0.1667$,$d_1 = 0.1 * sin(t)$; (a) Temperature deviation, (b) Concentration deviation, (c) Control action u_1, (d) Control action u_2

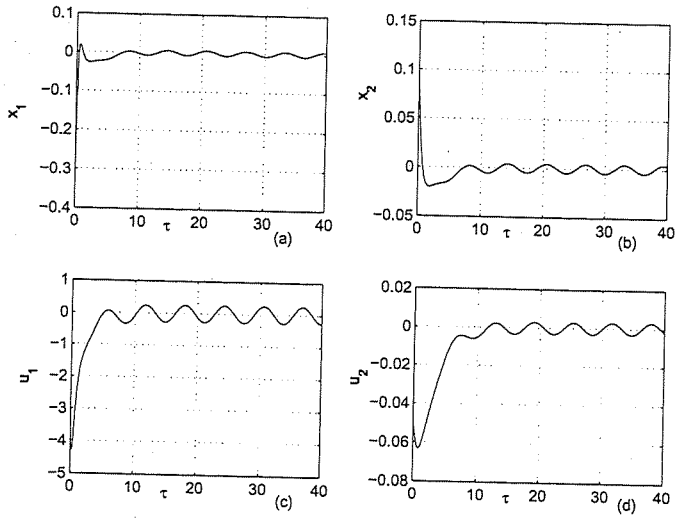

Figure 4.13: Transient response and PID-control signals for Example 1, $\beta_0 = 0.5$, $\alpha = 5.734e^{16}$, $\beta = 1.1468e^{16}$, $\alpha_0 = 0.1667$,$d_1 = e^{-4} + e^{-4} * sin(t)$,$d_2 = e^{-4} + e^{-2} * sin(t)$; (a) Temperature deviation, (b) Concentration deviation, (c) Control action u_1, (d) Control action u_2

The integral action (I) has the disadvantage that it increases the decay rate, that is it makes the stationary state to be reached slowly. However, it has the advantage to make the system insensible to the presence of disturbances in the case of temperature, which is the variable that directly receives the integral action. The integral action has not been applied over the concentration because in this way it would be not possible to reach the goal of having a globally asymptotically stable system.

If we have a set point for the temperature, x_{1s} and suddenly a disturbance appears, then the temperature will be in the same value showing its insensitivity to the presence of disturbances, and the concentrations set point is moving a little bit due to the presence of the disturbance.

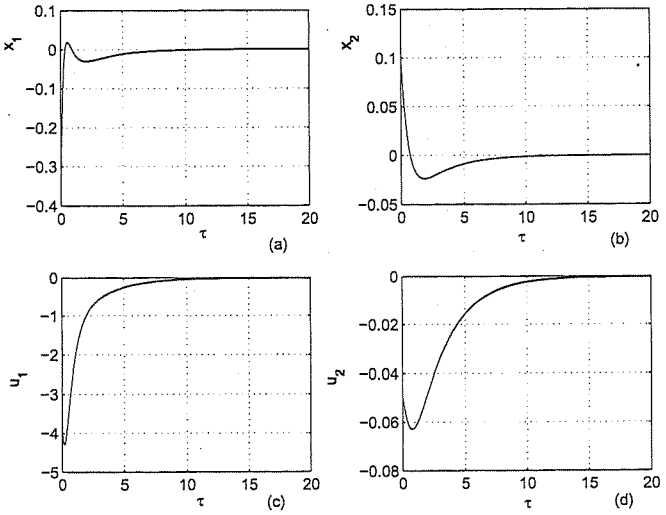

Figure 4.14: Transient response and PID-control signals for Example 1, $\beta_0 = 0.5$, $\alpha = 5.734e^{16}$, $\beta = 1.1468e^{16}$, $\alpha_0 = 0.1667$,$d_1 = 0.01$; (a) Temperature deviation, (b) Concentration deviation, (c) Control action u_1, (d) Control action u_2

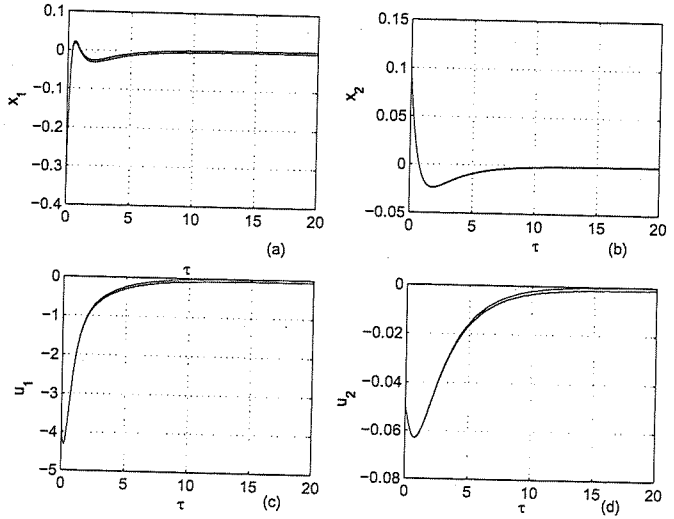

Figure 4.15: Transient response and PID-control signals for Example 1, $\beta_0 = 0.5$, $\alpha = 5.734e^{16}$, $\beta = 1.1468e^{16}$, $\alpha_0 = 0.1667$,$d_1 = 0.03$; (a) Temperature deviation, (b) Concentration deviation, (c) Control action u_1, (d) Control action u_2

4.2.4 Generalizations

In (4.16), (4.19) a more general PID-controller was obtained selecting u_2 as :

$$\begin{aligned} u_2 &= -\beta_0 y - \beta_1 w \\ \dot{y} &= w \end{aligned}$$

where

$$\beta_0 > 0; \quad \beta_1 > 0$$

In this case the closed loop linearized state equations become :

$$\begin{aligned} \dot{x}_1 &= -\frac{\alpha}{\beta}x_1 + \frac{m_2}{\beta}x_2 \qquad (4.37) \\ \dot{x}_2 &= -x_2 - a_0 x_1 - b_0 x_2 - \beta_0 y - \beta_1 (x_1 - \alpha_0 \frac{\alpha}{\beta}x_1 + \alpha_0 \frac{m_2}{\beta}x_2) \\ \dot{y} &= (1 - \frac{\alpha_0 \alpha}{\beta})x_1 + \frac{\alpha_0 m_2}{\beta}x_2 \end{aligned}$$

In vector form we have :

$$\dot{x} = A_c x \qquad (4.38)$$

with

$$A_c \triangleq \begin{bmatrix} -\frac{\alpha}{\beta} & \frac{m_2}{\beta} & 0 \\ -(a_0 + \beta_1 - \frac{\alpha_0 \alpha \beta_1}{\beta}) & -(1 + b_0) - \frac{\beta_1 \alpha_0 m_2}{\beta} & -\beta_0 \\ 1 - \frac{\alpha_0 \alpha}{\beta} & \frac{\alpha_0 m_2}{\beta} & 0 \end{bmatrix}$$

The characteristic equation becomes :

$$s(s + \frac{\alpha}{\beta})(s + 1 + b_0) + \frac{m_2}{\beta}[\beta_1 \alpha_0 s^2 + (a_0 + \beta_1 + \alpha_0 \beta_0)s + \beta_0] = 0 \qquad (4.39)$$

which can be written as :

$$s(s + \frac{\alpha}{\beta})(s + 1 + b_0) + \frac{m_2 \beta_1 \alpha_0}{\beta}(s - q_1)(s - q_2) = 0 \qquad (4.40)$$

where

$$\begin{aligned} q_1 + q_2 &= -[\frac{1}{\alpha_0} + \frac{\beta_0}{\beta_1} + \frac{a_0}{\beta_1 \alpha_0}] \\ q_1 q_2 &= \frac{\beta_0}{\beta_1 \alpha_0} \end{aligned}$$

The zeros q_1 and q_2 satisfy :

$$(\beta_0 + \beta_1 s)(1 + \alpha_0 s) + a_0 s = 0 \qquad (4.41)$$

A root locus plot for (4.41) with given values of β_0, β_1, α_0 and $0 < a_0 < +\infty$ shows that the full spectrum falls on the real axis of the complex plane. In other words q_1 and q_2 are real and either:

$$0 > q_1 > -\tfrac{1}{\alpha_0} > -\tfrac{\beta_0}{\beta_1} > q_2$$

or:

$$0 > q_1 > -\tfrac{\beta_0}{\beta_1} > -\tfrac{1}{\alpha_0} > q_2$$

A root locus for the characteristic equation (4.40) with $0 < \frac{1}{\beta} < +\infty$ is now displayed in Figure 4.16. We can make $-(q_1 + q_2)$ and $q_1 q_2$ both arbitrarily

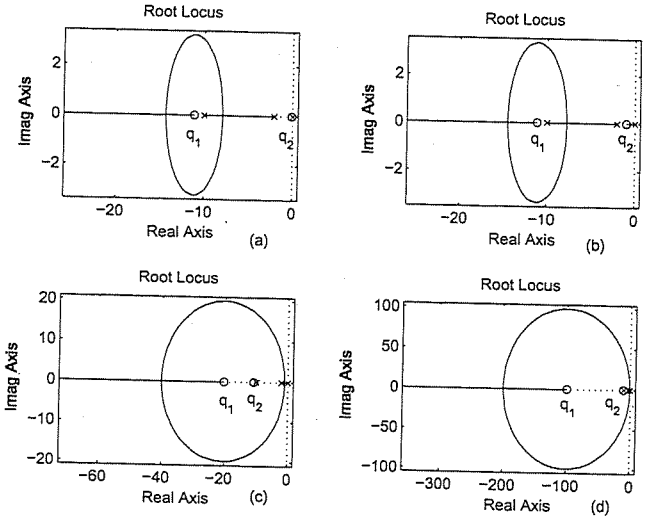

Figure 4.16: Root locus for Example 1, $\frac{\alpha}{\beta} = 10$, $\beta_1 = 5$, $\alpha_0 = 0.0909$; (a) $\beta_0 = 0.5$, (b) $\beta_0 = 5$, (c) $\beta_0 = 100$, (d) $\beta_0 = 500$

large by letting $\beta_0 \to +\infty$ and $\beta_1 \to 0$. So we can move the zeros q_1 and q_2 arbitrarily far to the left. This effect is observed in Figure 4.16 where we see that the spectrum moves towards the left for high values of the parameter β_0

Now the system has the following properties :

- There is an interval of values for β which yields an oscillatory response :

$$\frac{1}{\beta_a} < \frac{1}{\beta} < \frac{1}{\beta_b} \to \text{oscillatory response}$$

- The rate of decay of the response can be made arbitrarily large (by moving q_1 and q_2 to the left and taking $\frac{1}{\beta}$ sufficiently large).

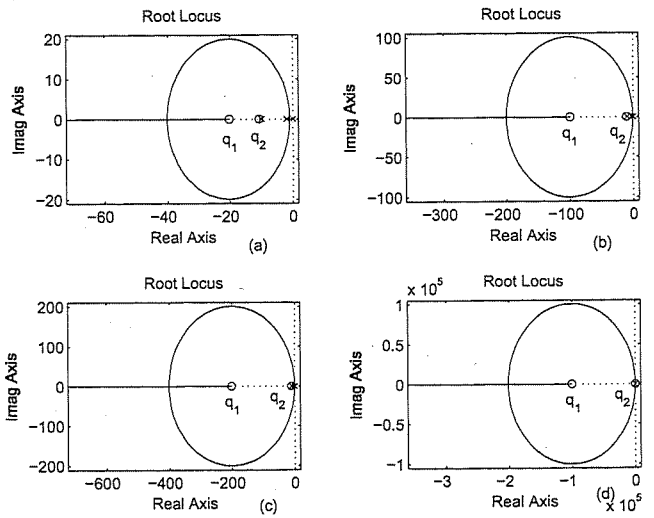

Figure 4.17: Root locus for Example 1, $\beta_0 = 100$, $\frac{\alpha}{\beta} = 10$, $\alpha_0 = 0.0909$; (a) $\beta_1 = 5$, (b) $\beta_1 = 1$, (c) $\beta_1 = 0.5$, (d) $\beta_1 = 0.001$

Figure 4.17 shows the effect on the eigenvalue spectrum when we change the parameter β_1. We again conclude that when this parameter goes to zero we push the zeros q_1 and q_2 towards the left .

4.2.5 Simulation results

In this section we display and discuss some computer generated step responses.

Figure 4.18 shows the simulation result for the nonlinear CSTR using the same parameters which were tuned for the linearized approximation of Figure 4.4. We obtain more or less the same behaviour as in the linear case. Figure 4.19

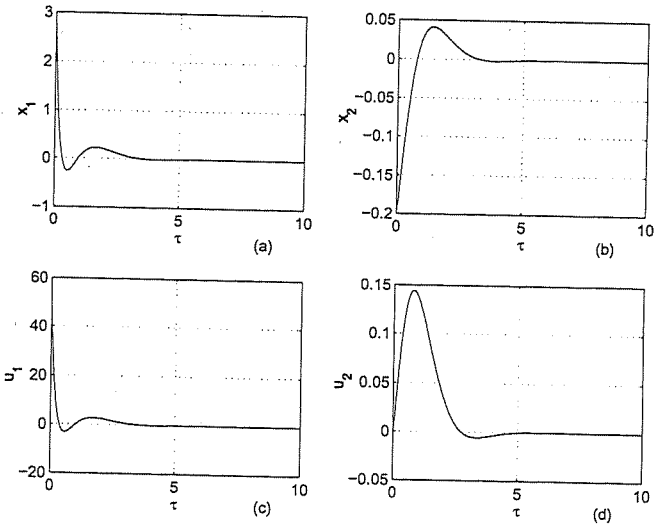

Figure 4.18: Transient response for Example 1, $\beta_0 = 0.5$, $\frac{1}{\beta} = 3.7.10^{-16}$, $\alpha = 1.35.10^{16}$, $\alpha_0 = 0.1667$; (a) Temperature deviation, (b) Concentration deviation, (c) Control action u_1, (d) Control action u_2

shows the simulation results using the same parameters which were tuned for the linearized approximation of Figure 4.5. We see that the response for the nonlinear system illustrates a stable behaviour with a small overshoot in the concentration response compared with the linear case. Besides in the controller signal u_2 we appreciate a small oscillation compared with a soft response observed in the linear system without oscillations in the signals.

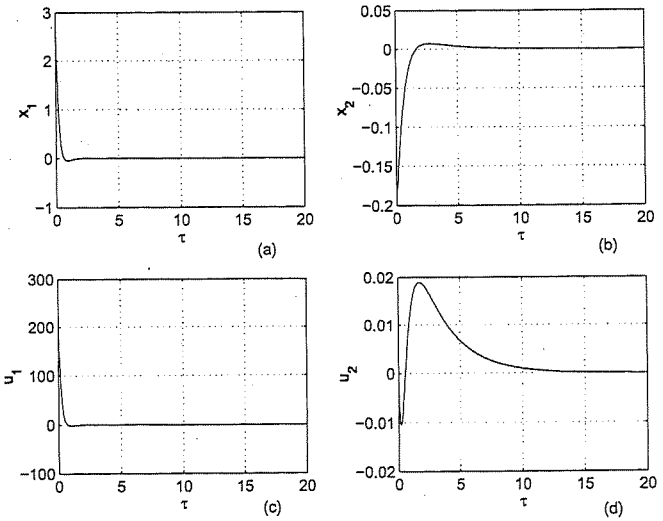

Figure 4.19: Transient response for Example 1, $\beta_0 = 0.5$, $\frac{1}{\beta} = 8.72.10^{-17}$, $\alpha = 5.73.10^{16}$, $\alpha_0 = 0.1667$, $x(0) = (3, -0.2, 0)$; (a) Temperature deviation, (b) Concentration deviation, (c) Control action u_1, (d) Control action u_2

So the controller parameters found with the root locus technique might be used as a first guess. Then if necessary retuning the controller parameters by trial and error can be done to obtain a better response.

Figure 4.20 shows a response which is obtained using the same parameters as in Figure 4.18 except that we have adopted a smaller value for β_0. As a result we obtain less overshoot on the temperature and concentration responses but the settling time becomes larger. By comparing Figure 4.20 and Figure 4.21 we

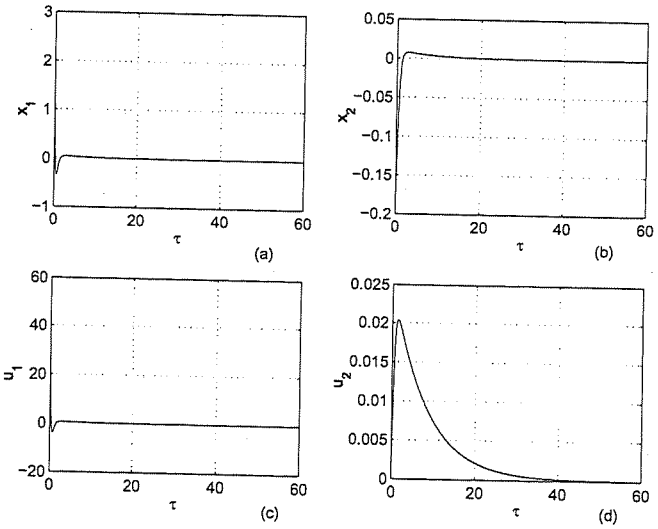

Figure 4.20: Transient response for Example 1, $\beta_0 = 0.05$, $\frac{1}{\beta} = 3.7.10^{-16}$, $\alpha = 1.35.10^{16}$, $\alpha_0 = 0.1667$, $x(0) = (3, -0.2, 0)$; (a) Temperature deviation, (b) Concentration deviation, (c) Control action u_1, (d) Control action u_2

conclude that using a two-input PD-controller has the advantage of reaching the steady state in a very short period of time. However the disadvantage is that a high value for the control effort is needed at the beginning of the transient where the temperature deviation reaches a high negative value.

For Example 2, good transients are observed in both temperature and concen-

tration deviations when using the two input PID-controller . Also the variations of the controller deviations are smooth (Figures 4.22 and 4.23).

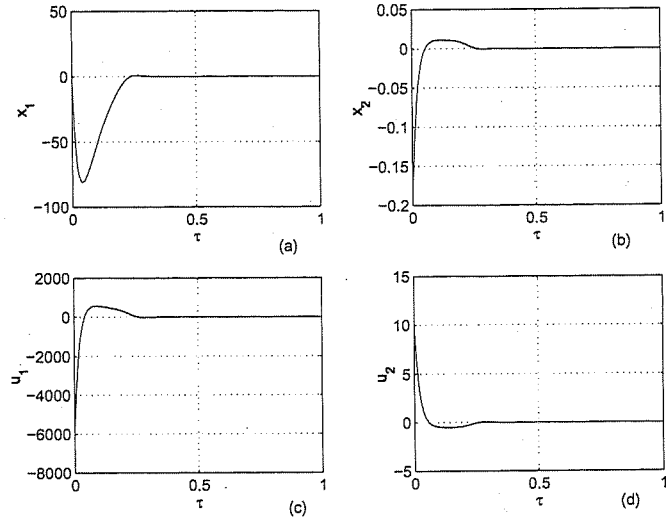

Figure 4.21: Transient response for Example 1 using a two input PD-controller, $\beta_1 = 0.01$, $\frac{1}{\beta} = 4.10^{-13}$, $\alpha = 1.25.10^{13}$, $\alpha_0 = 0.1667$, $x(0) = (3, -0.2)$; (a) Temperature deviation, (b) Concentration deviation, (c) Control action u_1, (d) Control action u_2

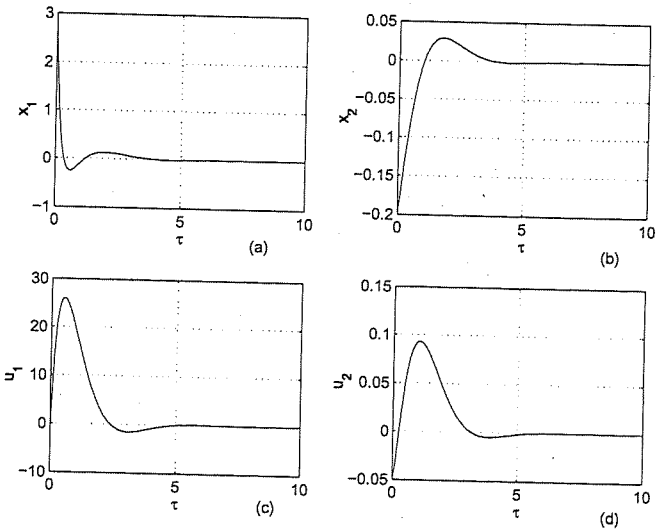

Figure 4.22: Transient response for the linearized system of Example 2, $\beta_0 = 0.5$, $\frac{1}{\beta} = 1.62.10^{-12}$, $\alpha = 3.08.10^{12}$, $\alpha_0 = 0.1667$, $x(0) = (3, -0.2, 0)$; (a) Temperature deviation, (b) Concentration deviation, (c) Control action u_1, (d) Control action u_2

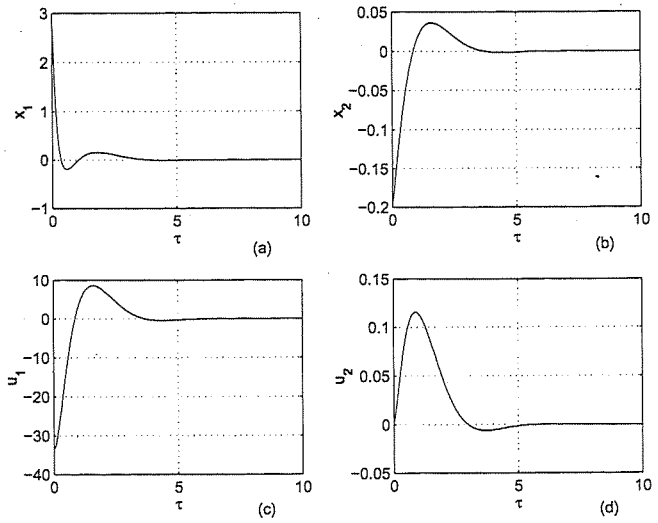

Figure 4.23: Transient response for the nonlinear system of Example 2, $\beta_0 = 0.5$, $\frac{1}{\beta} = 1.62.10^{-12}$, $\alpha = 3.08.10^{12}$, $\alpha_0 = 0.1667$, $x(0) = (3, -0.2, 0)$; (a) Temperature deviation, (b) Concentration deviation, (c) Control action u_1, (d) Control action u_2

4.3 Stability regions under state constraints

Here we consider a different aspect of the system's closed loop behaviour and the controller tuning problem. For technical reasons it may be neccesary to design the controller in such a way that during operation the control input variations and the state variable deviations from their set point values remain within given bounds.

We compute and maximize regions of initial states in state space from which the controller drives the system to its set point while satisfying such constraints. These regions show to what extent the set point is stabilized under practical operating conditions.

4.3.1 Theoretical analysis

To illustrate this technique we consider a reactor temperature constraint $x_1 \leq a$, $a > 0$. We use here a PID controller with u_2 of the form given by (4.15).

Let

$$P_a \triangleq \{x_c \in R^3; x_1 = a\}$$
$$S_k \triangleq \{x_c \in R^3; W(x_c) = k\}$$

(See Figure 4.24). On the plane P_a, $W(x_c)$ is a radially unbounded quadratic function of x_2 and y (because here x_1 is constant). Hence it possesses a unique minimum k_a :

$$k_a = minW(x_c) \text{ for } x_c \in P_a$$

This value k_a can be understood as the value of k where the surface S_k for the first time reaches the plane P_a.

If $k < k_a$ then $S_k \cap P_a$ is empty, if $k = k_a$ it is the single point A shown in Figure 4.24 and if $k > k_a$ the intersection is an ellipse in P_a. We have

$$\frac{d}{dt}W(x_c) = [grad \quad W(x_c)]'\dot{x}_c < 0; x_c \in P_a.$$

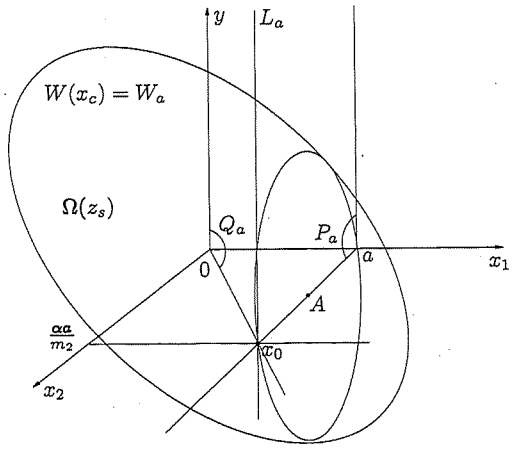

Figure 4.24: Computing stability regions under a reactor temperature constraint.

Therefore in the point A :

$\dot{x}_1 < 0$ since $\{S_k; \quad k = k_a\}$ and P_a are tangent in A, hence grad $W(x_c)$ and grad x_1 have the same direction in A.

Let

$$Q_a \triangleq \{x_c \in R^3; \dot{x}_1 = 0\} = \{x_c \in R^3; \quad m_2 x_2 = \alpha x_1\}$$
$$L_a \triangleq P_a \cap Q_a = \{x_c \in R^3; x_1 = a, x_2 = \frac{\alpha}{m_2} a\}$$

The minimum value of the Liapunov function over the line L_a, is

$$W_a \triangleq min W(x_c) \quad for \quad x_c \in L_a$$
$$\triangleq x_0' P x_0 + \alpha_0 \int_0^a \hat{f}_1(\theta) d\theta + \int_0^a \hat{f}_2(\theta) \theta d\theta;$$

where

$$x_0 \triangleq \begin{bmatrix} a \\ \frac{\alpha a}{m_2} \end{bmatrix}$$

We have :

Theorem 1 :

Any initial state in the set $\Omega(z_s) \triangleq \{x_c \in R^3; W(x_c) < W_a; x_1 < a\}$ generates a trajectory converging to $x_c = 0$ along which the constraint $x_1 < a$ is satisfied.

Indeed the trajectory cannot cross the boundary of $\Omega(z_s)$ through the surface $W(x_c) = W_a$ since $W(x_c)$ is non-increasing along the system's trajectories. **The trajectory cannot cross the boundary of $\Omega(z_s)$** through the plane P_a since $\dot{x}_1 < 0$ in A, hence in any point of intersection of P_a and $\{S_k; \quad k \leq W_a\}$.

So the trajectory cannot leave $\Omega(z_s)$. Since the closed loop set point is globally asymptotically stable the trajectory converges to $x_c = 0$ without leaving the set $\Omega(z_s)$.

A similar analysis applies to constraints on x_2 or constraints on the control variables. **However these cases are more difficult since here** we do not have a quadratic minimization problem with linear constraints, unless we replace $W(x_c)$ by its quadratic approximation and use the linearized system equations.

4.3.2 Simulation results

We compute stability regions with state constraints for two reactor examples. As explained before both examples possess two stable and one unstable open loop equilibrium points. The controller globally stabilizes the unstable equilibrium while the other equilibria disappear in closed loop.

Tuning the controller may require some trade-off between maximizing the stability regions and optimizing the controlled system's transients during convergence to the set point. For both examples a satisfactory choice of the controller parameters has been obtained and some simulation results have been displayed in Figures 4.25 and 4.26. These include an estimate of the set point's region

of attraction in state space and intersections of the estimate with the planes $x_1 = 0$, $x_2 = 0$ and y=0 respectively, under a temperature constraint $x_1 < 0.1$.
Making a comparison between maximizing the region of attraction and opti-

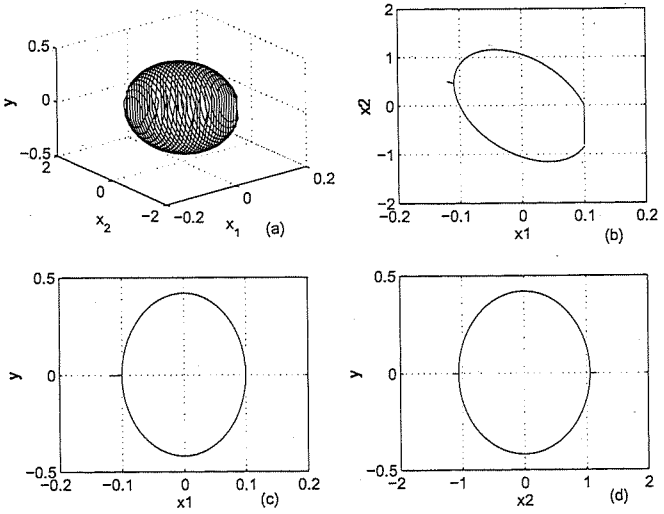

Figure 4.25: (a) Estimated region of attraction of the reactor set point for Example 1 with a temperature deviation constraint; (b) Intersection of $\Omega(z_s)$ with the plane $y = 0$; (c) Intersection of $\Omega(z_s)$ with the plane $x_2 = 0$; (d) Intersection of $\Omega(z_s)$ with the plane $x_1 = 0$; $\alpha = 10$; $\beta = 9.9.10^{17}$; $\alpha_0 = 3$; $\beta_0 = 1.5$

mizing the transient response we conclude that : By decreasing β_0 we obtain less oscillatory transient responses and the overshoot decreases significantly (Figures 4.18 and 4.20), while the region of attraction becomes slightly larger (Figure 4.27 and 4.28).

Concerning the control signals the main observation is that the quantity of energy needed to bring the system to the set point has diminished and less oscillations are obtained.

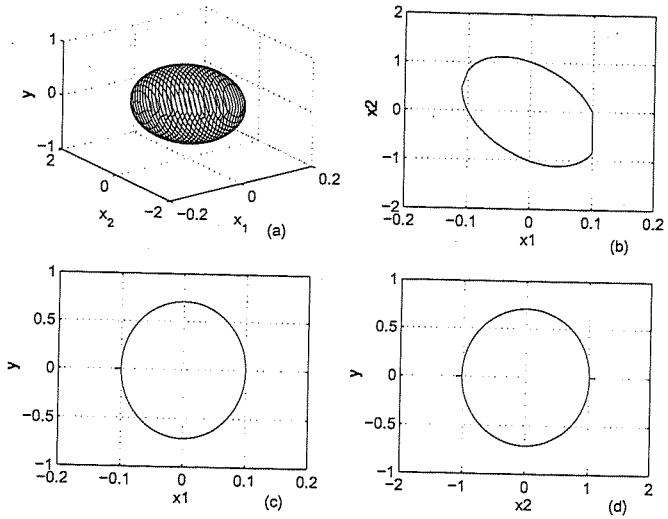

Figure 4.26: (a) Estimated region of attraction of the reactor set point for Example 2 with a temperature deviation constraint; (b) Intersection of $\Omega(z_s)$ with the plane $y = 0$; (c) Intersection of $\Omega(z_s)$ with the plane $x_2 = 0$; (d) Intersection of $\Omega(z_s)$ with the plane $x_1 = 0$; $\alpha = 10$; $\beta = 1.79.10^{14}$; $\alpha_0 = 3$; $\beta_0 = 0.5$

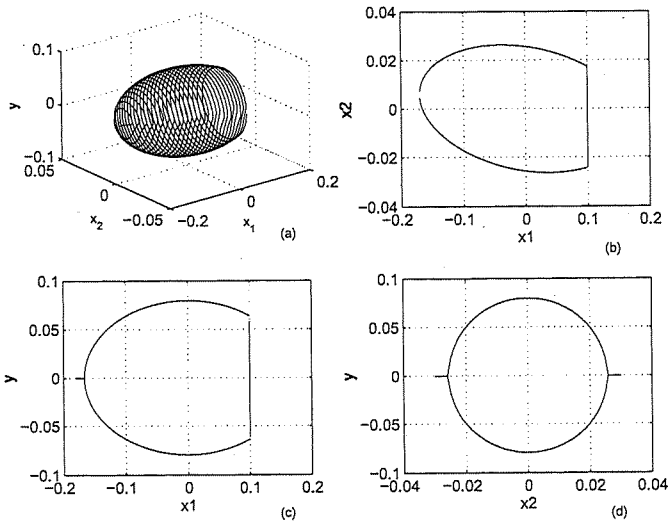

Figure 4.27: (a) Estimated region of attraction of the reactor set point for Example 1 with a temperature deviation constraint; (b) Intersection of $\Omega(z_s)$ with the plane $y = 0$; (c) Intersection of $\Omega(z_s)$ with the plane $x_2 = 0$; (d) Intersection of $\Omega(z_s)$ with the plane $x_1 = 0$;$\alpha = 1.35.10^{16}$; $\beta = 2.7.10^{15}$; $\alpha_0 = 0.1667$; $\beta_0 = 0.5$

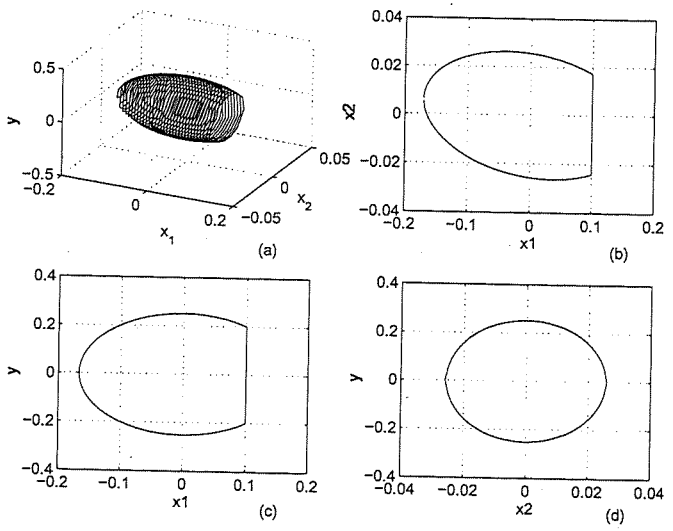

Figure 4.28: (a) Estimated region of attraction of the reactor set point for Example 1 with a temperature deviation constraint; (b) Intersection of $\Omega(z_s)$ with the plane $y = 0$; (c) Intersection of $\Omega(z_s)$ with the plane $x_2 = 0$; (d) Intersection of $\Omega(z_s)$ with the plane $x_1 = 0$;$\alpha = 1.35.10^{16}$; $\beta = 2.7.10^{15}$; $\alpha_0 = 0.1667$; $\beta_0 = 0.05$

In conclusion a method for stabilizing a nonlinear system using linear time invariant PID-control has been presented. Global asymptotic stabilization has been assured. A procedure based on the root locus technique permits to find good parameters values for the controller. Finally, a technique has been presented to compute regions of asymptotic stability in state space for the system's set point where the control or state variable fluctuations during convergence satisfy given upper bounds.

Chapter 5

Decoupling

In this chapter we explain how to design a controller which decouples one of the states of the system, specifically the temperature. Global asymptotic stability is proved using quadratic Liapunov functions. The controller parameter tuning problem is discussed. In the second part of the chapter we add robustness properties to the controller and we compute intervals for the controller parameters which guarantee global asymptotic stability of the set point. Some simulations are performed to study the transient responses.

5.1 Decoupling of the temperature dynamics

In many multivariable systems it is important in order to get a successful control system to properly assign a manipulated variable to each controlled variable. We may then try to decouple the system and design each loop separately.

We can say that there is interaction if the response of one controlled variable to the corresponding manipulated variable changes when we close another loop. A natural approach to the multivariable control problem is to break the system down into a set of well designed single input-single output loops. Here we design a partially decoupled system.

We again start from (1.3) and (1.4) or from (1.6). In deviation variables we obtained (1.7) which can be written as :

$$\dot{x}_1 = -(1+\vartheta)x_1 + m_2[f_1(x_1) + f_2(x_1)x_2] + u_1 \tag{5.1}$$
$$\dot{x}_2 = -x_2 - m_1[f_1(x_1) + f_2(x_1)x_2] + u_2 \tag{5.2}$$

with

$$x \triangleq \begin{bmatrix} x_1 \\ x_2 \end{bmatrix}, \; f_1(x_1) \triangleq \begin{bmatrix} f(x_1 + z_{1s}) - f(z_{1s}) \end{bmatrix} z_{2s},$$

and

$$f_2(x_1) \triangleq \begin{bmatrix} f(x_1 + z_{1s}) \end{bmatrix}$$

In vector form we have :

$$\dot{x} = Ax - b[f_0(x)] + u \tag{5.3}$$

where

$$f_0(x) \triangleq f_1(c'x) + f_2(c'x)g'x$$

and all the other variables as defined in Section 1.1.6, Chapter 1.
In analogy with (2.2) we have

$$m_1\dot{x}_1 + m_2\dot{x}_2 = -m_1(1+\vartheta)x_1 - m_2x_2 + u_0 \tag{5.4}$$

with u_0 given by (3.1).

Choose u_0 such that in closed loop :

$$(m_2+\eta)x_2 = \alpha x_1 + \beta \dot{x}_1 \tag{5.5}$$

Eliminating $m_2 x_2$ from (5.5) and (5.4) we obtain the control law for the single input case ($u_2 \equiv 0$) :

$$u_1(t) = (1+\vartheta+\frac{\alpha}{m_1})x_1 + (1+\frac{\beta}{m_1})\dot{x}_1 + \frac{1}{m_1}(m_2\dot{x}_2 - \eta x_2) \tag{5.6}$$

In Chapter 2 we have taken $\eta = 0$, hence

$$u_1(t) = (1+\vartheta+\frac{\alpha}{m_1})x_1 + (1+\frac{\beta}{m_1})\dot{x}_1 + \frac{m_2}{m_1}\dot{x}_2 \tag{5.7}$$

Another obvious choice is $\eta = -m_2$. Then

$$u_1(t) = (1+\vartheta+\frac{\alpha}{m_1})x_1 + (1+\frac{\beta}{m_1})\dot{x}_1 + \frac{m_2}{m_1}(\dot{x}_2 + x_2) \tag{5.8}$$

In closed loop we now obtain :

$$\begin{aligned} \beta\dot{x}_1 + \alpha x_1 &= 0 \\ \dot{x}_2 &= -x_2 - m_1[f_1(x_1) + f_2(x_1)x_2] \end{aligned} \tag{5.9}$$

such that the reactor temperature dynamics become linear and decoupled from the concentration dynamics.

The global asymptotic stability of (5.9) can easily be proved using a quadratic Liapunov function. Let

$$V(x) \triangleq \frac{1}{2}\kappa x_1^2 + \frac{1}{2}x_2^2; \quad \kappa > 0 \tag{5.10}$$

V(x) is positive definite and radially unbounded. Its derivative along the solutions of (5.9) is :

$$\begin{aligned} \dot{V}(x) &= \kappa x_1\dot{x}_1 + x_2\dot{x}_2 \\ &= -\frac{\alpha}{\beta}\kappa x_1^2 - x_2^2 - m_1 x_2 f_1(x_1) - m_1 x_2^2 \underbrace{f_2(x_1)}_{>0} \qquad (5.11) \\ &\leq -\frac{\alpha}{\beta}\kappa x_1^2 - x_2^2 - m_1 x_2 f_1(x_1) \qquad (5.12) \end{aligned}$$

According to Figure 5.1 we have :

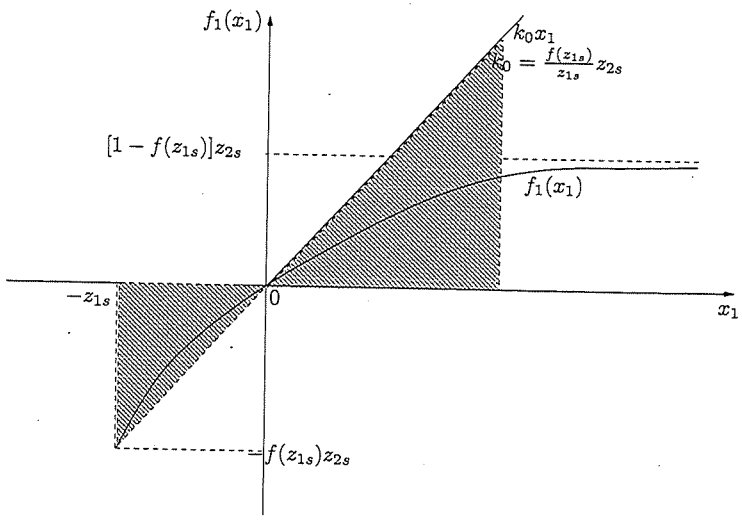

Figure 5.1: Evolution of the function $f_1(x_1)$.

$$0 < \frac{f_1(x_1)}{x_1} < \frac{f(z_{1s})}{z_{1s}} z_{2s} = e^{\frac{-10^4}{z_{1s}}} \frac{z_{2s}}{z_{1s}} \triangleq k_0$$

The derivative of the Liapunov function along the solutions of (5.9) is negative definite, that is :

$$\dot{V}(x) < 0 \tag{5.13}$$

for $x \neq 0$ if

$$(m_1 k_0)^2 < 4 \frac{\alpha}{\beta} \kappa$$

or if we choose

$$\kappa > \tfrac{1}{4} \tfrac{\beta}{\alpha} (m_1 k_0)^2$$

5.1.1 Parameter tuning

In this section we tune the obtained PD-controller. First, the system is represented in its linearized version and the characteristic equation is found. Then the eigenvectors are computed and some phase portrait diagrams are displayed for different values of the parameter $\frac{\alpha}{\beta}$.

Linearization of (5.9) at $x = 0$ yields :

$$\begin{aligned} \beta \dot{x}_1 + \alpha x_1 &= 0 \\ \dot{x}_2 &= -x_2 - m_1 [f_{1d}(0) x_1 + f_2(0) x_2] \end{aligned} \tag{5.14}$$

$$\begin{aligned} m_1 f_{1d}(0) &= 10^4 m_1 \frac{z_{2s}}{z_{1s}^2} e^{\frac{-10^4}{z_{1s}}} \triangleq a_0 \\ m_1 f_2(0) &= m_1 e^{\frac{-10^4}{z_{1s}}} \triangleq b_0 \end{aligned}$$

(5.14) becomes :

$$\begin{aligned} \dot{x}_1 &= -\frac{\alpha}{\beta} x_1 \\ \dot{x}_2 &= -(1 + b_0) x_2 - a_0 x_1 \end{aligned} \tag{5.15}$$

The characteristic values of the system (5.15) are :

$$s_1 = -\tfrac{\alpha}{\beta}; \quad s_2 = -(1 + b_0)$$

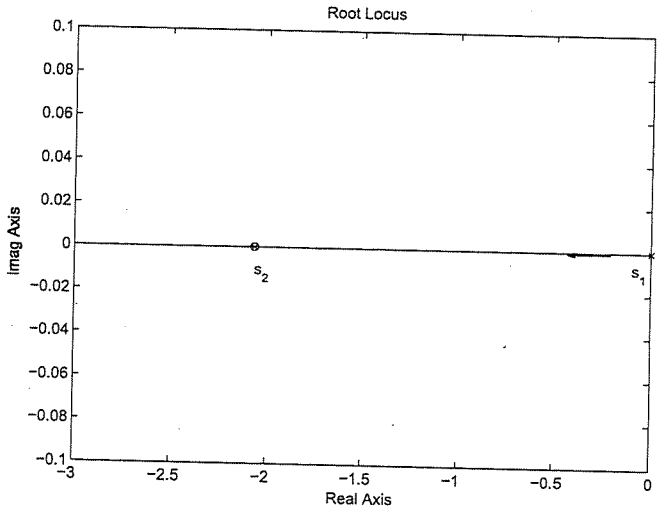

Figure 5.2: Effect of the parameter $\frac{\alpha}{\beta}$ on the location of the closed loop poles

where $\frac{\alpha}{\beta} > 0$ can be chosen arbitrarily while b_0 is a process parameter. Figure 5.2 illustrates that we can only move one of the poles (s_1) by changing the parameter $\frac{\alpha}{\beta}$ while the other pole (s_2) remains frozen in a value depending on the physical process.

Hence the reactor temperature time constant can be chosen arbitrarily while the concentration time constant is determined by the process. Now we compute the two eigenvectors :

$$(s_1 I - A)e_1 = 0 \tag{5.16}$$
$$(s_2 I - A)e_2 = 0 \tag{5.17}$$

with $A \triangleq \begin{bmatrix} -\frac{\alpha}{\beta} & 0 \\ -a_0 & -(1+b_0) \end{bmatrix}$

This results in :

$$e_1 = \begin{bmatrix} 1+b_0-\frac{\alpha}{\beta} \\ -a_0 \end{bmatrix} \tag{5.18}$$
$$e_2 = \begin{bmatrix} 0 \\ 1 \end{bmatrix} \tag{5.19}$$

The time response of (5.15) is :

$$x(t) = e_1 e^{\frac{-\alpha}{\beta}t} c_1 + e_2 e^{-(1+b_0)t} c_2 \tag{5.20}$$

Figure 5.3 shows phase portrait diagrams for two different values of the parameter $\frac{\alpha}{\beta}$.

If we choose $\frac{\alpha}{\beta} > (1+b_0)$ then the reactor temperature quickly converges to its set point value. Subsequently concentration converges with the time constant $\frac{1}{1+b_0}$. Figures 5.4(c), 5.4(d) show the transients for the linearized system and Figure 5.5 for the nonlinear system.

If we choose $0 < \frac{\alpha}{\beta} < (1+b_0)$ then both temperature and concentration converge to their set point values with the time constant $\frac{\beta}{\alpha}$ Figure 5.4(a),(b) illustrates these transients.

Figure 5.6 shows a comparison between the temperature transient response for the coupled(one-input PD-controller) and the decoupled nonlinear system. We

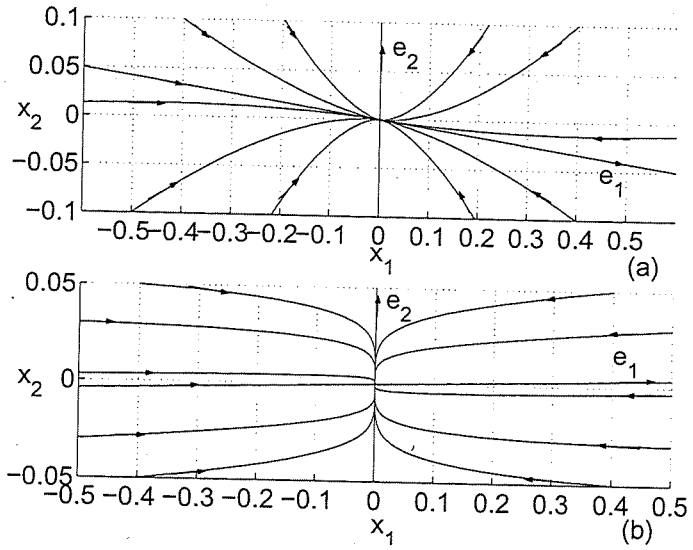

Figure 5.3: Phase portrait for the system with decoupled reactor temperature, Example 1. (a) $0 < \frac{\alpha}{\beta} < (1+b_0)$=1.3; (b) $\frac{\alpha}{\beta} = 10 > (1+b_0)$

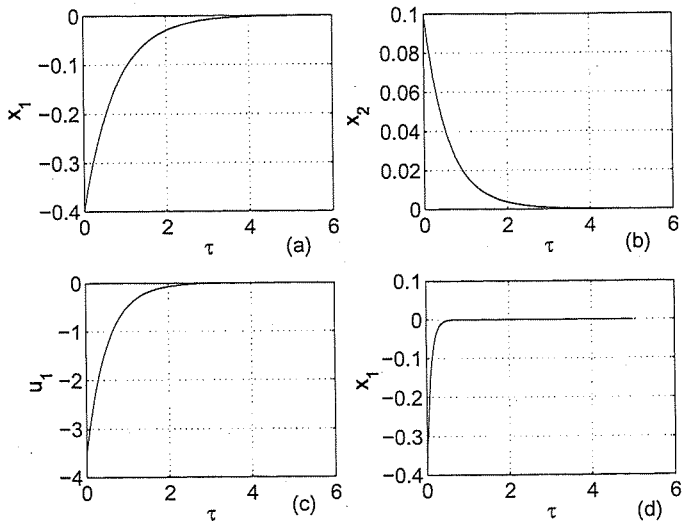

Figure 5.4: Transient response for the linearized system, Example 1. (a),(b) Temperature and concentration responses for $0 < \frac{\alpha}{\beta} < (1 + b_0)$=1.3; x(0)=(-0.4;0.1) (c) Control law (d) Temperature response for $\frac{\alpha}{\beta} = 10 > (1 + b_0)$

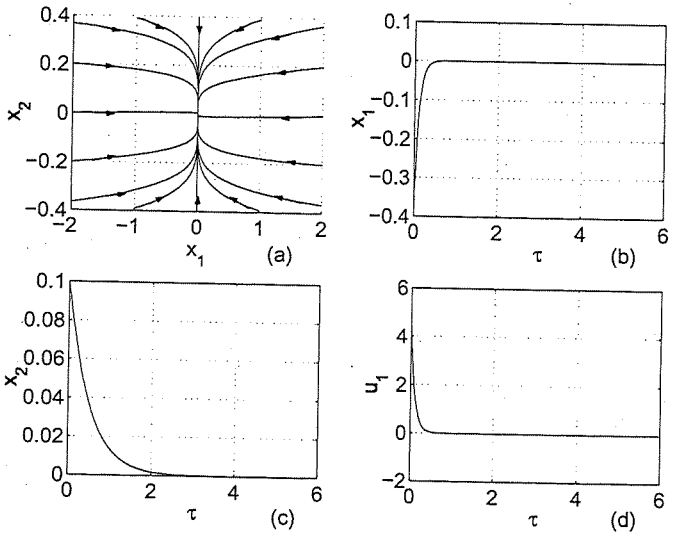

Figure 5.5: Transient response for the nonlinear system, Example 1; $\frac{\alpha}{\beta} = 10 > (1 + b_0)$; x(0)=(-0.4;0.1). (a) Phase portrait. (b) Temperature response. (c) Concentration response. (d) Control law, u_1

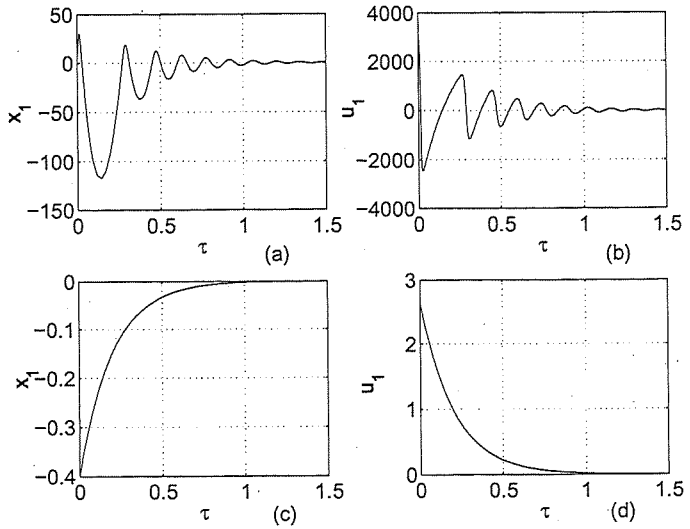

Figure 5.6: Transient response for the nonlinear system, Example 1; $\frac{\alpha}{\beta} = 5 > (1 + b_0)$; x(0)=(-0.4;0.1); $\alpha = 1.25.10^{13}$; $\beta = 2.5.10^{12}$. (a),(b) Temperature response and control signal u_1 without decoupling (Single input PD-controller). (c),(d) Temperature response and control signal u_1 with decoupled temperature.

see that for the decoupled system we have an overdamped response while for the coupled system oscillations appear in the transient. Also a stronger effort in the controller action is needed in the case of the coupled system and strong oscillations occur before reaching the steady state.

5.1.2 Some remarks

- In a similar way we can decouple and linearize the closed loop concentration dynamics using u_2 as an input.
- The decoupling control laws can be further generalized to two input PD-controllers or two input PID-controllers, in a similar way as the controller (5.7) has been generalized in Chapters 3 and 4. However we shall not further pursue this development. Instead we shall now concentrate on the robustness of the design.

5.2 The robustness problem

In practical applications modelling errors may occur, the system's dynamics may not be completely known or parameters can vary during the lifespan of the system. In this section we consider process models whose uncertainty is expressed in the form of a range of possible parameter values. We derive a robust linear multivariable feedback controller.

The control laws (5.7) and (5.8) are not robust. In (5.7) the coefficient of $\dot{x}_2$ and in (5.8) the coefficient of $(\dot{x}_2 + x_2)$ must exactly match the ratio $\frac{m_2}{m_1}$ of two process parameters. This is not true for the other controller parameters in (5.7) and (5.8), since α and β can be chosen positive but otherwise arbitrary.

To make the control law (5.8) robust, let

$$u_1(t) = (1 + \vartheta + \frac{\alpha}{m_1})x_1 + (1 + \frac{\beta}{m_1})\dot{x}_1 + (\frac{m_2 + \gamma}{m_1})(\dot{x}_2 + x_2) \quad (5.21)$$

We compute intervals for α, β and γ such that (5.21) globally asymptotically stabilizes the set point.

The closed loop dynamics become :

$$\alpha x_1 + \beta \dot{x}_1 + \gamma \dot{x}_2 + \gamma x_2 = 0$$

$$\dot{x}_2 = -x_2 - m_1[f_1(x_1) + f_2(x_1)x_2] \quad (5.22)$$

In vector form :

$$\begin{bmatrix} \beta & \gamma \\ 0 & 1 \end{bmatrix} \begin{bmatrix} \dot{x}_1 \\ \dot{x}_2 \end{bmatrix} = \begin{bmatrix} -\alpha & -\gamma \\ 0 & -1 \end{bmatrix} \begin{bmatrix} x_1 \\ x_2 \end{bmatrix} - \begin{bmatrix} 0 \\ m_1 \end{bmatrix} f_0(x)$$

We again introduce (5.10) as a candidate Liapunov function and compute its derivative as follows :

$$\begin{aligned} \dot{V}(x) &= \kappa x_1 \dot{x}_1 + x_2 \dot{x}_2 \\ &= -\frac{\alpha}{\beta}\kappa x_1^2 - x_2^2 - m_1 x_2 f_0(x) + \frac{\gamma}{\beta}\kappa m_1 x_1 f_0(x) \end{aligned} \quad (5.23)$$

or

$$\begin{aligned} -\dot{V}(x) &= \frac{\alpha}{\beta}\kappa x_1^2 + x_2^2 + m_1 x_2 [f_1(x_1) + \underbrace{f_2(x_1)}_{>0} x_2] - \\ &\quad \frac{\gamma}{\beta}\kappa m_1 \underbrace{x_1[f_1(x_1)}_{>0} + f_2(x_1)x_2] \end{aligned} \quad (5.24)$$

Choose $\frac{\gamma}{\beta} < 0$. Then

$$-\dot{V}(x) \geq \frac{\alpha}{\beta}\kappa x_1^2 + x_2^2 + m_1 \frac{f_1(x_1)}{x_1} x_1 x_2 + \frac{(-\gamma)}{\beta}\kappa m_1 x_1 f_2(x_1) x_2 \quad (5.25)$$

Choose $\frac{\alpha}{\beta} > 0$. Then without loss of generality we can assume

$$\alpha > 0; \beta > 0; \gamma < 0$$

From previous discussions we have:

$$0 < \frac{f(x_1)}{x_1} < k_0$$
$$0 < f_2(x_1) < 1$$

Hence $\dot{V}(x) < 0$ for $x \neq 0$ **(negative definite) if**

$$[m_1 k_0 - \frac{\gamma}{\beta}\kappa m_1]^2 < 4\kappa\frac{\alpha}{\beta}$$

or

$$\mu_1 \kappa^2 - \mu_2 \kappa + \mu_3 < 0 \quad (5.26)$$

with

$$\begin{aligned} \mu_1 &\triangleq \frac{\gamma^2}{\beta^2} m_1^2 \\ \mu_2 &\triangleq 4\frac{\alpha}{\beta} + 2m_1^2 k_0 \frac{\gamma}{\beta} \\ \mu_3 &\triangleq m_1^2 k_0^2 \end{aligned}$$

(5.26) cannot be satisfied unless $u_2 > 0$, or

$$4\frac{\alpha}{\beta} > 2m_1^2 k_0 \frac{(-\gamma)}{\beta} > 0 \Leftrightarrow -\gamma < \frac{2\alpha}{k_0 m_1^2} \quad (5.27)$$

Now the left hand side of (5.26) reaches its minimum for

$$2\mu_1\kappa - \mu_2 = 0$$

or :

$$\kappa = \frac{\mu_2}{2\mu_1} \quad (5.28)$$

So there exists an interval of positive κ-values such that (5.26) holds if and **only if (5.26) is satisfied for** $\kappa = \frac{\mu_2}{2\mu_1}$.

Replacing the optimum value of κ in (5.26) we obtain :

$$-\gamma < \frac{\alpha}{m_1^2 k_0} \quad (5.29)$$

From (5.27), (5.29) we conclude that the control law (5.21) globally asymptotically stabilizes the set point if

$$\alpha > 0 \quad ; \quad \beta > 0 \quad ; \quad 0 < -\gamma < \frac{\alpha}{m_1^2 k_0}$$

(5.21) is a robust version of (5.8). The control law (5.7) is somewhat simpler than (5.8). In the next Chapters we design a robust version of (5.7).

Note that with the control law (5.21) the closed loop system is no longer partially decoupled. The linearized closed loop dynamics become :

$$\alpha x_1 + \beta \dot{x}_1 + \gamma \dot{x}_2 + \gamma x_2 = 0 \quad (5.30)$$

$$\begin{aligned} \dot{x}_2 &= -x_2 - m_1[f_{1d}(0)x_1 + f_2(0)x_2] \\ &= -x_2 - a_0 x_1 - b_0 x_2 \end{aligned} \tag{5.31}$$

or

$$\dot{x}_1 = -\frac{[\alpha + (-\gamma)a_0]}{\beta}x_1 + \frac{\gamma}{\beta}(b_0 x_2) \tag{5.32}$$

$$\dot{x}_2 = -a_0 x_1 - (1 + b_0)x_2 \tag{5.33}$$

The characteristic equation is :

$$(s + \frac{\alpha}{\beta})(s + 1 + b_0) + \frac{(-\gamma)a_0}{\beta}(s + 1) = 0 \tag{5.34}$$

In conclusion, if for instance we take $\frac{\alpha}{\beta} > 1$, then making the control law robust

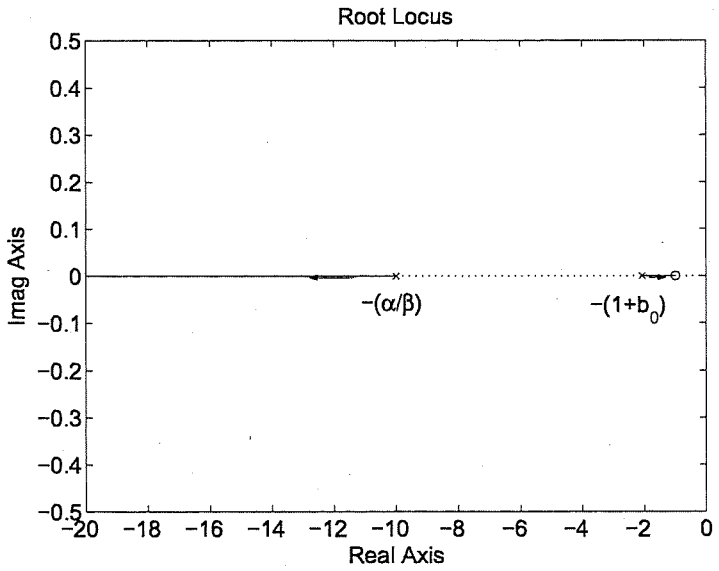

Figure 5.7: Example 1 : Effect of the parameter $-(\gamma)$ on the location of the closed loop poles.

deteriorates closed loop stability. Figure 5.7 illustrates this effect: When we

increase the value of $(-\gamma)$ one of the roots moves towards the imaginary axis and the largest time constant becomes larger than $\frac{1}{1+b_0}$.

Chapter 6

Robust single input PD-control

It is well known that no mathematical system can exactly model a physical system. In this sense when we use a model either obtained by ***identification*** *techniques (black box model) or by applying the relevant physical laws (white* ***model), modelling errors might adversely affect the performance*** *of the control* ***system. In this chapter we present a method to analyze the effect*** *of uncertainty on closed loop stability and performance. Section 6.1 is devoted to the controller design. In Section 6.2 we introduce conditions for the stability of the closed loop by using Liapunov concepts. In Section 6.3 we discuss the robustness of the system behaviour in a region of state space surrounding the set* ***point. The final*** *topic is discussed in Section 6.4 and corresponds to the controller tuning. New* ***contributions are reported in (Muñoz, Loccufier and Noldus,*** *2003)*

6.1 Controller structure

The concepts developed in this chapter have been discussed in (Muñoz, Loccufier and Noldus, 2004). We again start from the equations :

$$\dot{z}_1 = r - (1+\vartheta)z_1 + m_2 z_2 f(z_1) + u_1 \quad (6.1)$$

$$\dot{z}_2 = 1 - z_2 - m_1 z_2 f(z_1) + u_2 \quad (6.2)$$

with

$$f(z_1) = exp(\frac{-10^4}{z_1})$$

Let $u_2(t) \equiv 0$.

Since by definition z_1 can only assume positive values we have

$$0 < f(z_1) < 1$$

Equations (6.1), (6.2) imply that in the single input case

$$m_1\dot{z}_1 + m_2\dot{z}_2 = m_1 r + m_2 - m_1(1+\vartheta)z_1 - m_2 z_2 + m_1 u_1 \quad (6.3)$$

Choose u_1 such that in closed loop

$$m_2 z_2 = \alpha z_1 + \beta\dot{z}_1 + \gamma\dot{z}_2 + \delta \quad (6.4)$$

After eliminating z_2 from (6.3) and (6.4) we achieve the following single input PD-controller :

$$u_1 = (1+\vartheta+\frac{\alpha}{m_1})z_1 + (1+\frac{\beta}{m_1})\dot{z}_1 + (\frac{m_2+\gamma}{m_1})\dot{z}_2 + \frac{1}{m_1}(\delta - m_1 r - m_2) \quad (6.5)$$

Letting $u_1 = 0$ at $z = z_s$ results in

$$(1+\vartheta+\frac{\alpha}{m_1})z_{1s} + \frac{1}{m_1}(\delta - m_1 r - m_2) = 0 \quad (6.6)$$

Now u_1 can be expressed in terms of the deviation variables $x \triangleq z - z_s$ as

$$u_1 = (1+\vartheta+\frac{\alpha}{m_1})x_1 + (1+\frac{\beta}{m_1})\dot{x}_1 + (\frac{m_2+\gamma}{m_1})\dot{x}_2 \quad (6.7)$$

In closed loop the system is defined by :

$$m_2 z_2 = \alpha z_1 + \beta \dot{z}_1 + \gamma \dot{z}_2 + \delta \quad (6.8)$$
$$\dot{z}_2 = 1 - z_2 - m_1 z_2 f(z_1) \quad (6.9)$$

Taking $\alpha > 0$ ensures that there exists a unique closed loop equilibrium point z_s which satisfies

$$\alpha z_{1s} - m_2 z_{2s} + \delta = 0 \quad (6.10)$$
$$1 - z_{2s} - m_1 z_{2s} f(z_{1s}) = 0 \quad (6.11)$$

This is illustrated in Figure 6.1. (6.6), (6.11) determine z_s as a function of the

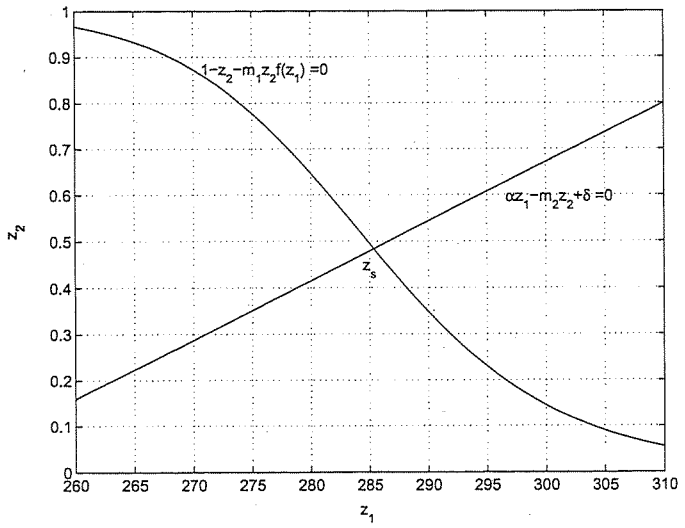

Figure 6.1: Closed loop equilibrium for Example 1 with controller parameters $\alpha = 10^{15}$ and $\delta = -2.476.10^7$

choice for α and δ. Combining (6.8) with (6.9) and using the relation (6.4) brings the closed loop state equations in the form :

$$M\dot{z} = A_0 z + k_0 - b_0 \left[f_1(z_1) + f_2(z_1)(\beta \dot{z}_1 + \gamma \dot{z}_2) \right] \quad (6.12)$$

with

$$M \triangleq \begin{bmatrix} \beta & \gamma \\ 0 & 1 \end{bmatrix}, A_0 \triangleq \begin{bmatrix} -\alpha & m_2 \\ 0 & -1 \end{bmatrix}, k_0 \triangleq \begin{bmatrix} -\delta \\ 1 \end{bmatrix},$$
$$b_0 \triangleq \begin{bmatrix} 0 \\ 1 \end{bmatrix}, f_1(z_1) \triangleq \frac{m_1}{m_2}(\alpha z_1 + \delta) e^{\frac{-10^4}{z_1}},$$
$$f_2(z_1) \triangleq \frac{m_1}{m_2} e^{\frac{-10^4}{z_1}}.$$

6.2 Stability analysis

We determine conditions on the controller parameters α, β and γ which ensure closed loop global asymptotic stability of the set point $z = z_s$ (or $x = 0$) using Liapunov theory.

In Chapters 2 to 4 we discussed an approach to the global asymptotic stabilization of the set point defining a positive definite and radially unbounded Liapunov function $V(x)$. Schematically we had :

$$\dot{V}(x) \leq -x'Qx$$
$$\dot{V}(x) = 0 \Rightarrow x = 0$$
$$E = M = \{0\}$$

where

$$Q = Q' > 0 (positive\ definite)$$
$$E = \{x \in R^n;\ \dot{V}(x) = 0\}$$
$$M = Largest\ invariant\ subset\ of\ E$$

In this section we propose the following modified approach :

$$\dot{V}(x) \leq -\dot{x}'Q\dot{x}$$
$$\dot{V}(x) = 0 \Rightarrow \dot{x} = 0$$
$$E = M = set\ of\ equilibria$$

Since the closed loop possesses a unique equilibrium point we again find :

$$E = M = \{0\}$$

Let

$$V(z) \triangleq z'Pz + \alpha_0 \int_0^{z_1} f_1(\theta)d\theta + p'z \tag{6.13}$$

be a candidate Liapunov function for the system (6.12). Recalling that we take $\alpha > 0$, $V(z)$ is radially unbounded if $P = P' > 0$ (positive definite) and $\alpha_0 > 0$. Along the solutions of (6.12) we have

$$\begin{aligned}\dot{V}(z) &= \dot{z}'Pz + z'P\dot{z} + \alpha_0 f_1(z_1)\dot{z}_1 + p'\dot{z} \\ &= \dot{z}'PA_0^{-1}[M\dot{z} - k_0 + b_0 f_1(z_1) + b_0 f_2(z_1)(\beta\dot{z}_1 + \gamma\dot{z}_2)] \\ &\quad + [M\dot{z} - k_0 + b_0 f_1(z_1) + b_0 f_2(z_1)(\beta\dot{z}_1 + \gamma\dot{z}_2)]' A_0^{-1'} P\dot{z} \\ &\quad + \alpha_0 f_1(z_1)\dot{z}_1 + p'\dot{z}\end{aligned} \tag{6.14}$$

Choose $p \triangleq 2PA_0^{-1}k_0$ and let

$$PA_0^{-1}M + M'A_0^{-1'}P = -qq' - \rho b_0 b_0'; \quad \rho > 0 \tag{6.15}$$

$$2PA_0^{-1}b_0 + \alpha_0 c = 0 \tag{6.16}$$

Then (6.14) simplifies to

$$\dot{V}(z) = (-q'\dot{z})^2 - \rho(b_0'\dot{z})^2 - \alpha_0 \dot{z}_1 f_2(z_1)(\beta\dot{z}_1 + \gamma\dot{z}_2) \tag{6.17}$$

By a straightforward application of the Kalman-Yacubovich-Popov (KYP) lemma (Lozano et al.,2000) the system (6.15), (6.16) has a real solution $P = P' > 0$, $q \in R^2$ if

$$A_0^{-1}M = \begin{bmatrix} -\frac{\beta}{\alpha} & -\frac{-(\gamma+m_2)}{\alpha} \\ 0 & -1 \end{bmatrix}$$

is a Hurwitz matrix, which is satisfied if $\frac{\beta}{\alpha} > 0$ and if

$$\begin{aligned}&\alpha_0 \mathrm{Re}c'(j\omega A_0 - M)^{-1}b_0 + \rho b_0'\overline{(j\omega A_0 - M)}^{-1}\cdot \\ &\qquad b_0 b_0'(j\omega A_0 - M)^{-1}b_0 < 0; \quad \forall\omega \in R\end{aligned} \tag{6.18}$$

After some mathematical manipulations (6.18) is reduced to the condition:

$$\frac{\alpha_0}{(\beta^2 + \alpha^2\omega^2)}\{\omega^2[m_2\beta + \alpha(\gamma + m_2)] - \beta\gamma\} > \rho; \quad \forall\omega \in R \tag{6.19}$$

A rational function $\frac{a+b\omega^2}{c+d\omega^2}$ with $ad \neq bc$ does not possess a minimum. Indeed, a minimum satisfies :

$$(a + b\omega^2)d - (c + d\omega^2)b = 0$$

$$ad - cb = 0$$

Hence (6.19) is satisfied if and only if the inequality holds for $\omega = 0$ and for $\omega = +\infty$:

$$\frac{\alpha_0}{\beta^2}(-\beta\gamma) > \rho \tag{6.20}$$

and

$$\frac{\alpha_0}{\alpha^2}[m_2\beta + \alpha(\gamma + m_2)] > \rho \tag{6.21}$$

Recall that we have taken $\alpha_0 > 0$, $\alpha > 0$, which also guarantees the existence of A_0^{-1}, and $\frac{\beta}{\alpha} > 0$, hence $\beta > 0$.

So (6.20) and (6.21) can be written as

$$\frac{\rho\beta}{\alpha_0} < -\gamma < m_2(1 + \frac{\beta}{\alpha}) - \frac{\rho\alpha}{\alpha_0} \tag{6.22}$$

Next rewrite (6.17) as :

$$-\dot{V}(z) = (q'\dot{z})^2 + f(z_1)[\alpha_0 \frac{m_1}{m_2}\beta\dot{z}_1^2 + \alpha_0 \frac{m_1}{m_2}\gamma\dot{z}_1\dot{z}_2 + \frac{\rho}{f(z_1)}\dot{z}_2^2] \tag{6.23}$$

where $0 < f(z_1) < 1$. An analysis of (6.23) leads us to the condition :

$$\gamma^2 \leq 4\rho\frac{\beta}{\alpha_0}\frac{m_2}{m_1} \tag{6.24}$$

which corresponds to values of the parameter γ for which $\dot{V}(z)$ is negative semidefinite, that is :

$$\begin{aligned}-\dot{V} &\geq 0; \quad \forall\dot{z} \in R^2 \\ &= 0 \Leftrightarrow \dot{z} = 0\end{aligned}$$

Assuming we choose

$$\gamma^2 = 4\rho\frac{\beta}{\alpha_0}\frac{m_2}{m_1} \tag{6.25}$$

we can easily verify that $\dot{V}(z) \leq 0$ for all $\dot{z}$ and that the largest invariant set where $\dot{V}(z)$ vanishes consists of the set where $\dot{z}(t) \equiv 0$, i.e. the system's unique equilibrium point $z = z_s$. Eliminating $\frac{\rho}{\alpha_0}$ from (6.22) and (6.25) yields the condition

$$\frac{1}{4}\frac{m_1}{m_2}\gamma^2 < -\gamma < m_2(1 + \frac{\beta}{\alpha}) - \frac{1}{4}\frac{m_1}{m_2}\gamma^2\frac{\alpha}{\beta} \tag{6.26}$$

(6.26) is satisfied for $\gamma < 0$ and $|\gamma|$ sufficiently small. For practical parameter values the first inequality of (6.26) imposes the strongest restriction on γ :

$$0 < -\gamma < 4\frac{m_2}{m_1} \tag{6.27}$$

The second inequality of (6.26) yields the condition:

$$0 < -\gamma < 2\frac{\beta}{\alpha}\frac{m_2}{m_1}[-1 + \sqrt{1 + m_1(1 + \frac{\alpha}{\beta})}] \tag{6.28}$$

Since $V(z)$ is radially unbounded and $\dot{V}(z)$ is negative semidefinite all closed loop trajectories remain bounded for increasing time. Hence under the obtained conditions every closed loop solution converges to the equilibrium point. So the feedback law (6.5) or (6.7) renders the set point $z = z_s$ globally asymptotically stable provided we choose $\alpha > 0$, $\beta > 0$ and γ satisfies (6.27).

6.3 Robust design with a finite stability region

For practical process parameter values the admissible interval (6.27) for γ is small, which results in a control system with limited robustness. In this section we extend the analysis to controllers yielding a finite stability region around the set point $x = 0$. The proposed solution can be seen as decreasing the system's stability but on the other hand increasing the degree of freedom of the parameter γ, producing better robustness properties.

By the analysis of Section 6.2, the control law

$$u = \xi_1 x_1 + \xi_2 \dot{x}_1 + \xi_3 \dot{x}_2 \tag{6.29}$$

represents a globally asymptotically stabilizing PD-controller provided $\xi_1 = (1 + s + \frac{\alpha}{m_1}) > (1 + s)$, $\xi_2 = (1 + \frac{\beta}{m_1}) > 1$ and

$$\frac{m_2}{m_1}(1 - \frac{4}{m_1}) < \xi_3 = (\frac{m_2 + \gamma}{m_1}) < \frac{m_2}{m_1} \tag{6.30}$$

Tuning the controller does not require a precise knowledge of the process parameters, however for practical parameter values the admissible interval for ξ_3 is small. The robustness of the controller can be improved if we restrict the system's operation to some finite stability region in state space surrounding

the set point.

Define

$$\Omega_a \triangleq \{z \in R^2; \quad z_1 < a; \quad V(z) < V_a\}$$

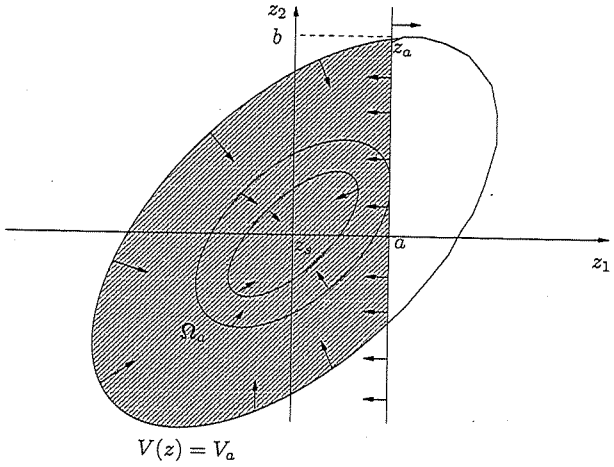

Figure 6.2: Level sets $\{V(z)$=constant$\}$ and stability region Ω_a under a state constraint $z_1 < a$.

where a is a scalar, $a > z_{1s}$. Choose V_a such that if $z(0) \in \Omega_a$ then $z(t) \in \Omega_a$ for all $t \geq 0$.

We can evaluate the first equation of (6.12) in $z_1 = a$, $\dot{z}_1 = 0$ obtaining:

$$z_2 = b \triangleq \frac{\alpha a + \delta + \gamma}{m_2 + \gamma + \gamma m_1 f(a)} \tag{6.31}$$

It is straightforward to verify that in each point z on the straight line segment $\{z_1 = a, \quad z_2 < b\}$ we have $\dot{z}_1 < 0$ (see Figure 6.2).

Let $z_a \triangleq \begin{bmatrix} a \\ b \end{bmatrix}$ and $V_a \triangleq V(z_a)$. For $z \in \Omega_a$ where we have the constraint $z_1 < a$ we obtain from (6.23) :

$$-\dot{V}(z) \geq (q'\dot{z})^2 + f(z_1)[\alpha_0 \frac{m_1}{m_2}\beta \dot{z}_1^2 + \alpha_0 \frac{m_1}{m_2}\gamma \dot{z}_1 \dot{z}_2 + \frac{\rho}{f_{max}}\dot{z}_2^2] \quad (6.32)$$

where

$$f_{max} = max f(z_1) = f(a); \quad z_1 \leq a$$

Now $\dot{V}$ is negative semidefinite in Ω_a, that is :

$$\begin{aligned} \dot{V} &\leq 0; \quad \forall z \in \Omega_a \\ &= 0 \Leftrightarrow \dot{z} = 0; \quad z \in \Omega_a \end{aligned}$$

if :

$$\gamma^2 \leq 4 \frac{\rho}{f(a)} \frac{\beta}{\alpha_0} \frac{m_2}{m_1} \quad (6.33)$$

We choose

$$\gamma^2 = 4 \frac{\rho}{f(a)} \frac{\beta}{\alpha_0} \frac{m_2}{m_1} \quad (6.34)$$

So obviously a trajectory starting in Ω_a at $t = 0$ remains in Ω_a for all $t \geq 0$ and Ω_a is a region of attraction of the set point. It follows that if we restrict the system's operation to the set Ω_a and we eliminate $\frac{\rho}{\alpha_0}$ from (6.34) and (6.22) then the condition (6.26) on γ is weakened to :

$$\frac{1}{4}\frac{m_1}{m_2}\gamma^2 e^{\frac{-10^4}{a}} < -\gamma < m_2(1 + \frac{\beta}{\alpha}) - \frac{1}{4}\frac{m_1}{m_2}\frac{\alpha}{\beta}\gamma^2 e^{\frac{-10^4}{a}} \quad (6.35)$$

Since

$$f(a) = e^{\frac{-10^4}{a}} < 1$$

(6.35) gives us a larger admissible interval for γ.

For practical parameter values (6.35) holds if

$$0 < -\gamma < \frac{4m_2}{m_1} e^{\frac{10^4}{a}} \quad (6.36)$$

As a conclusion we have shown that z_s is locally asymptotically stable with stability region Ω_a provided the control parameters satisfy $\alpha > 0$, $\beta > 0$ and γ satisfies (6.36)

For a given choice of ξ_1, ξ_2, ξ_3 there is a range of process parameters r,ϑ,m_1, m_2 for which the condition (6.36) remains satisfied. We do not have to know the exact values of the process parameters. So the controller robustly stabilizes the set point $x = 0$.

Let us illustrate the robustness property for Example 1:

$$\begin{aligned} \vartheta &= 0.1356 \\ m_1 &= 1.7685.10^{15} \end{aligned}$$

Suppose we choose $\alpha = 10^{12}$. Then we have $\xi_1 = 1.1362$. Recomputing α from ξ_1 gives us

$$\alpha = [\xi_1 - 1 - \vartheta]m_1$$

such that the stability condition $\alpha > 0$ yields :

$$\begin{aligned} [\xi_1 - 1 - \vartheta] &> 0 \\ \vartheta &< 0.1362 \end{aligned}$$

We conclude that because of the freedom in the choice of γ, the physical parameter s can vary in some range giving good robustness properties to the system.

For $-\gamma > 0$ and sufficiently small the quadratic approximation of Ω_a can readily be computed by solving the appropiate Riccati equation :

$$\begin{aligned} \Omega_a &= \{x; \quad x'P_0x \leq (z_a - z_s)'P_0(z_a - z_s); x_1 < a - z_{1s}\} \\ &= \{x; \quad [p_1 + \frac{1}{2}f_{1d}(z_{1s})]x_1^2 + 2p_2x_1x_2 + p_3x_2^2 \leq \\ &\quad [p_1 + \frac{1}{2}f_{1d}(z_{1s})](a - z_{1s})^2 + 2p_2(a - z_{1s})(b - z_{2s}) \\ &\quad + p_3(b - z_{2s})^2; x_1 < a - z_{1s}\} \end{aligned} \quad (6.37)$$

where

$$P_0 = \begin{bmatrix} p_1 + \frac{1}{2}f_{1d}(z_{1s}) & p_2 \\ p_2 & p_3 \end{bmatrix}$$

$$
\begin{aligned}
p_1 &= \frac{1}{2m_2}(\alpha+\beta) \\
p_2 &= -\frac{\beta}{2\alpha} \\
p_3 &= \frac{m_2\beta}{2\alpha^2} \\
f_{1d}(z_{1s}) &= \frac{m_1}{m_2}e^{\frac{-10^4}{z_{1s}}}[\alpha+(\alpha z_{1s}+\delta)\frac{10^4}{(z_{1s})^2}]
\end{aligned}
$$

6.4 Control parameter tuning

In this section we illustrate the tuning of the robust PD controller with a single input u_1. We show some simulations in closed loop for one of the examples.

The influence of the control parameters on the eigenvalue spectrum of the linearized closed loop system can be studied using the root locus technique. The linearized closed loop equations read :

$$\dot{x}_1 = \frac{1}{\beta}(a_0\gamma-\alpha)x_1+\frac{1}{\beta}(\gamma+\gamma b_0+m_2)x_2 \tag{6.38}$$

$$\dot{x}_2 = -a_0x_1-(1+b_0)x_2 \tag{6.39}$$

After some manipulations the characteristic equation is obtained as :

$$(s+\frac{\alpha}{\beta})(s+1+b_0)+\frac{a_0}{\beta}[(-\gamma)s+m_2]=0 \tag{6.40}$$

where

$$a_0 \triangleq m_1z_{2s}\frac{df(\sigma)}{d\sigma}|_{\sigma=z_{1s}} = m_1z_{2s}\frac{10^4}{z_{1s}^2}e^{\frac{-10^4}{z_{1s}}} > 0 \tag{6.41}$$

$$b_0 \triangleq m_1f(z_{1s}) = m_1e^{\frac{-10^4}{z_{1s}}} > 0 \tag{6.42}$$

Figure 6.3(a),(b) displays the root locus plots of (6.40) for given values of $\frac{\alpha}{\beta} > 0$ and$(-\gamma) > 0$ and for $0 < \frac{1}{\beta} < +\infty$ as compared to the nonrobust case $\gamma = 0$. The spectrum's shape depends on the controller parameters values $\frac{\alpha}{\beta}$ and $(-\gamma)$. With $\gamma < 0$ the system's time response is non-oscillatory for small values and for large values of β and oscillatory for intermediate values. The response dies out faster for increasing $\frac{\alpha}{\beta}$ and for increasing $\frac{1}{\beta}$. With $\gamma < 0$ a better damping is achievable than in the nonrobust case with $\gamma = 0$. Figure 6.4 shows two

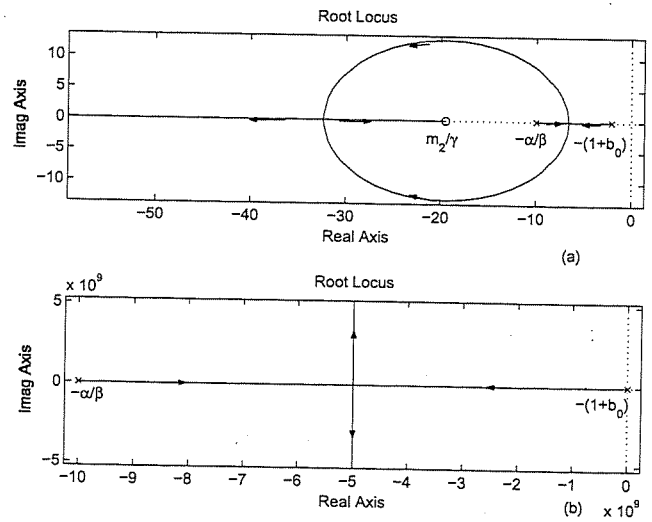

Figure 6.3: Root locus diagrams for the linearized closed loop dynamics for Example 1. (a) : robust control ($\gamma < 0$); (b) : nonrobust control ($\gamma = 0$).

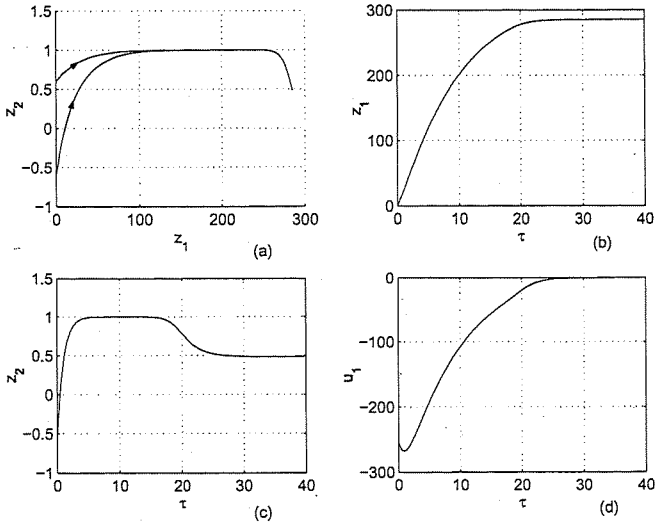

Figure 6.4: Transient response and robust PD-control signal for Example 1. $\alpha = 10^{15}; \beta = 10^{16}; \gamma = -0.1$; $z(0) = (0.4; -0.6)$; set point : $(285.3567; 0.4837)$ (a) Phase portrait,(b) Temperature response,(c) Concentration response,(d) Control law u_1 (Single input control). (a) also displays the trajectory starting at $z(0) = (0.4; 0.6)$.

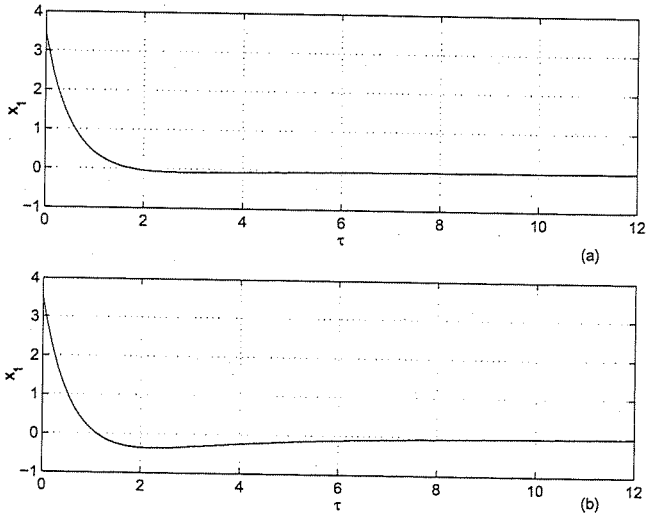

Figure 6.5: Temperature response for Example 1. $(-\gamma) = 1.28.10^7$; (a) Nonlinear system in deviation variables : $\alpha = 1.34.10^4; \beta = 8.5.10^{15}$; (b) Linearized system: $\alpha = 1.34.10^4; \beta = 8.5.10^{15}$

trajectories of the nonlinear system for two different initial conditions and the transient response corresponding to one of these. Figure 6.5 shows the temperature response curves corresponding to the linearized system and the nonlinear system starting at the initial condition x(0)=[3.5;-0.8]. We observe that in both cases there are no oscillations and the settling time is larger in the case of the linearized system.

Chapter 7

Conclusions

In the first section of this chapter we summarize the main topics of our research work. In Section 7.2 we talk about future research possibilities related to the application of the developed algorithms to industrial cases. We make a comparison with other design techniques such as artificial intelligence.

7.1 Summary

In this thesis it is shown how to apply Liapunov theory and passivity techniques in order to obtain the global asymptotic stabilization of an unstable set point of a CSTR. We use a nonlinear system model which is described dynamically by equations containing a product type nonlinearity in which one factor depends linearly and the other factor depends exponentially on the state variables.

The stabilization of the CSTR is achieved using linear dynamic output feedback control starting from a simple case which corresponds to a PD controller and finalizing with more complicated control structures such as the PID controller. Also to make the analysis simpler we start with only one input and subsequently we use the full multivariable system with two inputs.

Several conditions are derived under which it is possible for the different cases (PD, PID) to model the closed loop configurations as feedback interconnections of passive components, which allows the design of simple nonrobust stabilizing feedback laws initially and robust globally stabilizing feedback laws at the end.

The control parameters are tuned using simulations of the closed loop transients and phase portraits corresponding to the nonlinear and the linearized system. The root locus technique has been applied as an analytical tool for this tuning process. Besides passivity theory the underlying stabilization technique uses concepts from dissipative systems and from the direct method of Liapunov.

Using the Liapunov method it is possible to compute and numerically maximize stability regions in state space, defining sets of initial states from which convergence to the set point is ensured under given bounds on the admissible variations of state or control variables. However some trade-off may be required between the quality of the transient response and the extent of the region of attraction which can be fit by selecting appropriate controller parameters.

An important observation is that although at least in the multivariable case, linearizing state feedback laws could be obtained, in this research work we never tried to compensate the complex nonlinearities (originating from the Arrhenius law) of the controlled process. Instead, exploiting the special structure of these nonlinearities, simple linear time invariant control laws were synthesized which

globally asymptotically stabilize the selected set point.

It has been shown in the different chapters that every PD,PID controller globally stabilizes the system's set point if the controller parameters are selected in an appropriate way. By changing these parameter values we can obtain better transient responses or maximize the region of attraction of the set point under a control or state constraint. Although it is know that a better estimate of the true stability region is reached by taking the union of the different sets obtained from a family of Liapunov functions, we have shown that in our problem, for the control input constraint case, we only obtain a small increase of the estimated region of attraction in this way.

The two input PD controller produces smoother transients mainly in the temperature response, compared to the single input PD controller. Oscillations and a strong control effort appear in both cases of two PID-strategies we discussed. However less control amplitude is generated in the first case. In conclusion the two inputs give us better transient characteristics and better damping but more energy is needed to drive the system to its set point.

In the case of the PID approach it was concluded that although it is endowed with good disturbance rejection properties (at least for the temperature), the transient behaviour is worse when compared to the PD controller.

It is easily possible to partially decouple the system. For example we can decouple the temperature dynamics from the concentration dynamics or viceversa. However making the control law robust loses the decoupling effect and also deteriorates closed loop stability.

In the last part of this work a method to analyze the effect of model uncertainty on closed loop stability and performance has been proposed. We design controllers which yield a finite stability region around the set point but have good robustness properties. On the other hand controllers which globally stabilize the set point give us limited robustness. The robustness of the controller implies that it is not necessary to know the exact values of the process parameters.

7.2 Further research

In relation to the results that have been presented, we can formulate a number of important issues and extensions that need to be further focused upon. Some of them are summarized below.

7.2.1 Generalizations of the robust PD/PID controller

An alternative method to improve controller robustness is to use the reactor's feed concentration as a secondary input to the control system. Further extensions to the robust PD/PID controller could lead us to finding conditions under which global asymptotic stability remains ensured and robustness is improved. So an important research topic could be to obtain a generalization for the robustness problem based on the concepts exposed in Chapter 6. Some introductory ideas along these lines have been formulated in (Muñoz, Loccufier and Noldus 2003c).

7.2.2 Survey of and comparison with alternative controller design methods

An interesting approach would be to apply various controller design methods such as neural control or model based predictive control (MBPC) to the CSTR and compare the results with the algorithms developed in this work. In this way we can see the advantages and disadvantages of the proposed technique. If similar results are achieved, this would strengthen the possible usefulness of the methodology in real applications. Several control strategies could then be compared and conclusions could be established in order to know what can practically be done in any particular application.

For most complex industrial systems, the availability of a good system model for fully understanding the process behaviour is essential. Model- based control uses the available system model (CSTR) to incorporate the predicted future behaviour of the process into the controller design procedure. The general ideas of how this methodology is carried out are listed below :

- A model of the real plant to predict the process output at future time instants is needed.
- An objective function is defined, and the control sequence which mini-

mizes it is found. The receding horizon strategy principle is used.

A second approach could be the implementation of a model-based neural controller, consisting of multilayer feedforward neural networks. For such a control system sufficient conditions for global asymptotic closed loop stability and robust stability could be developed and then compared with our proposed method. A paper in this direction is in preparation and will be ready to be published in the near future.

7.2.3 Application to real world industrial plants

In future work it will be interesting to apply the proposed approach to specific industrial examples to test the practical applicability of the design method. Further studies are needed to determine if the suggested algorithms can be applied to real systems.

An important problem which we have not considered but which is similar to the present one is the monitoring and the control of biological reactors. Biological reactors, as most nonlinear systems, generally have multiple equilibrium states which can be stable or unstable. This is clearly the situation we have been studying in the present work. In particular, when substrate inhibition effects occur, not only the operating point can become unstable but the reactor may be irreversibly led to a wash-out state, that is to a situation where the microbial life has completely disappeared.

So, in the case of substrate inhibition, industrial CST biological reactors definitely require feedback control to stabilize the process. Some practical work has been developed in the direction of the application of nonlinear control theory to the stabilization of CST biological reactors. There are some similarities in the dynamical structure of the processes CSTR and CST biological reactor, in the sense that for instance the dynamics in the latter one contain product type nonlinearities resulting from the Monod growth law or its modifications in the process dynamics. Our suggested methods could be applied to these kinds of processes and then compared with the use of adaptive nonlinear feedback or any other techniques.

As an application we propose to apply the designed algorithms in our work to control the dissolved oxygen in an activated sludge pilot plant. The dissolved oxygen concentration(DO) in the aerobic part of an activated sludge process

should be sufficiently high to supply enough oxygen to the microorganisms in the sludge, so organic matter is degraded and ammonium is converted to nitrate. On the other hand an excessively high DO which requires a high airflow rate leads to a high energy consumption and may also deteriorate the sludge quality. Hence both for economical and process reasons it is of interest to control the DO. The dissolved oxygen dynamics involve a nonlinear term analogous to the type we have studied in the current thesis.

One problem with controlling the DO is that the process dynamics are nonlinear. This means that high control performance for all operating conditions may be hard to achieve with a linear controller. A research topic could be to show by practical experiments in the pilot plant that the linear PID controller behaves equally or better than the nonlinear controller currently used. Also a discussion about stability could be made.

Bequette, B. W. (2003), "Process Control, Modelling, Design and Simulation", Prentice Hall, New Jersey.

Brown,S.K. and Bordons,C. (1995), "Adaptive predictive controller for optimal process control", Los Alamos National Laboratory, Los Alamos, NM 87545.

Camacho, E.F. et al.(1993), "Model Predictive Control in the Process Industry", Springer, London.

Carlsson, B., Lindberg, S. and Xu, S. (1994), "On-line estimation of the respiration rate and the oxigen transfer rate at Kungsangen Wastewater plant in Upssala", Wat. Sci. Tech, 30, 255-263.

Clarke, D.W.(1988), "Application of generalized predictive control to industrial processes", I.E.E.E Cont. Sys. Mag., 49-55.

Dostal, P., Bobál, V. and Prokop, R. (2001), "One approach to adaptive control of nonlinear processes", IFAC Worshop on Adaptation and Learning in Control and Signal Processing ALCOSP, 407-412.

Efe, M.O. et al. (2001), "Radial basis function neural networks in variable structure control of a class of biochemical processes", I.E.E.E. Trans. on Automatic Control, 1, 13-18.

Eigenberger, G. (1985), "Dynamics and stability of chemical engineering processes", Int. Chem. Engineering, 25, 595-609.

Fogler, S.H. (2000), "Elements of Chemical Reaction Engineering", Prentice Hall, Michigan University.

Genesio, R., Tartaglia, M. and Vicino, A. (1985), "On the estimation of asymptotic stability regions : State of the art and new proposals", I.E.E.E. Trans. on Automatic Control, AC-30, 8, 747-755.

Glad, T. and Lyung, L. (2003), "Control Theory: Multivariable and Nonlinear Methods", Taylor and Francis, London and New York.

Golten, J. and Verwer, A.(1991), "Control System Design and Simulation", McGraw-Hill Education, England.

Guay, M., McLellan, J., Bacon, D.W.(1995), "Measurement of nonlinearity in chemical process control systems: the steady state map", Canadian Journal Chemical Engineering, 73, 868-882.

Guay, M.(1996), "Measurement of nonlinearity in chemical process control: PhD Thesis", Queen's University, Kingston, ON.

Harris, T.J. and Seppala, C.J. (2001), "Diagnosis and Analysis of Control Systems", preprints of CPC VI.

Hill, D.J. and Moylan, P.J. (1976), "The stability of nonlinear dissipative systems", I.E.E.E. Trans. on Automatic Control, AC-25, 5, 708-711.

Hill, D.J. and Moylan, P.J. (1980), "Connections between finite-gain and asymptotic stability", I.E.E.E. Trans. on Automatic Control, 5, 931-936.

Fantoni, I. and Lozano, R. (2002), "Non-linear control for underactuated mechanical systems", E.D.Sontag, London.

James, B.R. and Peter, L.L. (2001), "Multi-model decoupled generic model control", Control Engineering Practice, 9, 471-481.

Khalil, H. K. (1996), "Nonlinear Systems", Prentice-Hall, Upper Saddle River, NJ, 2nd edition.

Levenspiel, O.(1999), "Chemical Reaction Engineering", John Willey & Sons, New York.

Lindberg, C.(1997), "Control and estimation strategies applied to the activated sludge process : PhD Thesis", Uppsala University, systems and control group. UPTEC, Uppsala(Sweden).

Loccufier, M. and Noldus, E. (1994), "A combination of the direct method of Liapunov and simulation for the stability analysis of chemical reactors", Journal A, 35, 36-41.

Lozano, R., Brogliato, B., Egeland, O. and Maschke, B. (2000), "Dissipative Systems Analysis and Control", Springer, London.

Luyben, W.L. (1990), "Process Modelling, Simulation and Control for Chemical Engineers", McGraw-Hill, New York.

Marchand, N. and Alamir, M. (1998), "From open-loop trajectories to stabilizing state feedback. Application to a CSTR", IFAC Symposium on System Structure and Control, 2, 801-806.

Matsubara, M., Nishimura, Y. and Takahashi, N. C. (1973), "Periodic operation of a CSTR-Idealized control", Chem. Eng. Sci., 28, 1369-1377.

McColm, E.J., Manchanda, S. and Tham, M.T.(1994), "On the applicability of a nonlinear control strategy", Proc. IEE Conf. Contrl. '94, 1352-1357.

Muñoz, A.,Loccufier, M. and Noldus, E.(2002), "Passivity based modelling and simulation of nonlinear process control systems", IASTED Int. Conference on Applied Simulation and Modelling, Crete, 440-445.

Muñoz, A., Loccufier, M. and Noldus, E.(2003a), "Stabilizing PD-control of a nonlinear system in process engineering", Proc. 2nd Intern. Conference on System Identification and Control Problems, Moscow, 499-511.

Muñoz, A., Loccufier, M. and Noldus, E.(2003b),"Globally stabilizing linear PID-control of a nonlinear chemical process" , IASTED Int. Conference on Modelling, Identification and Control, Innsbruck, 275-279.

Muñoz, A., Loccufier, M. and Noldus, E.(2003c),"Design of a robust globally stabilizing PD-process control system", Computing Anticipatory Systems, CASYS 2003 - Sixth International Conference, *Liège*, Belgium; Chaos asbl, *Liège*, Symp. 9, p. 7.

Muñoz, A., Loccufier, M. and Noldus, E.(2004),"Design of a robust globally stabilizing PD-process control system" , Int. Journal of Computing Anticipatory Systems (to appear).

Muñoz, A., Loccufier, M. and Noldus, E.(2004a),"Decoupling control of a CSTR using linear dynamic feedback.6th Congress of the Colombian Association of Automatic Control", Ibagué, Colombia

Muske, K.R. and Rawlings, J.B.(1993), "Linear model predictive control of unstable processes", J.Proc. Control., 3, 85-96.

Nikolaou, M.(2001), "Linear Control of Nonlinear Processes : Recent Developments and Future Work", CEPAC, Guaruj, Sao Paulo (Brazil).

Noldus, E., Spriet,J., Veriest, E. and Van Cauwenberge,A. (1974), "A new Liapunov technique for the stability analysis of chemical reactors", Automatica, 10, 675-680.

Noldus, E.(1977), "Periodic optimization of a chemical reactor using perturbation methods", J. of Engineering Mathematics, 11, 49-66.

Ogata, K. (1998), "Modern Control Engineering", Prentice Hall, Mexico.

Rawlings, J., Tenny, M. and Wright, S.(2002), "A Tutorial to Nonlinear Model Predictive Control", University of Wisconsin, Washington.

Rigopoulos, K., Shu, X. and Cinar, A.(1988), "Forced periodic control of an exothermic CSTR with multiple input oscillations", AI CheE Journal, 34, 2041-2051.

Skogestad, S. and Postlethwaite, I.(1996), "Multivariable Feedback Control", Wiley, New York.

Smith, C.A. and Corripio, A.B.(1997), "Principles and Practice of Automatic Process Control", Wiley, New York.

Stephanopoulos, G. and Schuelke L. M.(1976), "Process design in a dynamic environment", AI Che E Journal, 22, 855-867.

Tan, Y. and Van Cauwenberghe, A.(1999), "Generalised nonlinear PID controller based on neural networks", Proceedings of Information, Desicion and Control, 99, 519-524.

Vidyasagar, M.(1993), "Nonlinear Systems Analysis", Prentice-Hall, Englewood Cliffs, N.J.

Warden, R.B., Aris, R. and Amundson, N.R. (1964), "An analysis of chemical reactor stability and control-VIII", Chemical Engineering Science, 19, 149-172.

Willems, J.C. (1971), "Least squares stationary optimal control and the algebraic Riccati equation", I.E.E.E. Trans. on Automatic Control, AC-16, 621-634.

Willems, J.C. (1972), "Dissipative dynamical systems, Part I : General theory", Arch. Rat.Mech. An., 45, 321-351.

Willems, J.L. (1969), "The computation of finite stability regions by means of open Liapunov surfaces", Int. J. Control, 10, 537-544.

Willems, J.L. (1970), "Stability Theory of Dynamical Systems", Nelson, London.

Willis, C. and Yham, M.T.(1994), "Globally linearizing control using artifitial neural networks", Proc. IEE Conf. Control'94, 967-972.